Electrically tunable excitonic light-emitting diodes base junctions

Nature Nanotechnology

9, 268-272

DOI: 10.1038/nnano.2014.26

Citation Report

#	Article	IF	Citations
4	Introduction to carbon-based nanostructures. , 0, , 1-10.		0
5	Electronic properties of carbon-based nanostructures. , 0, , 11-90.		0
6	Tuning the optical emission of MoS2 nanosheets using proximal photoswitchable azobenzene molecules. Applied Physics Letters, 2014, 105, .	1.5	32
7	Spin-resolved optical conductivity of two-dimensional group-VIB transition-metal dichalcogenides. Physical Review B, 2014, 90, .	1.1	33
8	Room Temperature Electroluminescence from Mechanically Formed van der Waals IIIâ€“VI Homojunctions and Heterojunctions. Advanced Optical Materials, 2014, 2, 1064-1069.	3.6	71
9	Carbon nanotube quantum dots on hexagonal boron nitride. Applied Physics Letters, 2014, 105, .	1.5	13
10	Air stable n-doping of WSe2 by silicon nitride thin films with tunable fixed charge density. APL Materials, 2014, 2, .	2.2	76
11	Quantum confined acceptors and donors in InSe nanosheets. Applied Physics Letters, 2014, 105, 221909.	1.5	58
12	Vapor-transport growth of high optical quality WSe2 monolayers. APL Materials, 2014, 2, .	2.2	52
13	Photoluminescence properties and exciton dynamics in monolayer WSe2. Applied Physics Letters, 2014, 105, .	1.5	149
14	Doping against the Native Propensity of MoS₂: Degenerate Hole Doping by Cation Substitution. Nano Letters, 2014, 14, 6976-6982.	4.5	574
15	High blue-near ultraviolet photodiode response of vertically stacked graphene-MoS2-metal heterostructures. Applied Physics Letters, 2014, 104, .	1.5	33
16	Two-dimensional material nanophotonics. Nature Photonics, 2014, 8, 899-907.	15.6	2,362
17	Measurement of the optical dielectric function of monolayer transition-metal dichalcogenides:<mml:math xmlns:mml="http://www.w3.org/1998/Math/MathML"><mml:msub><mml:mi>MoS</mml:mi><mml:mn>2</mml:mn></mml:msub></mml xmlns:mml="http://www.w3.org/1998/Math/MathML"><mml:mrow><mml:mi>Mo</mml:mi><mml:mi mathvariant="normal">S</mml:mi><mml:msub><mml:mi	1.1	1,017
18	Hot-electron cooling by acoustic and optical phonons in monolayers of<mml:math xmlns:mml="http://www.w3.org/1998/Math/MathML"><mml:msub><mml:mi mathvariant="normal">MoS</mml:mi><mml:mn>2</mml:mn></mml:msub></mml:math>and other transition-metal dichalcogenides. Physical Review B, 2014, 90, .	1.1	76
19	Spin-valley relaxation and quantum transport regimes in two-dimensional transition-metal dichalcogenides. Physical Review B, 2014, 90, .	1.1	38
20	Optoelectronic devices based on electrically tunable pâ€“n diodes in a monolayer dichalcogenide. Nature Nanotechnology, 2014, 9, 262-267.	15.6	1,270
21	Solar-energy conversion and light emission in an atomic monolayer pâ€“n diode. Nature Nanotechnology, 2014, 9, 257-261.	15.6	1,175

#	Article	IF	Citations
22	Electrically Switchable Chiral Light-Emitting Transistor. Science, 2014, 344, 725-728.	6.0	675
23	Enhancement of Photovoltaic Response in Multilayer MoS₂ Induced by Plasma Doping. ACS Nano, 2014, 8, 5270-5281.	7.3	344
24	Electronic Control of Circularly Polarized Light Emission. Science, 2014, 344, 702-703.	6.0	21
25	Formation and diffusion characteristics of Pt clusters on Graphene, 1Hâ€MoS₂ and 1Tâ€TaS₂. Annalen Der Physik, 2014, 526, 423-429.	0.9	13
26	Synthesis and Stability of Two-Dimensional Ge/Sn Graphane Alloys. Chemistry of Materials, 2014, 26, 6941-6946.	3.2	42
27	Broadband Coherent Absorption in Chirped-Planar-Dielectric Cavities for 2D-Material-Based Photovoltaics and Photodetectors. ACS Photonics, 2014, 1, 768-774.	3.2	101
28	Monolayer MoSe₂ Grown by Chemical Vapor Deposition for Fast Photodetection. ACS Nano, 2014, 8, 8582-8590.	7.3	515
29	Chemically Driven Tunable Light Emission of Charged and Neutral Excitons in Monolayer WS₂. ACS Nano, 2014, 8, 11320-11329.	7.3	236
30	Screw-Dislocation-Driven Growth of Two-Dimensional Few-Layer and Pyramid-like WSe₂ by Sulfur-Assisted Chemical Vapor Deposition. ACS Nano, 2014, 8, 11543-11551.	7.3	146
31	Two-dimensional heterostructures: fabrication, characterization, and application. Nanoscale, 2014, 6, 12250-12272.	2.8	323
32	Photovoltaic and Photothermoelectric Effect in a Double-Gated WSe₂ Device. Nano Letters, 2014, 14, 5846-5852.	4.5	232
33	Valley dynamics probed through charged and neutral exciton emission in monolayer<mml:math xmlns:mml="http://www.w3.org/1998/Math/MathML"><mml:msub><mml:mrow><mml:mi mathvariant="normal">WSe</mml:mi></mml:mrow><mml:mn>2</mml:mn></mml:msub></mml:math>. Physical Review B, 2014, 90, .	1.1	325
34	Atomically thin pâ€“n junctions. Nature Nanotechnology, 2014, 9, 664-665.	15.6	19
35	Monolayer MoS₂ Heterojunction Solar Cells. ACS Nano, 2014, 8, 8317-8322.	7.3	1,081
36	Photovoltaic Effect in an Electrically Tunable van der Waals Heterojunction. Nano Letters, 2014, 14, 4785-4791.	4.5	943
37	Photovoltaic effect in few-layer black phosphorus PN junctions defined by local electrostatic gating. Nature Communications, 2014, 5, 4651.	5.8	643
38	Vertical and in-plane heterostructures from WS2/MoS2 monolayers. Nature Materials, 2014, 13, 1135-1142.	13.3	1,918
39	Nonlinear Valley and Spin Currents from Fermi Pocket Anisotropy in 2D Crystals. Physical Review Letters, 2014, 113, 156603.	2.9	80

#	Article	IF	Citations
40	Atomically thin pâ€“n junctions with van der Waals heterointerfaces. Nature Nanotechnology, 2014, 9, 676-681.	15.6	1,953
41	Strong Enhancement of Raman Scattering from a Bulk-Inactive Vibrational Mode in Few-Layer MoTe₂. ACS Nano, 2014, 8, 3895-3903.	7.3	275
42	Dielectric Screening of Excitons and Trions in Single-Layer MoS₂. Nano Letters, 2014, 14, 5569-5576.	4.5	520
43	Lateral epitaxial growth of two-dimensional layered semiconductor heterojunctions. Nature Nanotechnology, 2014, 9, 1024-1030.	15.6	1,056
44	Electroluminescence and Photocurrent Generation from Atomically Sharp WSe₂/MoS₂ Heterojunction pâ€“n Diodes. Nano Letters, 2014, 14, 5590-5597.	4.5	937
45	Photodetectors based on graphene, other two-dimensional materials and hybrid systems. Nature Nanotechnology, 2014, 9, 780-793.	15.6	3,017
46	Engineering polar discontinuities in honeycomb lattices. Nature Communications, 2014, 5, 5157.	5.8	43
47	Generation and recombination in two-dimensional bipolar transistors. Applied Physics A: Materials Science and Processing, 2014, 115, 737-740.	1.1	3
48	Exciton Kinetics, Quantum Efficiency, and Efficiency Droop of Monolayer MoS₂ Light-Emitting Devices. Nano Letters, 2014, 14, 4125-4130.	4.5	146
49	Mono- and Bilayer WS₂ Light-Emitting Transistors. Nano Letters, 2014, 14, 2019-2025.	4.5	424
50	Monolayer diodes light up. Nature Nanotechnology, 2014, 9, 247-248.	15.6	34
51	Electron and Hole Mobilities in Single-Layer WSe₂. ACS Nano, 2014, 8, 7180-7185.	7.3	295
52	High Broadâ€Band Photoresponsivity of Mechanically Formed InSeâ€“Graphene van der Waals Heterostructures. Advanced Materials, 2015, 27, 3760-3766.	11.1	320
53	Simulation Evidence of Hexagonalâ€toâ€Tetragonal ZnSe Structure Transition: A Monolayer Material with a Wideâ€Range Tunable Direct Bandgap. Advanced Science, 2015, 2, 1500290.	5.6	44
54	Effect of Interlayer Coupling on Ultrafast Charge Transfer from Semiconducting Molecules to Mono- and Bilayer Graphene. Physical Review Applied, 2015, 4, .	1.5	19
55	Gate control of carrier distribution in<mml:math xmlns:mml="http://www.w3.org/1998/Math/MathML"><mml:mi>k</mml:mi></mml:math>-space in<mml:math xmlns:mml="http://www.w3.org/1998/Math/MathML"><mml:msub><mml:mi>MoS</mml:mi><mml:mn>2</mml:mn></mml:msub></mml:math> and bilayer crystals. Physical Review B, 2015, 91, .	1.1	19
56	Fast exciton annihilation by capture of electrons or holes by defects via Auger scattering in monolayer metal dichalcogenides. Physical Review B, 2015, 91, .	1.1	66
57	Binding energies of exciton complexes in transition metal dichalcogenide monolayers and effect of dielectric environment. Physical Review B, 2015, 92, .	1.1	223

#	Article	IF	Citations
58	Excitons in van der Waals heterostructures: The important role of dielectric screening. Physical Review B, 2015, 92, .	1.1	211
59	Selective Amplification of the Primary Exciton in a<mml:math xmlns:mml="http://www.w3.org/1998/Math/MathML" display="inline"><mml:mrow><mml:mi>Mo</mml:mi><mml:msub><mml:mi mathvariant="normal">S</mml:mi><mml:mn>2</mml:mn></mml:msub></mml:mrow></mml:math>Monolayer. Physical Review Letters, 2015, 115, 226801.	2.9	54
60	Ultraviolet Lasers Realized via Electrostatic Doping Method. Scientific Reports, 2015, 5, 13641.	1.6	14
61	Tunable Valley Polarization and Valley Orbital Magnetic Moment Hall Effect in Honeycomb Systems with Broken Inversion Symmetry. Scientific Reports, 2015, 5, 13906.	1.6	16
62	Plasmonic Gold Nanorods Coverage Influence on Enhancement of the Photoluminescence of Two-Dimensional MoS2 Monolayer. Scientific Reports, 2015, 5, 16374.	1.6	102
63	Robust Direct Bandgap Characteristics of One- and Two-Dimensional ReS2. Scientific Reports, 2015, 5, 13783.	1.6	68
64	A van der Waals pn heterojunction with organic/inorganic semiconductors. Applied Physics Letters, 2015, 107, 183103.	1.5	77
65	A comparative density functional study on electrical properties of layered penta-graphene. Journal of Applied Physics, 2015, 118, .	1.1	54
66	Unidirectional oxide hetero-interface thin-film diode. Applied Physics Letters, 2015, 107, .	1.5	3
67	Hopping conduction in p-type MoS2 near the critical regime of the metal-insulator transition. Applied Physics Letters, 2015, 107, .	1.5	20
68	Highâ€Performance, Airâ€Stable, Topâ€Gate, pâ€Channel WSe₂ Fieldâ€Effect Transistor with Fluoropolymer Buffer Layer. Advanced Functional Materials, 2015, 25, 7208-7214.	7.8	67
69	Lateral Builtâ€In Potential of Monolayer MoS₂â€“WS₂ Inâ€Plane Heterostructures by a Shortcut Growth Strategy. Advanced Materials, 2015, 27, 6431-6437.	11.1	191
70	Chemical Vapor Deposition of Largeâ€Sized Hexagonal WSe₂ Crystals on Dielectric Substrates. Advanced Materials, 2015, 27, 6722-6727.	11.1	152
71	Highâ€Performance Monolayer WS₂ Fieldâ€Effect Transistors on Highâ€κ Dielectrics. Advanced Materials, 2015, 27, 5230-5234.	11.1	218
72	Tunable Polarity Behavior and Selfâ€Driven Photoswitching in pâ€WSe₂/nâ€WS₂ Heterojunctions. Small, 2015, 11, 5430-5438.	5.2	114
73	Exciton and Trion Dynamics in Bilayer MoS₂. Small, 2015, 11, 6384-6390.	5.2	87
74	Highâ€Performance Transition Metal Dichalcogenide Photodetectors Enhanced by Selfâ€Assembled Monolayer Doping. Advanced Functional Materials, 2015, 25, 4219-4227.	7.8	247
75	Van der Waals pâ€“n Junction Based on an Organicâ€“Inorganic Heterostructure. Advanced Functional Materials, 2015, 25, 5865-5871.	7.8	98

#	Article	IF	Citations
76	Revealing Optical Properties of Reducedâ€Dimensionality Materials at Relevant Length Scales. Advanced Materials, 2015, 27, 5693-5719.	11.1	29
77	Hexagonal AlN: Dimensional-crossover-driven band-gap transition. Physical Review B, 2015, 91, .	1.1	121
78	Indirect Band Gap Emission by Hot Electron Injection in Metal/MoS₂ and Metal/WSe₂ Heterojunctions. Nano Letters, 2015, 15, 3977-3982.	4.5	60
79	Excitonic resonances in thin films of WSe₂: from monolayer to bulk material. Nanoscale, 2015, 7, 10421-10429.	2.8	275
80	Chemical Vapor Deposition Growth of Monolayer WSe₂ with Tunable Device Characteristics and Growth Mechanism Study. ACS Nano, 2015, 9, 6119-6127.	7.3	340
81	Robust Excitons and Trions in Monolayer MoTe₂. ACS Nano, 2015, 9, 6603-6609.	7.3	148
82	Charge trapping at the MoS2-SiO2 interface and its effects on the characteristics of MoS2 metal-oxide-semiconductor field effect transistors. Applied Physics Letters, 2015, 106, .	1.5	201
83	Electrostatically Reversible Polarity of Ambipolar Î±-MoTe₂ Transistors. ACS Nano, 2015, 9, 5976-5983.	7.3	113
84	WSe₂ Light-Emitting Tunneling Transistors with Enhanced Brightness at Room Temperature. Nano Letters, 2015, 15, 8223-8228.	4.5	231
85	Vibrational and optical properties of MoS2: From monolayer to bulk. Surface Science Reports, 2015, 70, 554-586.	3.8	178
86	Electronic and magnetic properties of 1 T-TiSe ₂ nanoribbons. 2D Materials, 2015, 2, 044002.	2.0	21
87	Exciton states in monolayer MoSe ₂ : impact on interband transitions. 2D Materials, 2015, 2, 045005.	2.0	71
88	Two-dimensional materials for nanophotonics application. Nanophotonics, 2015, 4, 128-142.	2.9	97
89	Optoelectric properties of gate-tunable MoS2/WSe2 heterojunction. , 2015, , .		0
90	Ultrafast Dynamics of Defect-Assisted Electronâ€“Hole Recombination in Monolayer MoS₂. Nano Letters, 2015, 15, 339-345.	4.5	509
91	Observation of Excitonic Fine Structure in a 2D Transition-Metal Dichalcogenide Semiconductor. ACS Nano, 2015, 9, 647-655.	7.3	288
92	Highâ€Gain Subnanowatt Power Consumption Hybrid Complementary Logic Inverter with WSe₂ Nanosheet and ZnO Nanowire Transistors on Glass. Advanced Materials, 2015, 27, 150-156.	11.1	43
93	Electronic Transport of Encapsulated Graphene and WSe₂ Devices Fabricated by Pick-up of Prepatterned hBN. Nano Letters, 2015, 15, 1898-1903.	4.5	115

#	Article	IF	Citations
94	Microwave Near-Field Imaging of Two-Dimensional Semiconductors. Nano Letters, 2015, 15, 1122-1127.	4.5	42
95	Self-Limiting Layer-by-Layer Oxidation of Atomically Thin WSe₂. Nano Letters, 2015, 15, 2067-2073.	4.5	204
96	Electrostatically Induced Superconductivity at the Surface of WS₂. Nano Letters, 2015, 15, 1197-1202.	4.5	140
97	Large-area synthesis of monolayer WSe₂ on a SiO₂/Si substrate and its device applications. Nanoscale, 2015, 7, 4193-4198.	2.8	128
98	Valley excitons in two-dimensional semiconductors. National Science Review, 2015, 2, 57-70.	4.6	254
99	Light-emitting diodes by band-structure engineering in van der Waals heterostructures. Nature Materials, 2015, 14, 301-306.	13.3	1,397
100	A 2D Semiconductorâ€“Selfâ€Assembled Monolayer Photoswitchable Diode. Advanced Materials, 2015, 27, 1426-1431.	11.1	52
101	Engineering Light Outcoupling in 2D Materials. Nano Letters, 2015, 15, 1356-1361.	4.5	138
102	MoS 2 and semiconductors in the flatland. Materials Today, 2015, 18, 20-30.	8.3	179
103	Lighten the Olympia of the Flatland: Probing and Manipulating the Photonic Properties of 2D Transitionâ€Metal Dichalcogenides. Small, 2015, 11, 3206-3220.	5.2	15
104	Helicity-Resolved Raman Scattering of MoS₂, MoSe₂, WS₂, and WSe₂ Atomic Layers. Nano Letters, 2015, 15, 2526-2532.	4.5	241
105	Modification of electronic structure and thermoelectric properties of hole-doped tungsten dichalcogenides. Physical Review B, 2015, 91, .	1.1	27
106	Giant Enhancement of the Optical Second-Harmonic Emission of<mml:math xmlns:mml="http://www.w3.org/1998/Math/MathML" display="inline"><mml:mrow><mml:msub><mml:mrow><mml:mi>WSe</mml:mi></mml:mrow><mml:mrow><mml:mn>2</mml:mn></r by Laser Excitation at Exciton Resonances. Physical Review Letters, 2015, 114, 097403.	2.9	464
107	Layer-Dependent Modulation of Tungsten Disulfide Photoluminescence by Lateral Electric Fields. ACS Nano, 2015, 9, 2740-2748.	7.3	50
108	Phonon and Raman scattering of two-dimensional transition metal dichalcogenides from monolayer, multilayer to bulk material. Chemical Society Reviews, 2015, 44, 2757-2785.	18.7	1,034
109	Surface transfer doping induced effective modulation on ambipolar characteristics of few-layer black phosphorus. Nature Communications, 2015, 6, 6485.	5.8	335
110	Thin-layer black phosphorus/GaAs heterojunction p-n diodes. Applied Physics Letters, 2015, 106, .	1.5	55
111	Enhanced device performances of WSe₂â€“MoS₂ van der Waals junction pâ€“n diode by fluoropolymer encapsulation. Journal of Materials Chemistry C, 2015, 3, 2751-2758.	2.7	74

#	Article	IF	Citations
112	Step-Edge-Guided Nucleation and Growth of Aligned WSe₂ on Sapphire via a Layer-over-Layer Growth Mode. ACS Nano, 2015, 9, 8368-8375.	7.3	168
113	Two-Step Growth of Two-Dimensional WSe₂/MoSe₂ Heterostructures. Nano Letters, 2015, 15, 6135-6141.	4.5	479
114	Modelling of stacked 2D materials and devices. 2D Materials, 2015, 2, 032003.	2.0	59
115	Nanoantenna-Enhanced Lightâ€"Matter Interaction in Atomically Thin WS₂. ACS Photonics, 2015, 2, 1260-1265.	3.2	114
116	Optically Pumped Two-Dimensional MoS₂ Lasers Operating at Room-Temperature. Nano Letters, 2015, 15, 5302-5306.	4.5	204
117	Highly sensitive and fast phototransistor based on large size CVD-grown SnS₂nanosheets. Nanoscale, 2015, 7, 14093-14099.	2.8	126
118	Recent developments in black phosphorus transistors. Journal of Materials Chemistry C, 2015, 3, 8760-8775.	2.7	146
119	Chemical Vapor Deposition Synthesized Atomically Thin Molybdenum Disulfide with Optoelectronic-Grade Crystalline Quality. ACS Nano, 2015, 9, 8822-8832.	7.3	132
120	Reversible Semiconducting-to-Metallic Phase Transition in Chemical Vapor Deposition Grown Monolayer WSe₂ and Applications for Devices. ACS Nano, 2015, 9, 7383-7391.	7.3	164
121	MoS2 Heterojunctions by Thickness Modulation. Scientific Reports, 2015, 5, 10990.	1.6	93
122	Raman analysis of gold on WSe₂ single crystal film. Materials Research Express, 2015, 2, 065009.	0.8	20
123	Tunable Electrical and Optical Characteristics in Monolayer Graphene and Few-Layer MoS₂ Heterostructure Devices. Nano Letters, 2015, 15, 5017-5024.	4.5	150
124	Towards photodetection with high efficiency and tunable spectral selectivity: graphene plasmonics for light trapping and absorption engineering. Nanoscale, 2015, 7, 13530-13536.	2.8	127
125	Metal Semiconductor Field-Effect Transistor with MoS₂/Conducting NiO_x van der Waals Schottky Interface for Intrinsic High Mobility and Photoswitching Speed. ACS Nano, 2015, 9, 8312-8320.	7.3	82
126	A sustainable future for photonic colloidal nanocrystals. Chemical Society Reviews, 2015, 44, 5897-5914.	18.7	115
127	Electric-field-induced strong enhancement of electroluminescence in multilayer molybdenum disulfide. Nature Communications, 2015, 6, 7509.	5.8	132
128	Synthesis, properties and applications of 2D non-graphene materials. Nanotechnology, 2015, 26, 292001.	1.3	101
129	Arrayed van der Waals Vertical Heterostructures Based on 2D GaSe Grown by Molecular Beam Epitaxy. Nano Letters, 2015, 15, 3571-3577.	4.5	146

#	Article	IF	Citations
130	Photocurrent generation with two-dimensional van der Waals semiconductors. Chemical Society Reviews, 2015, 44, 3691-3718.	18.7	802
131	Computational 2D Materials Database: Electronic Structure of Transition-Metal Dichalcogenides and Oxides. Journal of Physical Chemistry C, 2015, 119, 13169-13183.	1.5	902
132	Atomic Healing of Defects in Transition Metal Dichalcogenides. Nano Letters, 2015, 15, 3524-3532.	4.5	194
133	Novel Optical and Electrical Transport Properties in Atomically Thin WSe₂/MoS₂ pâ€“n Heterostructures. Advanced Electronic Materials, 2015, 1, 1400066.	2.6	67
134	Hybrid Grapheneâ€“Perovskite Phototransistors with Ultrahigh Responsivity and Gain. Advanced Optical Materials, 2015, 3, 1389-1396.	3.6	240
135	Lateral Growth of Composition Graded Atomic Layer MoS_{2(1â€“x)}Se_{2x} Nanosheets. Journal of the American Chemical Society, 2015, 137, 5284-5287.	6.6	191
136	Beyond Graphene: Progress in Novel Two-Dimensional Materials and van der Waals Solids. Annual Review of Materials Research, 2015, 45, 1-27.	4.3	537
137	Voltage-controlled quantum light from an atomically thin semiconductor. Nature Nanotechnology, 2015, 10, 507-511.	15.6	500
138	k Â· p theory for two-dimensional transition metal dichalcogenide semiconductors. 2D Materials, 2015, 2, 022001.	2.0	676
139	Nanostructured two-dimensional materials. , 2015, , 477-524.		0
140	Band Alignment in WSe₂â€“Graphene Heterostructures. ACS Nano, 2015, 9, 4527-4532.	7.3	138
141	TiS₃ Transistors with Tailored Morphology and Electrical Properties. Advanced Materials, 2015, 27, 2595-2601.	11.1	193
142	High-quality, large-area MoSe₂ and MoSe₂/Bi₂Se₃ heterostructures on AlN(0001)/Si(111) substrates by molecular beam epitaxy. Nanoscale, 2015, 7, 7896-7905.	2.8	122
143	Synthesis and Transfer of Large-Area Monolayer WS₂ Crystals: Moving Toward the Recyclable Use of Sapphire Substrates. ACS Nano, 2015, 9, 6178-6187.	7.3	200
144	Exciton dynamics and annihilation in WS₂ 2D semiconductors. Nanoscale, 2015, 7, 7402-7408.	2.8	388
145	Monolayer semiconductor nanocavity lasers with ultralow thresholds. Nature, 2015, 520, 69-72.	13.7	713
146	An Atomically Layered InSe Avalanche Photodetector. Nano Letters, 2015, 15, 3048-3055.	4.5	253
147	Low Power Consumption Complementary Inverters with n-MoS₂ and p-WSe₂ Dichalcogenide Nanosheets on Glass for Logic and Light-Emitting Diode Circuits. ACS Applied Materials & Interfaces, 2015, 7, 22333-22340.	4.0	113

#	Article	IF	Citations
148	Acoustic phonon assisted free-carrier optical absorption in an n-type monolayer MoS2 and other transition-metal dichalcogenides. Journal of Applied Physics, 2015, 118, 044308.	1.1	10
149	Nonvolatile Ferroelectric Memory Circuit Using Black Phosphorus Nanosheet-Based Field-Effect Transistors with P(VDF-TrFE) Polymer. ACS Nano, 2015, 9, 10394-10401.	7.3	130
150	Anisotropic Spin Transport and Strong Visible-Light Absorbance in Few-Layer SnSe and GeSe. Nano Letters, 2015, 15, 6926-6931.	4.5	290
151	Designing the shape evolution of SnSe₂nanosheets and their optoelectronic properties. Nanoscale, 2015, 7, 17375-17380.	2.8	121
152	Carrier Injection and Scattering in Atomically Thin Chalcogenides. Journal of the Physical Society of Japan, 2015, 84, 121011.	0.7	7
153	What We Talk About When We Talk About Light. ACS Central Science, 2015, 1, 354-363.	5.3	14
154	Recent Advances in Two-Dimensional Materials beyond Graphene. ACS Nano, 2015, 9, 11509-11539.	7.3	2,069
155	Control of Light-Matter Interaction in 2D Atomic Crystals Using Microcavities. IEEE Journal of Quantum Electronics, 2015, 51, 1-8.	1.0	5
156	Monolayers of WxMo1â^'xS2 alloy heterostructure with in-plane composition variations. Applied Physics Letters, 2015, 106, .	1.5	99
157	Visualizing nanoscale excitonic relaxation properties of disordered edges and grain boundaries in monolayer molybdenum disulfide. Nature Communications, 2015, 6, 7993.	5.8	204
158	Monolayer excitonic laser. Nature Photonics, 2015, 9, 733-737.	15.6	492
159	Two-dimensional transition metal dichalcogenides as atomically thin semiconductors: opportunities and challenges. Chemical Society Reviews, 2015, 44, 8859-8876.	18.7	917
160	Halide-assisted atmospheric pressure growth of large WSe2 and WS2 monolayer crystals. Applied Materials Today, 2015, 1, 60-66.	2.3	372
161	An Anomalous Formation Pathway for Dislocation-Sulfur Vacancy Complexes in Polycrystalline Monolayer MoS₂. Nano Letters, 2015, 15, 6855-6861.	4.5	90
162	Excitonâ€“polaritons in van der Waals heterostructures embedded in tunable microcavities. Nature Communications, 2015, 6, 8579.	5.8	377
163	Black Phosphorus: Narrow Gap, Wide Applications. Journal of Physical Chemistry Letters, 2015, 6, 4280-4291.	2.1	631
164	In-Plane Anisotropy in Mono- and Few-Layer ReS₂ Probed by Raman Spectroscopy and Scanning Transmission Electron Microscopy. Nano Letters, 2015, 15, 5667-5672.	4.5	406
165	3D Band Diagram and Photoexcitation of 2Dâ€“3D Semiconductor Heterojunctions. Nano Letters, 2015, 15, 5919-5925.	4.5	33

#	Article	IF	Citations
166	High-Mobility Holes in Dual-Gated WSe₂ Field-Effect Transistors. ACS Nano, 2015, 9, 10402-10410.	7.3	232
167	Bandgap Engineering of Phosphorene by Laser Oxidation toward Functional 2D Materials. ACS Nano, 2015, 9, 10411-10421.	7.3	126
168	Epitaxial Growth of Hetero-Nanostructures Based on Ultrathin Two-Dimensional Nanosheets. Journal of the American Chemical Society, 2015, 137, 12162-12174.	6.6	218
169	Wafer-scale arrayed p-n junctions based on few-layer epitaxial GaTe. Nano Research, 2015, 8, 3332-3341.	5.8	41
170	Flexible transition metal dichalcogenide nanosheets for band-selective photodetection. Nature Communications, 2015, 6, 8063.	5.8	192
171	Ambipolar Light-Emitting Transistors on Chemical Vapor Deposited Monolayer MoS₂. Nano Letters, 2015, 15, 8289-8294.	4.5	67
172	Ultrafast response of monolayer molybdenum disulfide photodetectors. Nature Communications, 2015, 6, 8831.	5.8	147
173	Crystalline and Amorphous Chalcogenides, High-Tech Materials with Structural Disorder and Many Important Applications. NATO Science for Peace and Security Series C: Environmental Security, 2015, , 151-238.	0.1	9
174	2D crystals of transition metal dichalcogenide and their iontronic functionalities. 2D Materials, 2015, 2, 044004.	2.0	28
175	High-performance a MoS2 nanosheet-based nonvolatile memory transistor with a ferroelectric polymer and graphene source-drain electrode. Journal of the Korean Physical Society, 2015, 67, 1499-1503.	0.3	25
176	Exciton band structure in layered MoSe₂: from a monolayer to the bulk limit. Nanoscale, 2015, 7, 20769-20775.	2.8	163
177	Surface Recombination Limited Lifetimes of Photoexcited Carriers in Few-Layer Transition Metal Dichalcogenide MoS₂. Nano Letters, 2015, 15, 8204-8210.	4.5	153
178	Band Engineering for Novel Twoâ€Ðimensional Atomic Layers. Small, 2015, 11, 1868-1884.	5.2	96
179	Electronic structures and theoretical modelling of two-dimensional group-VIB transition metal dichalcogenides. Chemical Society Reviews, 2015, 44, 2643-2663.	18.7	528
180	Physical and chemical tuning of two-dimensional transition metal dichalcogenides. Chemical Society Reviews, 2015, 44, 2664-2680.	18.7	694
181	Two-dimensional transition metal dichalcogenide nanosheet-based composites. Chemical Society Reviews, 2015, 44, 2713-2731.	18.7	1,405
182	Science and technology roadmap for graphene, related two-dimensional crystals, and hybrid systems. Nanoscale, 2015, 7, 4598-4810.	2.8	2,452
183	Photonic Structure-Integrated Two-Dimensional Material Optoelectronics. Electronics (Switzerland), 2016, 5, 93.	1.8	19

#	Article	IF	Citations
184	Graphene against Other Twoâ€Dimensional Materials: A Comparative Study on the Basis of Electronic Applications. , 2016, , .		4
185	Optoelectronic Devices Based on Atomically Thin Transition Metal Dichalcogenides. Applied Sciences (Switzerland), 2016, 6, 78.	1.3	96
186	Two-Dimensional Semiconductor Optoelectronics Based on van der Waals Heterostructures. Nanomaterials, 2016, 6, 193.	1.9	107
187	Neutral and charged excitons in tungsten dichalcogenides monolayer. International Journal of Nanotechnology, 2016, 13, 619.	0.1	0
188	Direct observation of strong light-exciton coupling in thin WS_2 flakes. Optics Express, 2016, 24, 7151.	1.7	43
189	Layer Control of WSe₂ via Selective Surface Layer Oxidation. ACS Nano, 2016, 10, 6836-6842.	7.3	77
190	Broad Detection Range Rhenium Diselenide Photodetector Enhanced by (3â€Aminopropyl)Triethoxysilane and Triphenylphosphine Treatment. Advanced Materials, 2016, 28, 6711-6718.	11.1	72
191	Large-scale synthesis of WSe2 atomic layers on SiO2/Si. Modern Physics Letters B, 2016, 30, 1650267.	1.0	3
192	A Floating Sheet for Efficient Photocatalytic Water Splitting. Advanced Energy Materials, 2016, 6, 1600510.	10.2	74
193	Nonvolatile Charge Injection Memory Based on Black Phosphorous 2D Nanosheets for Charge Trapping and Active Channel Layers. Advanced Functional Materials, 2016, 26, 5701-5707.	7.8	49
194	Site Selective Doping of Ultrathin Metal Dichalcogenides by Laserâ€Assisted Reaction. Advanced Materials, 2016, 28, 341-346.	11.1	101
195	Enhanced Photoresponse from Phosphoreneâ€“Phosphoreneâ€Suboxide Junction Fashioned by Focused Laser Micromachining. Advanced Materials, 2016, 28, 4090-4096.	11.1	38
196	Recent Advances in Controlling Syntheses and Energy Related Applications of MX₂ and MX₂/Graphene Heterostructures. Advanced Energy Materials, 2016, 6, 1600459.	10.2	43
197	Mo_{1â€“x}W_xSe₂-Based Schottky Junction Photovoltaic Cells. ACS Applied Materials & Interfaces, 2016, 8, 33811-33820.	4.0	24
198	Tunable photoresponse in graphene photodetector with novel split local back-gates based on heavily doped silicon. , 2016, , .		0
199	Hybrid quantum dot-tin disulfide field-effect transistors with improved photocurrent and spectral responsivity. Applied Physics Letters, 2016, 108, .	1.5	23
200	Plasma functionalization for cyclic transition between neutral and charged excitons in monolayer MoS2. Scientific Reports, 2016, 6, 21405.	1.6	48
201	Distance-dependent energy transfer between CdSe/CdS quantum dots and a two-dimensional semiconductor. Applied Physics Letters, 2016, 108, .	1.5	54

#	Article	IF	Citations
202	Laser energy dependence of valley polarization in transition-metal dichalcogenides. Physical Review B, 2016, 94, .	1.1	18
203	Demonstration of electric double layer p-i-n junction in WSe<inf>2</inf>. , 2016, , .		2
204	High circular polarization in electroluminescence from MoSe2. Applied Physics Letters, 2016, 108, .	1.5	38
205	Hidden quantum mirage by negative refraction in semiconductor P-N junctions. Physical Review B, 2016, 94, .	1.1	6
206	Photodetection in pâ€“n junctions formed by electrolyte-gated transistors of two-dimensional crystals. Applied Physics Letters, 2016, 109, .	1.5	15
207	Elastic properties of suspended multilayer WSe2. Applied Physics Letters, 2016, 108, .	1.5	121
208	Improved photoswitching response times of MoS2 field-effect transistors by stacking p-type copper phthalocyanine layer. Applied Physics Letters, 2016, 109, .	1.5	29
209	Integration of 2D materials on a silicon photonics platform for optoelectronics applications. Nanophotonics, 2016, 6, 1205-1218.	2.9	87
210	P-doping and efficient carrier injection induced by graphene oxide for high performing WSe2 rectification devices. Applied Physics Letters, 2016, 108, .	1.5	8
211	Charge neutral MoS2 field effect transistors through oxygen plasma treatment. Journal of Applied Physics, 2016, 120, .	1.1	20
212	Defect-Tolerant Monolayer Transition Metal Dichalcogenides. Nano Letters, 2016, 16, 2234-2239.	4.5	111
213	Controlled Exfoliation of MoS₂ Crystals into Trilayer Nanosheets. Journal of the American Chemical Society, 2016, 138, 5143-5149.	6.6	207
214	Photonics and optoelectronics of 2D semiconductor transition metal dichalcogenides. Nature Photonics, 2016, 10, 216-226.	15.6	2,779
215	Green's function modeling of response of two-dimensional materials to point probes for scanning probe microscopy. Physics Letters, Section A: General, Atomic and Solid State Physics, 2016, 380, 1750-1756.	0.9	5
216	Laser Direct Writing Process for Making Electrodes and High-k Solâ€“Gel ZrO₂ for Boosting Performances of MoS₂ Transistors. ACS Applied Materials & Interfaces, 2016, 8, 9314-9318.	4.0	21
217	Photo-Electrical Properties of Trilayer MoSe₂ Nanoflakes. Nano, 2016, 11, 1650082.	0.5	19
218	Quantum mechanical modeling the emission pattern and polarization of nanoscale light emitting diodes. Nanoscale, 2016, 8, 13168-13173.	2.8	12
219	T-ZrS nanoribbons: structure and electronic properties. Philosophical Magazine, 2016, 96, 2074-2087.	0.7	8

#	Article	IF	Citations
220	Valley-Coherent Hot Carriers and Thermal Relaxation in Monolayer Transition Metal Dichalcogenides. Journal of Physical Chemistry Letters, 2016, 7, 2032-2038.	2.1	9
221	Ultrafast Coulomb-Induced Intervalley Coupling in Atomically Thin WS₂. Nano Letters, 2016, 16, 2945-2950.	4.5	139
222	Lateral black phosphorene Pâ€“N junctions formed via chemical doping for high performance near-infrared photodetector. Nano Energy, 2016, 25, 34-41.	8.2	162
223	Van der Waals stacked 2D layered materials for optoelectronics. 2D Materials, 2016, 3, 022001.	2.0	213
224	Simultaneous Hosting of Positive and Negative Trions and the Enhanced Direct Band Emission in MoSe₂/MoS₂ Heterostacked Multilayers. ACS Nano, 2016, 10, 6211-6219.	7.3	62
225	Single Defect Light-Emitting Diode in a van der Waals Heterostructure. Nano Letters, 2016, 16, 3944-3948.	4.5	115
226	Electrical generation and control of the valley carriers in a monolayer transition metal dichalcogenide. Nature Nanotechnology, 2016, 11, 598-602.	15.6	259
227	Optoelectric Properties of Gate-Tunable MoS₂/WSe₂Heterojunction. IEEE Nanotechnology Magazine, 2016, 15, 499-505.	1.1	16
228	A microscopic study investigating the structure of SnSe surfaces. Surface Science, 2016, 651, 5-9.	0.8	33
229	Multilayer ReS₂ lateral pâ€“n homojunction for photoemission and photodetection. Applied Physics Express, 2016, 9, 055201.	1.1	19
230	Percolative switching in transition metal dichalcogenide field-effect transistors at room temperature. Nanotechnology, 2016, 27, 125706.	1.3	23
231	Controlling nucleation of monolayer WSe 2 during metal-organic chemical vapor deposition growth. 2D Materials, 2016, 3, 025015.	2.0	42
232	Photochemical Reaction in Monolayer MoS₂ via Correlated Photoluminescence, Raman Spectroscopy, and Atomic Force Microscopy. ACS Nano, 2016, 10, 5230-5236.	7.3	101
233	Optoelectronic devices based on two-dimensional transition metal dichalcogenides. Nano Research, 2016, 9, 1543-1560.	5.8	186
234	Black Phosphorus-Based Nanodevices. Semiconductors and Semimetals, 2016, 95, 279-303.	0.4	5
235	Observation of Switchable Photoresponse of a Monolayer WSe₂â€“MoS₂ Lateral Heterostructure via Photocurrent Spectral Atomic Force Microscopic Imaging. Nano Letters, 2016, 16, 3571-3577.	4.5	86
236	Pressure-induced Kâ€“Î› crossing in monolayer WSe₂. Nanoscale, 2016, 8, 10843-10848.	2.8	35
237	Valley Zeeman Splitting and Valley Polarization of Neutral and Charged Excitons in Monolayer MoTe₂ at High Magnetic Fields. Nano Letters, 2016, 16, 3624-3629.	4.5	102

#	Article	IF	Citations
238	Luminescent transition metal dichalcogenide nanosheets through one-step liquid phase exfoliation. 2D Materials, 2016, 3, 035014.	2.0	42
239	Hybrid Bilayer WSe₂â€“CH₃NH₃PbI₃ Organolead Halide Perovskite as a Highâ€Performance Photodetector. Angewandte Chemie - International Edition, 2016, 55, 11945-11949.	7.2	91
240	Significant Exciton Brightening in Monolayer Tungsten Disulfides via Fluorination: nâ€Type Gas Sensing Semiconductors. Advanced Functional Materials, 2016, 26, 7551-7559.	7.8	33
241	Photodetectors based on two dimensional materials. Journal of Semiconductors, 2016, 37, 091001.	2.0	29
242	Chemical doping modulation of nonlinear photoluminescence properties in monolayer MoS₂. Applied Physics Express, 2016, 9, 055202.	1.1	16
243	Visualization of Defect-Induced Excitonic Properties of the Edges and Grain Boundaries in Synthesized Monolayer Molybdenum Disulfide. Journal of Physical Chemistry C, 2016, 120, 24080-24087.	1.5	20
244	NaSn₂As₂: An Exfoliatable Layered van der Waals Zintl Phase. ACS Nano, 2016, 10, 9500-9508.	7.3	39
245	Vertically oriented few-layered HfS ₂ nanosheets: growth mechanism and optical properties. 2D Materials, 2016, 3, 035024.	2.0	88
246	Enhanced Light Emission from Monolayer Semiconductors by Forming Heterostructures with ZnO Thin Films. ACS Applied Materials & Interfaces, 2016, 8, 28809-28815.	4.0	47
247	Reconfigurable van der Waals Heterostructured Devices with Metalâ€“Insulator Transition. Nano Letters, 2016, 16, 6746-6754.	4.5	35
248	Atomically thin lateral pâ€“n junction photodetector with large effective detection area. 2D Materials, 2016, 3, 041001.	2.0	78
249	Luminescence of 2D TMDC. Springer Series in Materials Science, 2016, , 295-320.	0.4	0
250	Nano-optical imaging of<mml:math xmlns:mml="http://www.w3.org/1998/Math/MathML"><mml:mrow><mml:mi>WS</mml:mi><mml:msub><mml:mi mathvariant="normal">e</mml:mi><mml:mn>2</mml:mn></mml:msub></mml:mrow></mml:math>waveguide modes revealing light-exciton interactions. Physical Review B, 2016, 94, .	1.1	82
251	Piezophototronic Effect in Singleâ€Atomicâ€Layer MoS₂ for Strainâ€Gated Flexible Optoelectronics. Advanced Materials, 2016, 28, 8463-8468.	11.1	187
252	Performance Upper Limit of subâ€10 nm Monolayer MoS₂ Transistors. Advanced Electronic Materials, 2016, 2, 1600191.	2.6	97
253	An AlAs/germanene heterostructure with tunable electronic and optical properties via external electric field and strain. Journal of Materials Chemistry C, 2016, 4, 8171-8178.	2.7	81
254	Tunable photoresponse with small drain voltage in few-layer grapheneâ€“WSe2 heterostructures. Physics Letters, Section A: General, Atomic and Solid State Physics, 2016, 380, 2575-2579.	0.9	3
255	Electronic Structure and Luminescence of Quasi-Freestanding MoS₂ Nanopatches on Au(111). Nano Letters, 2016, 16, 5163-5168.	4.5	61

#	Article	IF	Citations
256	Review of photo response in semiconductor transition metal dichalcogenides based photosensitive devices. Optical Materials Express, 2016, 6, 2313.	1.6	44
257	Progress in pulsed laser deposited two-dimensional layered materials for device applications. Journal of Materials Chemistry C, 2016, 4, 8859-8878.	2.7	124
258	Valley Polarization by Spin Injection in a Light-Emitting van der Waals Heterojunction. Nano Letters, 2016, 16, 5792-5797.	4.5	117
259	Synthesis, properties and applications of 2D layered M^{III}X^{VI}(M = Ga, In; X = S,) Tj ETQq1 1 0.784314 rgBT /Ov	2.8	142
260	Ultrafast Self-Limited Growth of Strictly Monolayer WSe₂Crystals. Small, 2016, 12, 5741-5749.	5.2	57
261	Magnetic-Field-Induced Rotation of Polarized Light Emission from Monolayer<mml:math xmlns:mml="http://www.w3.org/1998/Math/MathML" display="inline"><mml:msub><mml:mi>WS</mml:mi><mml:mn>2</mml:mn></mml:msub></mml:math>. Physical Review Letters, 2016, 117, 077402.	2.9	76
262	Strong Quantum Confinement Effect in the Optical Properties of Ultrathin Î±â€In₂Se₃. Advanced Optical Materials, 2016, 4, 1939-1943.	3.6	89
263	High-Performance MoS₂/CuO Nanosheet-on-One-Dimensional Heterojunction Photodetectors. ACS Applied Materials & Interfaces, 2016, 8, 33955-33962.	4.0	64
264	Surface-enhanced Raman scattering for 2-D WSe_2 hybridized with functionalized gold nanoparticles. Optics Express, 2016, 24, 27546.	1.7	10
265	Focused helium-ion beam irradiation effects on electrical transport properties of few-layer WSe2: enabling nanoscale direct write homo-junctions. Scientific Reports, 2016, 6, 27276.	1.6	99
266	Transitionâ€Metal Substitution Doping in Synthetic Atomically Thin Semiconductors. Advanced Materials, 2016, 28, 9735-9743.	11.1	208
267	Surface Analysis of WSe₂ Crystals: Spatial and Electronic Variability. ACS Applied Materials & Interfaces, 2016, 8, 26400-26406.	4.0	73
268	Single layer PbI2: hydrogenation-driven reconstructions. RSC Advances, 2016, 6, 89708-89714.	1.7	10
269	Surface Charge Transfer Doping of Lowâ€Dimensional Nanostructures toward Highâ€Performance Nanodevices. Advanced Materials, 2016, 28, 10409-10442.	11.1	144
270	Hybrid Bilayer WSe₂â€“CH₃NH₃PbI₃ Organolead Halide Perovskite as a Highâ€Performance Photodetector. Angewandte Chemie, 2016, 128, 12124-12128.	1.6	51
271	Controllable growth of layered selenide and telluride heterostructures and superlattices using molecular beam epitaxy. Journal of Materials Research, 2016, 31, 900-910.	1.2	85
272	Layer-modulated, wafer scale and continuous ultra-thin WS₂ films grown by RF sputtering via post-deposition annealing. Journal of Materials Chemistry C, 2016, 4, 7846-7852.	2.7	26
273	Theoretical Study of Transition Metal Dichalcogenides. , 2016, , 157-178.		1

#	Article	IF	Citations
274	Tunable Electronic Transport Properties of 2D Layered Double Hydroxide Crystalline Microsheets with Varied Chemical Compositions. Small, 2016, 12, 4471-4476.	5.2	27
275	Spin- and valley-polarized transport across line defects in monolayer<mml:math xmlns:mml="http://www.w3.org/1998/Math/MathML"><mml:msub><mml:mi>MoS</mml:mi><mml:mn>2</mml:mn></mml:msub></mml:math> Physical Review B, 2016, 93, .	1.1	53
276	Optical properties of GaS-Ca(OH)<mml:math xmlns:mml="http://www.w3.org/1998/Math/MathML"><mml:msub><mml:mrow /><mml:mn>2</mml:mn></mml:msub></mml:math>bilayer heterostructure. Physical Review B, 2016, 93, .	1.1	18
277	Probing the uniaxial strains in<mml:math xmlns:mml="http://www.w3.org/1998/Math/MathML"><mml:msub><mml:mtext>MoS</mml:mtext><mml:mn>2</mml:mn></mml:msub></mml:math> polarized Raman spectroscopy: A first-principles study. Physical Review B, 2016, 93, .	1.1	36
278	Edge states in dichalcogenide nanoribbons and triangular quantum dots. Physical Review B, 2016, 93, .	1.1	29
279	Bilayer<mml:math xmlns:mml="http://www.w3.org/1998/Math/MathML"><mml:msub><mml:mi>SnS</mml:mi><mml:mn>2</mml:mn></mml:msub></mml:math> Stark shift and electric-field-induced dissociation of excitons in monolayer<mml:math xmlns:mml="http://www.w3.org/1998/Math/MathML"><mml:msub><mml:mi mathvariant="bold">MoS</mml:mi><mml:mn mathvariant="bold">2</mml:mn></mml:msub></mml:math>and<mml:math xmlns:mml="http://www.w3.org/1998/Math/MathML"><mml:mrow><mml:mi>h</mml:mi><mml:mrow><mml:mi mathvariant="bold">BN</mml:mi><mml:mo>/</mml:mo><mml:msub><mml:mi mathvariant="bold">MoS<	1.1	51
281	Van der Waals heterostructures and devices. Nature Reviews Materials, 2016, 1, .	23.3	1,897
282	Valleytronics in 2D materials. Nature Reviews Materials, 2016, 1, .	23.3	1,712
283	Atomically thin quantum light-emitting diodes. Nature Communications, 2016, 7, 12978.	5.8	242
284	Transition metal dichalcogenide heterojunction PN diode toward ultimate photovoltaic benefits. 2D Materials, 2016, 3, 045011.	2.0	45
285	High-performance black phosphorus top-gate ferroelectric transistor for nonvolatile memory applications. Journal of the Korean Physical Society, 2016, 69, 1347-1351.	0.3	6
286	Two-dimensional GaSe/MoSe ₂ misfit bilayer heterojunctions by van der Waals epitaxy. Science Advances, 2016, 2, e1501882.	4.7	239
287	Giant photoluminescence enhancement in tungsten-diselenideâ€“gold plasmonic hybrid structures. Nature Communications, 2016, 7, 11283.	5.8	244
288	Photonics and optoelectronics of two-dimensional materials beyond graphene. Nanotechnology, 2016, 27, 462001.	1.3	259
289	Recent progress of photodetectors based on MX2/graphene van der Waals heterostructures. , 2016, , .		1
290	Sensitivity Enhancement of Transition Metal Dichalcogenides/Silicon Nanostructure-based Surface Plasmon Resonance Biosensor. Scientific Reports, 2016, 6, 28190.	1.6	299
291	Excitonic properties of semiconducting monolayer and bilayer <mml:math xmlns:mml="http://www.w3.org/1998/Math/MathML"><mml:mrow><mml:mi>MoT</mml:mi><mml:msub><mml:mi mathvariant="normal">e</mml:mi><mml:mn>2</mml:mn></mml:msub></mml:mrow></mml:math>. Physical Review B, 2016, 94, .	1.1	60

#	Article	IF	Citations
292	Ab initio study of electronic excitations and the dielectric function in molybdenum disulfide monolayer. Physical Review B, 2016, 94, .	1.1	14
293	Towards functional assembly of 3D and 2D nanomaterials. Proceedings of SPIE, 2016, , .	0.8	0
294	Engineering the optoelectronic properties of MoS₂ photodetectors through reversible noncovalent functionalization. Chemical Communications, 2016, 52, 14365-14368.	2.2	37
295	Piezotronics and piezo-phototronics for adaptive electronics and optoelectronics. Nature Reviews Materials, 2016, 1, .	23.3	438
296	Influence of lattice vibrations on luminescence and transfer of excitons in WS₂monolayer semiconductors. Journal Physics D: Applied Physics, 2016, 49, 465101.	1.3	4
297	Two-dimensional hexagonal semiconductors beyond graphene. Advances in Natural Sciences: Nanoscience and Nanotechnology, 2016, 7, 043001.	0.7	19
298	Modulating Electronic Properties of Monolayer MoS₂ via Electron-Withdrawing Functional Groups of Graphene Oxide. ACS Nano, 2016, 10, 10446-10453.	7.3	41
299	Synthesis of Large-Area WS2 monolayers with Exceptional Photoluminescence. Scientific Reports, 2016, 6, 19159.	1.6	153
300	Engineering Bandgaps of Monolayer MoS₂ and WS₂ on Fluoropolymer Substrates by Electrostatically Tuned Manyâ€Body Effects. Advanced Materials, 2016, 28, 6457-6464.	11.1	116
301	pâ€Type MoS₂ and nâ€Type ZnO Diode and Its Performance Enhancement by the Piezophototronic Effect. Advanced Materials, 2016, 28, 3391-3398.	11.1	143
302	Realization of Roomâ€Temperature Phononâ€Limited Carrier Transport in Monolayer MoS₂ by Dielectric and Carrier Screening. Advanced Materials, 2016, 28, 547-552.	11.1	218
303	Nanostructured Photodetectors: From Ultraviolet to Terahertz. Advanced Materials, 2016, 28, 403-433.	11.1	492
304	Coherent Coupling of WS₂ Monolayers with Metallic Photonic Nanostructures at Room Temperature. Nano Letters, 2016, 16, 4368-4374.	4.5	256
305	First principles kinetic Monte Carlo study on the growth patterns of WSe ₂ monolayer. 2D Materials, 2016, 3, 025029.	2.0	59
306	Bipolar Junction Transistors in Two-Dimensional WSe₂ with Large Current and Photocurrent Gains. Nano Letters, 2016, 16, 4355-4360.	4.5	50
307	Electrically pumped single-defect light emitters in WSe ₂. 2D Materials, 2016, 3, 025038.	2.0	66
308	Air-Stable n-Doping of WSe₂ by Anion Vacancy Formation with Mild Plasma Treatment. ACS Nano, 2016, 10, 6853-6860.	7.3	202
309	Bulk Fabrication of WS₂ Nanoplates: Investigation on the Morphology Evolution and Electrochemical Performance. ACS Applied Materials & Interfaces, 2016, 8, 16876-16884.	4.0	25

#	Article	IF	Citations
310	Revealing Defect-State Photoluminescence in Monolayer WS₂ by Cryogenic Laser Processing. ACS Nano, 2016, 10, 5847-5855.	7.3	91
311	Electrostatically tunable lateral MoTe₂pâ€“n junction for use in high-performance optoelectronics. Nanoscale, 2016, 8, 13245-13250.	2.8	49
312	Layer Engineering of 2D Semiconductor Junctions. Advanced Materials, 2016, 28, 5126-5132.	11.1	63
313	Intercalation in two-dimensional transition metal chalcogenides. Inorganic Chemistry Frontiers, 2016, 3, 452-463.	3.0	181
314	Impurity-induced ferromagnetism and metallicity of WS2 monolayer. Ceramics International, 2016, 42, 2364-2369.	2.3	25
315	Biexciton Formation in Bilayer Tungsten Disulfide. ACS Nano, 2016, 10, 2176-2183.	7.3	57
316	Transport Properties of a MoS₂/WSe₂ Heterojunction Transistor and Its Potential for Application. Nano Letters, 2016, 16, 1359-1366.	4.5	430
317	Synthesis of WS_{2x}Se_{2â€“2x} Alloy Nanosheets with Composition-Tunable Electronic Properties. Nano Letters, 2016, 16, 264-269.	4.5	308
318	Electroluminescence Dynamics across Grain Boundary Regions of Monolayer Tungsten Disulfide. ACS Nano, 2016, 10, 1093-1100.	7.3	31
319	Heterostructures based on two-dimensional layered materials and their potential applications. Materials Today, 2016, 19, 322-335.	8.3	469
320	Electronic Structure, Surface Doping, and Optical Response in Epitaxial WSe₂ Thin Films. Nano Letters, 2016, 16, 2485-2491.	4.5	147
321	A polarizing situation: Taking an in-plane perspective for next-generation near-field studies. Frontiers of Physics, 2016, 11, 1.	2.4	8
322	Spatially resolved optical absorption spectroscopy of single- and few-layer MoS₂by hyperspectral imaging. Nanotechnology, 2016, 27, 115705.	1.3	145
323	Metalâ€“Insulatorâ€“Semiconductor Diode Consisting of Two-Dimensional Nanomaterials. Nano Letters, 2016, 16, 1858-1862.	4.5	74
324	Broadband Photovoltaic Detectors Based on an Atomically Thin Heterostructure. Nano Letters, 2016, 16, 2254-2259.	4.5	322
325	Solid state carbon nanotube device for controllable trion electroluminescence emission. Nanoscale, 2016, 8, 6761-6769.	2.8	20
326	Nanoscale Control of Rewriteable Doping Patterns in Pristine Graphene/Boron Nitride Heterostructures. Nano Letters, 2016, 16, 1620-1625.	4.5	60
327	Electrically Tunable Valley-Light Emitting Diode (vLED) Based on CVD-Grown Monolayer WS₂. Nano Letters, 2016, 16, 1560-1567.	4.5	175

#	Article	IF	Citations
328	Solution-processable exfoliation and suspension of atomically thin WSe2. Journal of Colloid and Interface Science, 2016, 468, 247-252.	5.0	28
329	Surface functionalization of two-dimensional metal chalcogenides by Lewis acidâ€“base chemistry. Nature Nanotechnology, 2016, 11, 465-471.	15.6	197
330	Interactions between lasers and two-dimensional transition metal dichalcogenides. Chemical Society Reviews, 2016, 45, 2494-2515.	18.7	61
331	Gas adsorption on MoS₂/WS₂ in-plane heterojunctions and the Iâ€“V response: a first principles study. RSC Advances, 2016, 6, 17494-17503.	1.7	56
332	Stable electrical performance observed in large-scale monolayer WSe_{2(1â^'x)}S_{2x}with tunable band gap. Nanotechnology, 2016, 27, 13LT01.	1.3	33
333	Thickness-Dependent Thermal Conductivity of Suspended Two-Dimensional Single-Crystal In₂Se₃Layers Grown by Chemical Vapor Deposition. Journal of Physical Chemistry C, 2016, 120, 4753-4758.	1.5	56
334	Near-Infrared Photodetector Based on MoS₂/Black Phosphorus Heterojunction. ACS Photonics, 2016, 3, 692-699.	3.2	446
335	Photoinduced doping and photoluminescence signature in an exfoliated WS₂ monolayer semiconductor. RSC Advances, 2016, 6, 27677-27681.	1.7	26
336	Broadband Absorption Enhancement in Solar Cells with an Atomically Thin Active Layer. ACS Photonics, 2016, 3, 571-577.	3.2	62
337	Field-effect transistors based on wafer-scale, highly uniform few-layer p-type WSe₂. Nanoscale, 2016, 8, 2268-2276.	2.8	58
338	Modulating Optoelectronic Properties of Two-Dimensional Transition Metal Dichalcogenide Semiconductors by Photoinduced Charge Transfer. ACS Nano, 2016, 10, 1671-1680.	7.3	154
339	Photo-Induced Bandgap Renormalization Governs the Ultrafast Response of Single-Layer MoS₂. ACS Nano, 2016, 10, 1182-1188.	7.3	272
340	Strain engineering of electronic properties of transition metal dichalcogenide monolayers. Solid State Communications, 2016, 227, 33-39.	0.9	48
341	Does p-type ohmic contact exist in WSe₂â€“metal interfaces?. Nanoscale, 2016, 8, 1179-1191.	2.8	166
342	Picosecond photoresponse in van der Waals heterostructures. Nature Nanotechnology, 2016, 11, 42-46.	15.6	493
343	Rapid preparation of single-layer transition metal dichalcogenide nanosheets via ultrasonication enhanced lithium intercalation. Chemical Communications, 2016, 52, 529-532.	2.2	102
344	Elastic and Inelastic Lightâ€“Matter Interactions in 2D Materials. IEEE Journal of Selected Topics in Quantum Electronics, 2017, 23, 206-213.	1.9	6
345	Substrate induced changes in atomically thin 2-dimensional semiconductors: Fundamentals, engineering, and applications. Applied Physics Reviews, 2017, 4, 011301.	5.5	97

#	Article	IF	Citations
346	Realization of vertical and lateral van der Waals heterojunctions using two-dimensional layered organic semiconductors. Nano Research, 2017, 10, 1336-1344.	5.8	30
347	Strong Adlayerâ€“Substrate Interactions â€œBreakâ€•the Patching Growth of h-BN onto Graphene on Re(0001). ACS Nano, 2017, 11, 1807-1815.	7.3	27
348	Significantly enhanced optoelectronic performance of tungsten diselenide phototransistor via surface functionalization. Nano Research, 2017, 10, 1282-1291.	5.8	30
349	Study of chemical vapour transport (CVT) grown WSe1.93 single crystals. Materials Science in Semiconductor Processing, 2017, 61, 11-16.	1.9	7
350	Microsteganography on WS₂ Monolayers Tailored by Direct Laser Painting. ACS Nano, 2017, 11, 713-720.	7.3	43
351	A comparative study of hydrogen evolution reaction on pseudo-monolayer WS₂ and PtS₂: insights based on the density functional theory. Catalysis Science and Technology, 2017, 7, 687-692.	2.1	51
352	Gate tunable photovoltaic effect in MoS₂ vertical pâ€“n homostructures. Journal of Materials Chemistry C, 2017, 5, 854-861.	2.7	50
353	Electronic and Optoelectronic Devices based on Twoâ€Dimensional Materials: From Fabrication to Application. Advanced Electronic Materials, 2017, 3, 1600364.	2.6	123
354	Exciton Emission Intensity Modulation of Monolayer MoS2 via Au Plasmon Coupling. Scientific Reports, 2017, 7, 41175.	1.6	50
355	Strong coupling between Tamm plasmon polariton and two dimensional semiconductor excitons. Applied Physics Letters, 2017, 110, .	1.5	51
356	Dark excitons and the elusive valley polarization in transition metal dichalcogenides. 2D Materials, 2017, 4, 025016.	2.0	71
357	Room-temperature electrically driven phase transition of two-dimensional 1T-TaS₂layers. Nanoscale, 2017, 9, 2436-2441.	2.8	19
358	Theoretical study on dynamic acoustic modulation of free carriers, excitons, and trions in 2D MoS₂ flake. Journal Physics D: Applied Physics, 2017, 50, 114005.	1.3	16
359	Grapheneâ€Assisted Antioxidation of Tungsten Disulfide Monolayers: Substrate and Electricâ€Field Effect. Advanced Materials, 2017, 29, 1603898.	11.1	47
360	Arrayed Van Der Waals Broadband Detectors for Dualâ€Band Detection. Advanced Materials, 2017, 29, 1604439.	11.1	218
361	Franckeite as a naturally occurring van der Waals heterostructure. Nature Communications, 2017, 8, 14409.	5.8	103
362	Microcavity-Controlled Chirality-Sorted Carbon Nanotube Film Infrared Light Emitters. ACS Photonics, 2017, 4, 435-442.	3.2	14
363	Enhanced optical activity of atomically thin MoSe 2 proximal to nanoscale plasmonic slot-waveguides. 2D Materials, 2017, 4, 021011.	2.0	13

#	Article	IF	Citations
364	Interfacial Defect Engineering on Electronic States of Two-Dimensional AlN/MoS₂ Heterostructure. Journal of Physical Chemistry C, 2017, 121, 6605-6613.	1.5	31
365	Direct Observation of 2D Electrostatics and Ohmic Contacts in Template-Grown Graphene/WS₂ Heterostructures. ACS Nano, 2017, 11, 2785-2793.	7.3	74
366	Recent progress in van der Waals heterojunctions. Nanoscale, 2017, 9, 4324-4365.	2.8	155
367	Quantitative Agreement between Electron-Optical Phase Images of<mml:math xmlns:mml="http://www.w3.org/1998/Math/MathML" display="inline"><mml:mrow><mml:msub><mml:mrow><mml:mi>WSe</mml:mi></mml:mrow><mml:mrow><mml:mn>2</mml:mn> Simulations Based on Electrostatic Potentials that Include Bonding Effects. Physical Review Letters, 2017, 118, 086101.	2.9	15
368	Control of interlayer valley excitons in atomically-thin MoSe2-WSe2heterostructures. , 2017, , .		0
369	Determination of band offsets, hybridization, and exciton binding in 2D semiconductor heterostructures. Science Advances, 2017, 3, e1601832.	4.7	293
370	Carrier transfer across a 2D-3D semiconductor heterointerface: The role of momentum mismatch. Physical Review B, 2017, 95, .	1.1	14
371	<mml:math xmlns:mml="http://www.w3.org/1998/Math/MathML"><mml:mi>h</mml:mi><mml:mtext>-AlN-</mml:mtext><mml:mtext>Mg</mml:mtext> van der Waals bilayer heterostructure: Tuning the excitonic characteristics. Physical Review B, 2017, 95, .	1.1	20
372	Electric-field tunable electronic structure in WSe 2 /arsenene van der Waals heterostructure. Superlattices and Microstructures, 2017, 104, 518-524.	1.4	17
373	2D Organicâ€“Inorganic Hybrid Thin Films for Flexible UVâ€“Visible Photodetectors. Advanced Functional Materials, 2017, 27, 1605554.	7.8	125
374	Interfacial Engineering of Van der Waals Coupled 2D Layered Materials. Advanced Materials Interfaces, 2017, 4, 1601054.	1.9	26
375	Spectral focusing of broadband silver electroluminescence in nanoscopic FRET-LEDs. Nature Nanotechnology, 2017, 12, 637-641.	15.6	18
376	Inhomogeneous composition distribution in monolayer transition metal dichalcogenide alloys. Materials Research Express, 2017, 4, 045004.	0.8	4
377	Electrical and Photoresponse Properties of Inversion Asymmetric Topological Insulator BiTeCl Nanoplates. ChemNanoMat, 2017, 3, 406-410.	1.5	5
378	Broken Symmetry Induced Strong Nonlinear Optical Effects in Spiral WS₂ Nanosheets. ACS Nano, 2017, 11, 4892-4898.	7.3	123
379	Thermal dissociation of inter-layer excitons in MoS₂/MoSe₂ hetero-bilayers. Nanoscale, 2017, 9, 6674-6679.	2.8	64
380	1Â/Âf noise in van der Waals materials and hybrids. Advances in Physics: X, 2017, 2, 428-449.	1.5	21
381	Tunable Schottky Barrier at MoSe₂/Metal Interfaces with a Buffer Layer. Journal of Physical Chemistry C, 2017, 121, 9305-9311.	1.5	45

#	Article	IF	Citations
382	Interlayerâ€Stateâ€Coupling Dependent Ultrafast Charge Transfer in MoS₂/WS₂ Bilayers. Advanced Science, 2017, 4, 1700086.	5.6	87
383	A Versatile and Simple Approach to Generate Light Emission in Semiconductors Mediated by Electric Double Layers. Advanced Materials, 2017, 29, 1606918.	11.1	37
384	Reconfigurable Complementary Monolayer MoTe₂ Field-Effect Transistors for Integrated Circuits. ACS Nano, 2017, 11, 4832-4839.	7.3	108
385	Twoâ€Dimensional Semiconductors: From Materials Preparation to Electronic Applications. Advanced Electronic Materials, 2017, 3, 1700045.	2.6	94
386	+Cerenkov emission of terahertz acoustic phonons generated electrically from monolayers of transition metal dichalcogenides. Journal of Applied Physics, 2017, 121, .	1.1	4
387	Elastic, electronic, and dielectric properties of bulk and monolayer ZrS₂, ZrSe₂, HfS₂, HfSe₂ from van der Waals densityâ€functional theory. Physica Status Solidi (B): Basic Research, 2017, 254, 1700033.	0.7	110
388	Nonlinear photoluminescence in monolayer WS₂: parabolic emission and excitation fluence-dependent recombination dynamics. Nanoscale, 2017, 9, 7235-7241.	2.8	41
389	Thermal Light Emission from Monolayer MoS₂. Advanced Materials, 2017, 29, 1701304.	11.1	45
390	Surface Functionalization of Black Phosphorus via Potassium toward High-Performance Complementary Devices. Nano Letters, 2017, 17, 4122-4129.	4.5	117
391	High-quality single-layer nanosheets of MS₂(M = Mo, Nb, Ta, Ti) directly exfoliated from AMS₂(A = Li, Na, K) crystals. Journal of Materials Chemistry C, 2017, 5, 5977-5983.	2.7	35
392	Defect-mediated phonon dynamics in TaS2 and WSe2. Structural Dynamics, 2017, 4, 044019.	0.9	35
393	Exciton center-of-mass localization and dielectric environment effect in monolayer WS2. Journal of Applied Physics, 2017, 121, 235702.	1.1	20
394	Progress on Electronic and Optoelectronic Devices of 2D Layered Semiconducting Materials. Small, 2017, 13, 1604298.	5.2	65
395	Graphene and related two-dimensional materials: Structure-property relationships for electronics and optoelectronics. Applied Physics Reviews, 2017, 4, .	5.5	476
396	Synthetic approaches to two-dimensional transition metal dichalcogenide nanosheets. Progress in Materials Science, 2017, 89, 411-478.	16.0	176
397	Progress in 2D semiconductor optoelectronics. Proceedings of SPIE, 2017, , .	0.8	0
398	Fast gate-tunable photodetection in the graphene sandwiched WSe₂/GaSe heterojunctions. Nanoscale, 2017, 9, 8388-8392.	2.8	112
399	Enriched Fluorescence Emission from WS₂ Monoflake Empowered by Au Nanoexplorers. Advanced Optical Materials, 2017, 5, 1700156.	3.6	7

#	Article	IF	Citations
400	Two-dimensional transition metal dichalcogenide-based counter electrodes for dye-sensitized solar cells. RSC Advances, 2017, 7, 28234-28290.	1.7	171
401	Defect Healing and Charge Transfer-Mediated Valley Polarization in MoS₂/MoSe₂/MoS₂ Trilayer van der Waals Heterostructures. Nano Letters, 2017, 17, 4130-4136.	4.5	56
402	Two-dimensional non-volatile programmable pâ€“n junctions. Nature Nanotechnology, 2017, 12, 901-906.	15.6	278
403	Gateâ€Controlled BPâ€“WSe₂ Heterojunction Diode for Logic Rectifiers and Logic Optoelectronics. Small, 2017, 13, 1603726.	5.2	86
404	Functional two/three-dimensional assembly of monolayer WS₂ and nickel oxide. Journal of Photonics for Energy, 2017, 7, 014001.	0.8	1
405	Photodetecting and light-emitting devices based on two-dimensional materials. Chinese Physics B, 2017, 26, 036801.	0.7	30
406	The Prospect of Two-Dimensional Heterostructures: A Review of Recent Breakthroughs. IEEE Nanotechnology Magazine, 2017, 11, 6-17.	0.9	27
407	Recent advances in preparation, properties and device applications of two-dimensional h-BN and its vertical heterostructures. Journal of Semiconductors, 2017, 38, 031004.	2.0	15
408	Ab initioelectronic transport study of two-dimensional silicon carbide-based pâ€“n junctions. Journal of Semiconductors, 2017, 38, 033002.	2.0	5
409	High-Performance Broadband Floating-Base Bipolar Phototransistor Based on WSe₂/BP/MoS₂ Heterostructure. ACS Photonics, 2017, 4, 823-829.	3.2	89
410	Photodetectors based on junctions of two-dimensional transition metal dichalcogenides. Chinese Physics B, 2017, 26, 038504.	0.7	56
411	Electronic structure of the <mml:math xmlns:mml="http://www.w3.org/1998/Math/MathML"><mml:mrow><mml:mrow><mml:mi>Co</mml:mi><mml:mo>(</mml:mo></mml:mrow><mml:mathvariant="normal">S</mml:mi><mml:mn>2</mml:mn></mml:msub></mml:mrow></mml:math> interface and its possible use for electrical spin injection in a single <mml:math xmlns:mml="http://www.w3.org/1998/Math/MathML"><mml:mrow><mml:mi>Mo</mml:mi>. Physical Review B, 2017, 95, .	1.1	16
412	Interlayer Exciton Optoelectronics in a 2D Heterostructure pâ€“n Junction. Nano Letters, 2017, 17, 638-643.	4.5	253
413	Broadband Highâ€Responsivity Photodetectors Based on Largeâ€Scale Topological Crystalline Insulator SnTe Ultrathin Film Grown by Molecular Beam Epitaxy. Advanced Optical Materials, 2017, 5, 1600727.	3.6	48
414	Interlayer Excitons and Band Alignment in MoS₂/hBN/WSe₂ van der Waals Heterostructures. Nano Letters, 2017, 17, 938-945.	4.5	174
415	Nanocavity Integrated van der Waals Heterostructure Light-Emitting Tunneling Diode. Nano Letters, 2017, 17, 200-205.	4.5	129
416	Alâ€Doped Black Phosphorus pâ€“n Homojunction Diode for High Performance Photovoltaic. Advanced Functional Materials, 2017, 27, 1604638.	7.8	145
417	Atomically Thin-Layered Molybdenum Disulfide (MoS₂) for Bulk-Heterojunction Solar Cells. ACS Applied Materials & Interfaces, 2017, 9, 3223-3245.	4.0	207

#	Article	IF	Citations
418	Evolution of Surface and Interface Structures in Molecular-Beam Epitaxy of MoSe2 on GaAs(111)A and (111)B. Crystal Growth and Design, 2017, 17, 363-367.	1.4	10
419	Electric Field Effect in Twoâ€Dimensional Transition Metal Dichalcogenides. Advanced Functional Materials, 2017, 27, 1602404.	7.8	57
420	Ultrafast Laser Spectroscopy of Twoâ€Dimensional Materials Beyond Graphene. Advanced Functional Materials, 2017, 27, 1604509.	7.8	122
421	The structural, magnetic and electronic properties of p-type and n-type doped monolayer WS 2 systems. Superlattices and Microstructures, 2017, 112, 619-627.	1.4	14
422	Floating-Gate Manipulated Graphene-Black Phosphorus Heterojunction for Nonvolatile Ambipolar Schottky Junction Memories, Memory Inverter Circuits, and Logic Rectifiers. Nano Letters, 2017, 17, 6353-6359.	4.5	87
423	Three-band k.p Hamiltonian of monolayer MoS 2 based on the group theory and infinitesimal basis transformations approach. Physica B: Condensed Matter, 2017, 527, 66-71.	1.3	4
424	Chiral topological excitons in a Chern band insulator. Physical Review B, 2017, 96, .	1.1	8
425	Atomic-Monolayer Two-Dimensional Lateral Quasi-Heterojunction Bipolar Transistors with Resonant Tunneling Phenomenon. ACS Nano, 2017, 11, 11015-11023.	7.3	45
426	Mixedâ€Dimensional 1D ZnOâ€“2D WSe₂ van der Waals Heterojunction Device for Photosensors. Advanced Functional Materials, 2017, 27, 1703822.	7.8	98
427	Unidirectional Doubly Enhanced MoS₂ Emission via Photonic Fano Resonances. Nano Letters, 2017, 17, 6715-6720.	4.5	69
428	Two-dimensional and three-dimensional hybrid assemblies based on graphene oxide and other layered structures: A carbon science perspective. Carbon, 2017, 125, 437-453.	5.4	21
429	Diffusion quantum Monte Carlo study of excitonic complexes in two-dimensional transition-metal dichalcogenides. Physical Review B, 2017, 96, .	1.1	76
430	Grapheneâ€TMDCâ€Graphene Hybrid Plasmonic Metasurface for Enhanced Biosensing: A Theoretical Analysis. Physica Status Solidi (A) Applications and Materials Science, 2017, 214, 1700563.	0.8	13
431	A MoTe2-based light-emitting diode and photodetector for silicon photonic integrated circuits. Nature Nanotechnology, 2017, 12, 1124-1129.	15.6	344
432	Hydrogenation-driven phase transition in single-layer TiSe₂. Nanotechnology, 2017, 28, 495709.	1.3	6
433	On-Demand Spinâ€“Orbit Interaction from Which-Layer Tunability in Bilayer Graphene. Nano Letters, 2017, 17, 7003-7008.	4.5	42
434	Characterization of Few layer Tungsten diselenide based FET under Thermal Excitation. MRS Advances, 2017, 2, 3721-3726.	0.5	0
435	Dielectric environment and/or random disorder effects on free, charged and localized excitonic states in monolayer WS₂. Journal of Physics Condensed Matter, 2017, 29, 435305.	0.7	17

#	Article	IF	Citations
436	Modulation of electronic structures of MoSe2/WSe2 van der Waals heterostructure by external electric field. Solid State Communications, 2017, 266, 11-15.	0.9	10
437	Metal Thioâ€•and Selenophosphates as Multifunctional van der Waals Layered Materials. Advanced Materials, 2017, 29, 1602852.	11.1	256
438	Excitonic Linewidth Approaching the Homogeneous Limit in <mml:math xmlns:mml="http://www.w3.org/1998/Math/MathML" display="inline"><mml:mrow><mml:msub><mml:mrow><mml:mi>MoS</mml:mi></mml:mrow><mml:mrow><mml:mn>2</mml:mn></mml:mrow></mml:msub></mml:mrow></mml:math>-Based van der Waals Heterostructures. Physical Review X, 2017, 7, .	2.8	389
439	Enhancing Multifunctionalities of Transition-Metal Dichalcogenide Monolayers via Cation Intercalation. ACS Nano, 2017, 11, 9390-9396.	7.3	35
440	Room-temperature 2D semiconductor activated vertical-cavity surface-emitting lasers. Nature Communications, 2017, 8, 543.	5.8	102
441	Interplay of valley polarization and dynamic nuclear polarization in 2D transition metal dichalcogenides. Physical Review B, 2017, 96, .	1.1	12
442	Exciton trapping is responsible for the long apparent lifetime in acid-treated <mml:math xmlns:mml="http://www.w3.org/1998/Math/MathML"><mml:msub><mml:mi>MoS</mml:mi><mml:mn>2</mml:mn></mml:msub></mml:math> Physical Review B, 2017, 96, .	1.1	55
443	Ultrasensitive all-2D MoS2 phototransistors enabled by an out-of-plane MoS2 PN homojunction. Nature Communications, 2017, 8, 572.	5.8	181
444	Tailoring Semiconductor Lateral Multijunctions for Giant Photoconductivity Enhancement. Advanced Materials, 2017, 29, 1703680.	11.1	21
445	Deposition of porous few-layer WSe 2 flakes with high density of exposed edge sites. Vacuum, 2017, 145, 4-10.	1.6	5
446	Controlled Layer Thinning and pâ€Type Doping of WSe₂ by Vapor XeF₂. Advanced Functional Materials, 2017, 27, 1702455.	7.8	103
447	Synthesis of Ultrathin Composition Graded Doped Lateral WSe2/WS2Heterostructures. ACS Applied Materials & Interfaces, 2017, 9, 34204-34212.	4.0	22
448	Noble gas ion beams in materials science for future applications and devices. MRS Bulletin, 2017, 42, 660-666.	1.7	23
449	Wafer-scale two-dimensional ferromagnetic Fe3GeTe2 thin films grown by molecular beam epitaxy. Npj 2D Materials and Applications, 2017, 1, .	3.9	157
450	Tuning electronic and magnetic properties in monolayer MoSe2 by metal adsorption. Chemical Physics Letters, 2017, 687, 54-59.	1.2	12
451	Optical properties and band alignments in ZnTe nanoparticles/MoS₂layer hetero-interface using SE and KPFM studies. Nanotechnology, 2017, 28, 445701.	1.3	15
452	A new insight for ohmic contacts to MoS₂: by tuning MoS₂ affinity energies but not metal work-functions. Physical Chemistry Chemical Physics, 2017, 19, 26151-26157.	1.3	18
453	Piezotronic effect in 1D van der Waals solid of elemental tellurium nanobelt for smart adaptive electronics. Semiconductor Science and Technology, 2017, 32, 104004.	1.0	32

#	Article	IF	Citations
454	Progress of Largeâ€Scale Synthesis and Electronic Device Application of Twoâ€Dimensional Transition Metal Dichalcogenides. Small, 2017, 13, 1700098.	5.2	54
455	Suppression of exciton-exciton annihilation in tungsten disulfide monolayers encapsulated by hexagonal boron nitrides. Physical Review B, 2017, 95, .	1.1	92
456	Efficient Carrier-to-Exciton Conversion in Field Emission Tunnel Diodes Based on MIS-Type van der Waals Heterostack. Nano Letters, 2017, 17, 5156-5162.	4.5	71
457	Pressure-Dependent Light Emission of Charged and Neutral Excitons in Monolayer MoSe₂. Journal of Physical Chemistry Letters, 2017, 8, 3556-3563.	2.1	36
458	Room-temperature continuous-wave lasing from monolayer molybdenum ditelluride integrated with a silicon nanobeam cavity. Nature Nanotechnology, 2017, 12, 987-992.	15.6	241
459	Synthesis of WO_nâ€WX₂ (n=2.7, 2.9; X=S, Se) Heterostructures for Highly Efficient Green Quantum Dot Lightâ€Emitting Diodes. Angewandte Chemie, 2017, 129, 10622-10626.	1.6	7
460	Synthesis of WO_nâ€WX₂ (n=2.7, 2.9; X=S, Se) Heterostructures for Highly Efficient Green Quantum Dot Lightâ€Emitting Diodes. Angewandte Chemie - International Edition, 2017, 56, 10486-10490.	7.2	21
461	Imaging of Interlayer Coupling in van der Waals Heterostructures Using a Bright-Field Optical Microscope. Nano Letters, 2017, 17, 5342-5349.	4.5	74
462	Large array fabrication of high performance monolayer MoS2 photodetectors. Applied Physics Letters, 2017, 111, .	1.5	38
463	Kondo screening in two-dimensional p -type transition-metal dichalcogenides. Physical Review B, 2017, 95, .	1.1	2
464	A kinetic Monte Carlo simulation method of van der Waals epitaxy for atomistic nucleation-growth processes of transition metal dichalcogenides. Scientific Reports, 2017, 7, 2977.	1.6	72
465	High Conduction Hopping Behavior Induced in Transition Metal Dichalcogenides by Percolating Defect Networks: Toward Atomically Thin Circuits. Advanced Functional Materials, 2017, 27, 1702829.	7.8	52
466	Planar p -n Junction Based on a TMDs/Boron Nitride Heterostructure. Physica Status Solidi (B): Basic Research, 2017, 254, 1700180.	0.7	5
467	Enhanced Directional Emission from Monolayer WSe₂ Integrated onto a Multiresonant Silicon-Based Photonic Structure. ACS Photonics, 2017, 4, 3031-3038.	3.2	38
468	Excitonic effects and related properties in semiconductor nanostructures: roles of size and dimensionality. Materials Research Express, 2017, 4, 085017.	0.8	19
469	Measuring the Edge Recombination Velocity of Monolayer Semiconductors. Nano Letters, 2017, 17, 5356-5360.	4.5	19
470	2D hetero-structures based on transition metal dichalcogenides: fabrication, properties and applications. Science Bulletin, 2017, 62, 1148-1161.	4.3	32
471	TMDs â€“ Optoelectronic Devices. , 0, , 329-343.		0

#	Article	IF	Citations
472	Synthesis of Transition Metal Dichalcogenides. , 0, , 344-358.		0
473	Optical Properties and Optoelectronic Applications of Black Phosphorus. , 0, , 435-457.		0
474	Hydrogenation of monolayer molybdenum diselenide via hydrogen plasma treatment. Journal of Materials Chemistry C, 2017, 5, 11294-11300.	2.7	20
475	Stability, electronic and phononic properties ofÎ²and 1T structures of SiTe_x(x= 1, 2) and their vertical heterostructures. Journal of Physics Condensed Matter, 2017, 29, 395504.	0.7	6
476	Few-Layer WSe₂ Schottky Junction-Based Photovoltaic Devices through Site-Selective Dual Doping. ACS Applied Materials & Interfaces, 2017, 9, 42912-42918.	4.0	17
477	Facile Electrochemical Synthesis of 2D Monolayers for High-Performance Thin-Film Transistors. ACS Applied Materials & Interfaces, 2017, 9, 44617-44624.	4.0	22
478	High-Performance Sub-Micrometer Channel WSe₂ Field-Effect Transistors Prepared Using a Floodâ€“Dike Printing Method. ACS Nano, 2017, 11, 12536-12546.	7.3	7
479	Contact morphology and revisited photocurrent dynamics in monolayer MoS2. Npj 2D Materials and Applications, 2017, 1, .	3.9	16
480	Strain effects on the energy band structure and electronic states of single-layer MoTe₂, WTe₂ and their heterostructures. Integrated Ferroelectrics, 2017, 182, 30-38.	0.3	5
481	Potential Profile of Stabilized Field-Induced Lateral pâ€“n Junction in Transition-Metal Dichalcogenides. ACS Nano, 2017, 11, 12583-12590.	7.3	27
482	Enhanced Electrical and Optoelectronic Characteristics of Few-Layer Type-II SnSe/MoS₂ van der Waals Heterojunctions. ACS Applied Materials & Interfaces, 2017, 9, 42149-42155.	4.0	54
483	Synthesis of Large-Area Tungsten Disulfide Films on Pre-Reduced Tungsten Suboxide Substrates. ACS Applied Materials & Interfaces, 2017, 9, 43021-43029.	4.0	29
484	Half metallicity and pressure-induced electronic structure of monolayer FeX2 (X = S, Se). Materials Research Express, 2017, 4, 116305.	0.8	6
485	Wide-Range Controllable Doping of Tungsten Diselenide (WSe₂) based on Hydrochloric Acid Treatment. Journal of Physical Chemistry C, 2017, 121, 14367-14372.	1.5	15
486	Single Atomically Sharp Lateral Monolayer pâ€n Heterojunction Solar Cells with Extraordinarily High Power Conversion Efficiency. Advanced Materials, 2017, 29, 1701168.	11.1	111
487	Lifting the mist of flatland: The recent progress in the characterizations of two-dimensional materials. Progress in Crystal Growth and Characterization of Materials, 2017, 63, 72-93.	1.8	12
488	Universal Substrate-Trapping Strategy To Grow Strictly Monolayer Transition Metal Dichalcogenides Crystals. Chemistry of Materials, 2017, 29, 6095-6103.	3.2	40
489	Lateral multilayer/monolayer MoS2 heterojunction for high performance photodetector applications. Scientific Reports, 2017, 7, 4505.	1.6	35

#	Article	IF	Citations
490	Water-Assisted Synthesis of Molybdenum Disulfide Film with Single Organic Liquid Precursor. Scientific Reports, 2017, 7, 1983.	1.6	27
491	Rapid Wafer-Scale Growth of Polycrystalline 2H-MoS₂ by Pulsed Metalâ€“Organic Chemical Vapor Deposition. Chemistry of Materials, 2017, 29, 6279-6288.	3.2	68
492	Intervalley dark trion states with spin lifetimes of 150 ns in <mml:math xmlns:mml="http://www.w3.org/1998/Math/MathML"><mml:msub><mml:mi>WSe</mml:mi><mml:mn>2</mml:mn></mml:msub></mml:mr Physical Review B, 2017, 95, .	3.1	49
493	Cationâ€“Eutectic Transition via Sublattice Melting in CuInP₂S₆/In_{4/3}P₂S₆ van der Waals Layered Crystals. ACS Nano, 2017, 11, 7060-7073.	7.3	54
494	Development of electronic devices based on two-dimensional materials. FlatChem, 2017, 3, 43-63.	2.8	23
495	Photo-tunable transfer characteristics in MoTe2â€“MoS2 vertical heterostructure. Npj 2D Materials and Applications, 2017, 1, .	3.9	35
496	Enhanced current rectification and self-powered photoresponse in multilayer p-MoTe₂/n-MoS₂ van der Waals heterojunctions. Nanoscale, 2017, 9, 10733-10740.	2.8	75
497	Functionalization of MoS2 with 1,2-dithiolanes: toward donor-acceptor nanohybrids for energy conversion. Npj 2D Materials and Applications, 2017, 1, .	3.9	85
498	Gate tunable photovoltaic effect in a MoSe₂ homojunction enabled with different thicknesses. Journal of Materials Chemistry C, 2017, 5, 7051-7056.	2.7	45
499	Excitons in atomically thin 2D semiconductors and their applications. Nanophotonics, 2017, 6, 1309-1328.	2.9	154
500	Monolayered MoSe ₂ : a candidate for room temperature polaritonics. 2D Materials, 2017, 4, 015006.	2.0	50
501	Synergistic Effect of Hybrid PbS Quantum Dots/2Dâ€“WSe₂ Toward High Performance and Broadband Phototransistors. Advanced Functional Materials, 2017, 27, 1603605.	7.8	193
502	Metalâ€“Semiconductor Phaseâ€Transition in WSe_{2(1â€“}_x₎Te₂_x Monolayer. Advanced Materials, 2017, 29, 1603991.	11.1	123
503	High-efficiency omnidirectional photoresponses based on monolayer lateral pâ€“n heterojunctions. Nanoscale Horizons, 2017, 2, 37-42.	4.1	21
504	Photodetectors Based on Twoâ€Dimensional Layered Materials Beyond Graphene. Advanced Functional Materials, 2017, 27, 1603886.	7.8	534
505	Physics and chemistry of oxidation of twoâ€dimensional nanomaterials by molecular oxygen. Wiley Interdisciplinary Reviews: Computational Molecular Science, 2017, 7, e1280.	6.2	47
506	Electronic and magnetic properties of Mn-doped WSe 2 monolayer under strain. Physica E: Low-Dimensional Systems and Nanostructures, 2017, 88, 11-17.	1.3	13
507	Control of interlayer physics in 2H transition metal dichalcogenides. Journal of Applied Physics, 2017, 122, .	1.1	21

#	Article	IF	Citations
508	Ordered and Disordered Phases in Mo1â^'xWxS2 Monolayer. Scientific Reports, 2017, 7, 15124.	1.6	21
509	WSe<inf>2</inf>-In<inf>2</inf>O<inf>3</inf> nanowire infrared phototransistor. , 2017, , .		0
510	Two Step Chemical Vapor Deposition of In2Se3/MoSe2 van der Waals Heterostructures. Chinese Journal of Chemical Physics, 2017, 30, 325-332.	0.6	14
511	Large-area highly crystalline WSe_2 atomic layers for ultrafast pulsed lasers. Optics Express, 2017, 25, 30020.	1.7	59
512	Recent Advances in Electronic and Optoelectronic Devices Based on Two-Dimensional Transition Metal Dichalcogenides. Electronics (Switzerland), 2017, 6, 43.	1.8	68
513	Graphene against Other Two-Dimensional Materials: A Comparative Study on the Basis of Photonic Applications. , 0, , .		2
514	Pronounced Photovoltaic Response from Multi-layered MoTe2 Phototransistor with Asymmetric Contact Form. Nanoscale Research Letters, 2017, 12, 603.	3.1	7
515	Stability of two orientations of MoS2 on Î±-Al2O3(0001). Japanese Journal of Applied Physics, 2017, 56, 105701.	0.8	2
516	Modification of degenerative photoluminescence in aged monolayer WS_2 by PC_61BM surface processing. Applied Optics, 2017, 56, 890.	2.1	5
517	Highly Enhanced Photoresponsivity of a Monolayer WSe₂ Photodetector with Nitrogen-Doped Graphene Quantum Dots. ACS Applied Materials & Interfaces, 2018, 10, 10322-10329.	4.0	114
518	Local Enhancement of Exciton Emission of Monolayer MoS₂ by Copper Phthalocyanine Nanoparticles. Journal of Physical Chemistry C, 2018, 122, 6794-6800.	1.5	19
519	Device physics of van der Waals heterojunction solar cells. Npj 2D Materials and Applications, 2018, 2, .	3.9	100
520	Spatially controlled doping of two-dimensional SnS2 through intercalation for electronics. Nature Nanotechnology, 2018, 13, 294-299.	15.6	269
521	Strong Depletion in Hybrid Perovskite pâ€“n Junctions Induced by Local Electronic Doping. Advanced Materials, 2018, 30, e1705792.	11.1	141
522	The effect of air stable n-doping through mild plasma on the mechanical property of WSe₂ layers. Nanotechnology, 2018, 29, 175703.	1.3	5
523	Coupling-Assisted Renormalization of Excitons and Vibrations in Compressed MoSe₂â€“WSe₂ Heterostructure. Journal of Physical Chemistry C, 2018, 122, 5820-5828.	1.5	19
524	Highly Enhanced Many-Body Interactions in Anisotropic 2D Semiconductors. Accounts of Chemical Research, 2018, 51, 1164-1173.	7.6	34
525	Probing excitons in transition metal dichalcogenides by Drude-like exciton intraband absorption. Nanoscale, 2018, 10, 9538-9546.	2.8	21

#	Article	IF	Citations
526	3D Network nanostructured NiCoP nanosheets supported on N-doped carbon coated Ni foam as a highly active bifunctional electrocatalyst for hydrogen and oxygen evolution reactions. Frontiers of Chemical Science and Engineering, 2018, 12, 417-424.	2.3	28
527	Atomically thin pâ€“n junctions based on two-dimensional materials. Chemical Society Reviews, 2018, 47, 3339-3358.	18.7	231
528	Distributed Bragg Reflectors as Broadband and Large-Area Platforms for Light-Coupling Enhancement in 2D Transition-Metal Dichalcogenides. ACS Applied Materials & Interfaces, 2018, 10, 16874-16880.	4.0	16
529	Strain-Tuning Atomic Substitution in Two-Dimensional Atomic Crystals. ACS Nano, 2018, 12, 4853-4860.	7.3	75
530	Lanthanide Yb/Er co-doped semiconductor layered WSe₂ nanosheets with near-infrared luminescence at telecommunication wavelengths. Nanoscale, 2018, 10, 9261-9267.	2.8	62
531	Terahertz surface emission from layered semiconductor WSe2. Applied Surface Science, 2018, 448, 416-423.	3.1	38
532	High-Performance WSe₂ Phototransistors with 2D/2D Ohmic Contacts. Nano Letters, 2018, 18, 2766-2771.	4.5	105
533	Dual nanocomposite carrier transport layers enhance the efficiency of planar perovskite photovoltaics. RSC Advances, 2018, 8, 12526-12534.	1.7	20
534	Colloquium : Excitons in atomically thin transition metal dichalcogenides. Reviews of Modern Physics, 2018, 90, .	16.4	1,292
535	Reconfigurable Diodes Based on Vertical WSe₂ Transistors with van der Waals Bonded Contacts. Advanced Materials, 2018, 30, e1707200.	11.1	31
536	Piezoelectric properties in two-dimensional materials: Simulations and experiments. Materials Today, 2018, 21, 611-630.	8.3	219
537	Interfacial electronic states and self-formed pâ€“n junctions in hydrogenated MoS₂/SiC heterostructure. Journal of Materials Chemistry C, 2018, 6, 4523-4530.	2.7	37
538	Laser-induced fabrication of nanoporous monolayer WS ₂ membranes. 2D Materials, 2018, 5, 035011.	2.0	19
539	Janus single layers of <mml:math xmlns:mml="http://www.w3.org/1998/Math/MathML"><mml:msub><mml:mi>In</mml:mi><mml:mn>2</mml:mn></mml:msub></mml:math> : A first-principles study. Physical Review B, 2018, 97, .	3.7	57
540	The organicâ€“2D transition metal dichalcogenide heterointerface. Chemical Society Reviews, 2018, 47, 3241-3264.	18.7	158
541	Microwatts continuous-wave pumped second harmonic generation in few- and mono-layer GaSe. Light: Science and Applications, 2018, 7, 17126-17126.	7.7	68
542	2D Photovoltaic Devices: Progress and Prospects. Small Methods, 2018, 2, 1700294.	4.6	135
543	Dynamic Photochemical and Optoelectronic Control of Photonic Fano Resonances via Monolayer MoS₂ Trions. Nano Letters, 2018, 18, 957-963.	4.5	31

#	Article	IF	Citations
544	Laser Tuning in van der Waals Crystals. ACS Nano, 2018, 12, 2001-2007.	7.3	31
545	2D Layered Materialâ€Based van der Waals Heterostructures for Optoelectronics. Advanced Functional Materials, 2018, 28, 1706587.	7.8	279
546	Observation of Tunable Charged Exciton Polaritons in Hybrid Monolayer WS₂â"Plasmonic Nanoantenna System. Nano Letters, 2018, 18, 1777-1785.	4.5	200
547	Exploring Two-Dimensional Materials toward the Next-Generation Circuits: From Monomer Design to Assembly Control. Chemical Reviews, 2018, 118, 6236-6296.	23.0	410
548	Chemical Vapor Deposition Growth and Applications of Two-Dimensional Materials and Their Heterostructures. Chemical Reviews, 2018, 118, 6091-6133.	23.0	1,000
549	Phase engineering of seamless heterophase homojunctions with co-existing 3R and 2H phases in WS₂ monolayers. Nanoscale, 2018, 10, 3320-3330.	2.8	27
550	Effect of vacancy defect on optoelectronic properties of monolayer tungsten diselenide. Optical and Quantum Electronics, 2018, 50, 1.	1.5	105
551	Reversible and Precisely Controllable p/nâ€Type Doping of MoTe₂ Transistors through Electrothermal Doping. Advanced Materials, 2018, 30, e1706995.	11.1	68
552	Three-Dimensional Self-Assembled Columnar Arrays of AlInP Quantum Wires for Polarized Micrometer-Sized Amber Light Emitting Diodes. ACS Photonics, 2018, 5, 1318-1325.	3.2	4
553	Broadband nonlinear optical response of monolayer MoSe2 under ultrafast excitation. Applied Physics Letters, 2018, 112, .	1.5	25
554	The interplay between excitons and trions in a monolayer of MoSe2. Applied Physics Letters, 2018, 112, .	1.5	35
555	Gate-Tunable WSe₂/SnSe₂ Backward Diode with Ultrahigh-Reverse Rectification Ratio. ACS Applied Materials & Interfaces, 2018, 10, 5657-5664.	4.0	65
556	Dielectric Engineering of Electronic Correlations in a van der Waals Heterostructure. Nano Letters, 2018, 18, 1402-1409.	4.5	39
557	Superior Electro-Oxidation and Corrosion Resistance of Monolayer Transition Metal Disulfides. ACS Applied Materials & Interfaces, 2018, 10, 4285-4294.	4.0	23
558	Mechanical Properties of 2D Materials Studied by In Situ Microscopy Techniques. Advanced Materials Interfaces, 2018, 5, 1701246.	1.9	71
559	Direct Observation of Ultrafast Exciton Dissociation in Lead Iodide Perovskite by 2D Electronic Spectroscopy. ACS Photonics, 2018, 5, 852-860.	3.2	57
560	Double-Channel Piezotronic Transistors for Highly Sensitive Pressure Sensing. ACS Nano, 2018, 12, 1732-1738.	7.3	33
561	Direct determination of monolayer MoS₂and WSe₂exciton binding energies on insulating and metallic substrates. 2D Materials, 2018, 5, 025003.	2.0	142

#	Article	IF	Citations
562	Probing Excitons, Trions, and Dark Excitons in Monolayer WS₂ Using Resonance Raman Spectroscopy. Nano Letters, 2018, 18, 1428-1434.	4.5	25
563	Gate Tunable Self-Biased Diode Based on Few Layered MoS₂ and WSe₂. Chemistry of Materials, 2018, 30, 1011-1016.	3.2	20
564	Novel Optoelectronic Devices: Transitionâ€Metalâ€Dichalcogenideâ€Based 2D Heterostructures. Advanced Electronic Materials, 2018, 4, 1700335.	2.6	91
565	Probing Exciton Complexes and Charge Distribution in Inkslab-Like WSe₂ Homojunction. ACS Nano, 2018, 12, 4959-4967.	7.3	21
566	Magnetic Field Enhanced Superconductivity in Epitaxial Thin Film WTe2. Scientific Reports, 2018, 8, 6520.	1.6	31
567	Light Sources and Photodetectors Enabled by 2D Semiconductors. Small Methods, 2018, 2, 1800019.	4.6	35
568	Enhanced Hole Injection Into Single Layer WSe2. IEEE Journal of the Electron Devices Society, 2018, 6, 309-313.	1.2	2
569	Material platforms for spin-based photonic quantum technologies. Nature Reviews Materials, 2018, 3, 38-51.	23.3	453
570	Dissociation of two-dimensional excitons in monolayer WSe2. Nature Communications, 2018, 9, 1633.	5.8	116
571	Material Synthesis and Device Aspects of Monolayer Tungsten Diselenide. Scientific Reports, 2018, 8, 5221.	1.6	18
572	Suspended SnS₂ Layers by Light Assistance for Ultrasensitive Ammonia Detection at Room Temperature. Advanced Functional Materials, 2018, 28, 1801035.	7.8	81
573	In Situ Synthesis of WSe₂/CMK-5 Nanocomposite for Rechargeable Lithium-Ion Batteries with a Long-Term Cycling Stability. ACS Sustainable Chemistry and Engineering, 2018, 6, 4688-4694.	3.2	47
574	Affinity capture surface carboxyl-functionalized MoS2 sheets to enhance the sensitivity of surface plasmon resonance immunosensors. Talanta, 2018, 185, 174-181.	2.9	42
575	Large-area and bright pulsed electroluminescence in monolayer semiconductors. Nature Communications, 2018, 9, 1229.	5.8	146
576	Nonlinear Optics with 2D Layered Materials. Advanced Materials, 2018, 30, e1705963.	11.1	485
577	Optoelectronic response of a WS ₂ tubular p - n junction. 2D Materials, 2018, 5, 035002.	2.0	41
578	Strain mapping in single-layer two-dimensional crystals via Raman activity. Physical Review B, 2018, 97, .	1.1	43
579	Dimensional Crossover Transport Induced by Substitutional Atomic Doping in SnSe₂. Advanced Electronic Materials, 2018, 4, 1700563.	2.6	18

#	Article	IF	Citations
580	Computational study of phase engineered transition metal dichalcogenides heterostructures. Computational Materials Science, 2018, 142, 129-134.	1.4	11
581	Realizing p-Type MoS₂ with Enhanced Thermoelectric Performance by Embedding VMo₂S₄ Nanoinclusions. Journal of Physical Chemistry B, 2018, 122, 713-720.	1.2	44
582	Plasma-assisted synthesis of MoS ₂. 2D Materials, 2018, 5, 015005.	2.0	19
583	Electronic structures and optical properties of arsenene and antimonene under strain and an electric field. Journal of Materials Chemistry C, 2018, 6, 83-90.	2.7	68
584	Multimodal Kelvin Probe Force Microscopy Investigations of a Photovoltaic WSe₂/MoS₂ Type-II Interface. ACS Applied Materials & Interfaces, 2018, 10, 1363-1373.	4.0	58
585	Pronounced Photovoltaic Effect in Electrically Tunable Lateral Blackâ€Phosphorus Heterojunction Diode. Advanced Electronic Materials, 2018, 4, 1700442.	2.6	27
586	Capacitanceâ€“voltage analysis of electrical properties for WSe2field effect transistors with high-k encapsulation layer. Nanotechnology, 2018, 29, 065703.	1.3	4
587	Tuning the activity of the inert MoS₂ surface via graphene oxide support doping towards chemical functionalization and hydrogen evolution: a density functional study. Physical Chemistry Chemical Physics, 2018, 20, 1861-1871.	1.3	22
588	Carrier Modulation of Ambipolar Fewâ€Layer MoTe₂ Transistors by MgO Surface Charge Transfer Doping. Advanced Functional Materials, 2018, 28, 1704539.	7.8	88
589	Group 6 transition metal dichalcogenide nanomaterials: synthesis, applications and future perspectives. Nanoscale Horizons, 2018, 3, 90-204.	4.1	309
590	Band Structure and Photoelectric Characterization of GeSe Monolayers. Advanced Functional Materials, 2018, 28, 1704855.	7.8	133
591	Structural stability and magnetic-exchange coupling in Mn-doped monolayer/bilayer MoS₂. Physical Chemistry Chemical Physics, 2018, 20, 553-561.	1.3	37
592	Electrical and optical transport properties of single layer WSe 2. Physica E: Low-Dimensional Systems and Nanostructures, 2018, 97, 184-190.	1.3	12
593	Conversion of Multi-layered MoTe2 Transistor Between P-Type and N-Type and Their Use in Inverter. Nanoscale Research Letters, 2018, 13, 291.	3.1	30
594	Ultra-sensitive and plasmon-tunable graphene photodetectors for micro-spectrometry. Nanoscale, 2018, 10, 20013-20019.	2.8	34
595	New Directions in Science Technologyâ€”Atomically-Thin Metal Dichalcogenides. , 2018, , 181-250.		1
596	DFT Study of Skutterudite CoSb₃ and In_{0.2}Co₄Sb₁₂ Thermoelectric Heterostructures with 2Dâ€“WSe₂. ChemistrySelect, 2018, 3, 9336-9347.	0.7	3
597	Photovoltaic effects in reconfigurable heterostructured black phosphorus transistors. Chinese Physics B, 2018, 27, 128502.	0.7	10

#	Article	IF	Citations
598	van der Waals interaction-induced photoluminescence weakening and multilayer growth in epitaxially aligned WS₂. Physical Chemistry Chemical Physics, 2018, 20, 29790-29797.	1.3	7
599	Controlled p-type substitutional doping in large-area monolayer WSe₂crystals grown by chemical vapor deposition. Nanoscale, 2018, 10, 21374-21385.	2.8	58
600	Gate-tunable and high optoelectronic performance in multilayer WSe₂ Pâ€“N diode. Journal of Materials Chemistry C, 2018, 6, 11673-11678.	2.7	23
601	Gate Switching of Ultrafast Photoluminescence in Graphene. Nano Letters, 2018, 18, 7985-7990.	4.5	23
602	Electrically and Optically Tunable Responses in Graphene/Transition-Metal-Dichalcogenide Heterostructures. ACS Applied Materials & Interfaces, 2018, 10, 44102-44108.	4.0	29
603	Flexoelectricity in Monolayer Transition Metal Dichalcogenides. Journal of Physical Chemistry Letters, 2018, 9, 6841-6846.	2.1	51
604	Environmental Effects on the Electrical Characteristics of Back-Gated WSe2 Field-Effect Transistors. Nanomaterials, 2018, 8, 901.	1.9	58
605	Atomically-Thin Quantum Light Emitting Diodes. Springer Theses, 2018, , 71-89.	0.0	13
606	Exciton transport in strained monolayer WSe2. Applied Physics Letters, 2018, 113, .	1.5	58
607	Ultimate limit in size and performance of WSe2 vertical diodes. Nature Communications, 2018, 9, 5371.	5.8	63
608	Radiative lifetime of localized excitons in transition-metal dichalcogenides. Physical Review B, 2018, 98, .	1.1	22
609	Reversible Mechanochromic Delayed Fluorescence in 2D Metalâ€“Organic Micro/Nanosheets: Switching Singletâ€“Triplet States through Transformation between Exciplex and Excimer. Advanced Science, 2018, 5, 1801187.	5.6	61
610	Band Structure Engineering in 2D Materials for Optoelectronic Applications. Advanced Materials Technologies, 2018, 3, 1800072.	3.0	78
611	Recent Advances in Synthesis and Applications of 2D Junctions. Small, 2018, 14, e1801606.	5.2	19
612	Efficient Energy Transfer in In₂Se₃â€“MoSe₂ van der Waals Heterostructures. ACS Omega, 2018, 3, 11930-11936.	1.6	18
613	Charge carrier injection and transport engineering in two-dimensional transition metal dichalcogenides. Chemical Science, 2018, 9, 7727-7745.	3.7	70
614	Strong two-dimensional plasmon in Li-intercalated hexagonal boron-nitride film with low damping. Npj 2D Materials and Applications, 2018, 2, .	3.9	15
615	Efficient Charge Separation in 2D Janus van der Waals Structures with Built-in Electric Fields and Intrinsic pâ€“n Doping. Journal of Physical Chemistry C, 2018, 122, 24520-24526.	1.5	79

#	Article	IF	Citations
616	Diverse Atomically Sharp Interfaces and Linear Dichroism of 1T' ReS₂â€ReSe₂ Lateral pâ€“n Heterojunctions. Advanced Functional Materials, 2018, 28, 1804696.	7.8	50
617	Nonvolatile and Programmable Photodoping in MoTe₂ for Photoresistâ€Free Complementary Electronic Devices. Advanced Materials, 2018, 30, e1804470.	11.1	70
618	High-Efficiency Monolayer Molybdenum Ditelluride Light-Emitting Diode and Photodetector. ACS Applied Materials & Interfaces, 2018, 10, 43291-43298.	4.0	56
619	Defect-Induced Modification of Low-Lying Excitons and Valley Selectivity in Monolayer Transition Metal Dichalcogenides. Physical Review Letters, 2018, 121, 167402.	2.9	109
620	Deterministic coupling of site-controlled quantum emitters in monolayer WSe2 to plasmonic nanocavities. Nature Nanotechnology, 2018, 13, 1137-1142.	15.6	198
621	Controlling Lattice Defects and Inter-Exciton Interactions in Monolayer Transition Metal Dichalcogenides for Efficient Light Emission. ACS Photonics, 2018, 5, 4187-4194.	3.2	16
622	Black phosphorus with a unique rectangular shape and its anisotropic properties. AIP Advances, 2018, 8, .	0.6	5
623	Efficient Energy Transfer across Organicâ€“2D Inorganic Heterointerfaces. ACS Applied Materials & Interfaces, 2018, 10, 39336-39342.	4.0	27
624	Interface excitons at lateral heterojunctions in monolayer semiconductors. Physical Review B, 2018, 98, .	1.1	28
625	Thickness-Dependent Differential Reflectance Spectra of Monolayer and Few-Layer MoS2, MoSe2, WS2 and WSe2. Nanomaterials, 2018, 8, 725.	1.9	156
626	Two-Dimensional MoxW1â^'xS2 Graded Alloys: Growth and Optical Properties. Scientific Reports, 2018, 8, 12889.	1.6	24
627	Multiple Optical Frequency Conversions in Fewâ€Layer GaSe Assisted by a Photonic Crystal Cavity. Advanced Optical Materials, 2018, 6, 1800698.	3.6	15
628	Ultrahigh Photoresponsive Device Based on ReS₂/Graphene Heterostructure. Small, 2018, 14, e1802593.	5.2	75
629	Self-consistent dielectric constant determination for monolayer WSe₂. Optics Express, 2018, 26, 23061.	1.7	4
630	Recent advances of low-dimensional materials in lasing applications. FlatChem, 2018, 10, 22-38.	2.8	14
631	Transformation of 2D group-III selenides to ultra-thin nitrides: enabling epitaxy on amorphous substrates. Nanotechnology, 2018, 29, 47LT02.	1.3	6
632	Flexible Vertical pâ€“n Diode Photodetectors with Thin N-type MoSe₂ Films Solution-Processed on Water Surfaces. ACS Applied Materials & Interfaces, 2018, 10, 34543-34552.	4.0	25
633	Exciton physics and device application of two-dimensional transition metal dichalcogenide semiconductors. Npj 2D Materials and Applications, 2018, 2, .	3.9	526

#	Article	IF	Citations
634	Compact mid-infrared graphene thermopile enabled by a nanopatterning technique of electrolyte gates. New Journal of Physics, 2018, 20, 083050.	1.2	5
635	Thermally Induced 2D Alloyâ€Heterostructure Transformation in Quaternary Alloys. Advanced Materials, 2018, 30, e1804218.	11.1	29
636	Enhanced Emission from WSe₂ Monolayers Coupled to Circular Bragg Gratings. ACS Photonics, 2018, 5, 3950-3955.	3.2	31
637	Monitoring the effect of asymmetrical vertical strain on Janus single layers of MoSSe via vibrational spectrum. Journal of Chemical Physics, 2018, 149, 084707.	1.2	13
638	In situ exploration of the thermodynamic evolution properties in the type II interface from the WSe₂â€“WS₂ lateral heterojunction. Nanotechnology, 2018, 29, 435703.	1.3	7
639	pH-Dependent Photoluminescence Properties of Monolayer Transition-Metal Dichalcogenides Immersed in an Aqueous Solution. Journal of Physical Chemistry C, 2018, 122, 13175-13181.	1.5	12
640	UV-active plasmons in alkali and alkaline-earth intercalated graphene. Physical Review B, 2018, 97, .	1.1	8
641	Doping with Nb enhances the photoresponsivity of WSe2 thin sheets. AIP Advances, 2018, 8, .	0.6	13
642	Enhanced Performance of Field-Effect Transistors Based on Black Phosphorus Channels Reduced by Galvanic Corrosion of Al Overlayers. ACS Applied Materials & Interfaces, 2018, 10, 18895-18901.	4.0	9
643	Atomic scale electronic structure of the ferromagnetic semiconductor Cr2Ge2Te6. Science Bulletin, 2018, 63, 825-830.	4.3	40
644	MoS₂ Synaptic Transistor With Tunable Weight Profile. IEEE Transactions on Electron Devices, 2018, 65, 3543-3547.	1.6	13
645	Semiconductor Nanomembrane Materials for High-Performance Soft Electronic Devices. Journal of the American Chemical Society, 2018, 140, 9001-9019.	6.6	34
646	Piezoâ€Phototronic Effect for Enhanced Flexible MoS₂/WSe₂ van der Waals Photodiodes. Advanced Functional Materials, 2018, 28, 1802849.	7.8	130
647	Unraveling Spatially Heterogeneous Ultrafast Carrier Dynamics of Single-Layer WSe₂ by Femtosecond Time-Resolved Photoemission Electron Microscopy. Nano Letters, 2018, 18, 5172-5178.	4.5	42
648	DFT study of optical properties of MoS2 and WS2 compared to spectroscopic results on liquid phase exfoliated nanoflakes. Optical and Quantum Electronics, 2018, 50, 1.	1.5	8
649	A two-band spinful k.p Hamiltonian of monolayer MoS2 from a nine-band model based on group theory. Superlattices and Microstructures, 2018, 120, 812-823.	1.4	4
650	Interfacial Charge Behavior Modulation in Perovskite Quantum Dotâ€Monolayer MoS₂ 0Dâ€2D Mixedâ€Dimensional van der Waals Heterostructures. Advanced Functional Materials, 2018, 28, 1802015.	7.8	107
651	Two-dimensional light-emitting materials: preparation, properties and applications. Chemical Society Reviews, 2018, 47, 6128-6174.	18.7	167

#	Article	IF	Citations
652	Excitation-induced transition to indirect band gaps in atomically thin transition-metal dichalcogenide semiconductors. Physical Review B, 2018, 98, .	1.1	31
653	Recent Progress and Future Prospects of 2Dâ€Based Photodetectors. Advanced Materials, 2018, 30, e1801164.	11.1	408
654	Nanophotonics with 2D transition metal dichalcogenides [Invited]. Optics Express, 2018, 26, 15972.	1.7	134
655	Two-photon absorption arises from two-dimensional excitons. Optics Express, 2018, 26, 16093.	1.7	22
656	An atom-to-circuit modeling approach to all-2D metalâ€“insulatorâ€“semiconductor field-effect transistors. Npj 2D Materials and Applications, 2018, 2, .	3.9	20
657	A gate-free monolayer WSe2 pn diode. Nature Communications, 2018, 9, 3143.	5.8	108
658	Intrinsic excitonic emission and valley Zeeman splitting in epitaxial MS2 (M = Mo and W) monolayers on hexagonal boron nitride. Nano Research, 2018, 11, 6227-6236.	5.8	8
659	Electronic and vibrational properties of TMDs heterogeneous bilayers, nontwisted bilayers silicene/TMDs heterostructures and photovoltaic heterojunctions of fullerenes with TMDs monolayers. Physica E: Low-Dimensional Systems and Nanostructures, 2018, 104, 155-164.	1.3	30
660	Two-dimensional multibit optoelectronic memory with broadband spectrum distinction. Nature Communications, 2018, 9, 2966.	5.8	211
661	Co6Se8(PEt3)6 superatoms as tunable chemical dopants for two-dimensional semiconductors. Npj Computational Materials, 2018, 4, .	3.5	20
662	Synthesis of hexagonal boron nitride heterostructures for 2D van der Waals electronics. Chemical Society Reviews, 2018, 47, 6342-6369.	18.7	114
663	Semi-metallic bilayer MS2 (M=W, Mo) induced by Boron, Carbon, and Nitrogen impurities. Solid State Communications, 2018, 282, 28-32.	0.9	17
664	Influence of Polar Pressure Transmission Medium on the Pressure Coefficient of Excitonic Interband Transitions in Monolayer WSe 2. Chinese Physics Letters, 2018, 35, 066201.	1.3	1
665	Electronics and Optoelectronics Based on Two-Dimensional Materials. Journal of the Korean Physical Society, 2018, 73, 1-15.	0.3	16
666	Tuning Band Alignments and Charge-Transport Properties through MoSe₂ Bridging between MoS₂ and Cadmium Sulfide for Enhanced Hydrogen Production. ACS Applied Materials & Interfaces, 2018, 10, 26153-26161.	4.0	43
667	Progress on Crystal Growth of Two-Dimensional Semiconductors for Optoelectronic Applications. Crystals, 2018, 8, 252.	1.0	7
668	Quantum plasmonic hot-electron injection in lateral WSe2/MoSe2 heterostructures. Physical Review B, 2018, 98, .	1.1	31
669	Competition between Free Carriers and Excitons Mediated by Defects Observed in Layered WSe₂ Crystal with Timeâ€Resolved Terahertz Spectroscopy. Advanced Optical Materials, 2018, 6, 1800290.	3.6	39

#	Article	IF	Citations
670	High performance self-gating graphene/MoS₂ diode enabled by asymmetric contacts. Nanotechnology, 2018, 29, 395201.	1.3	7
671	Synthesis, properties, and optoelectronic applications of two-dimensional MoS₂and MoS₂-based heterostructures. Chemical Society Reviews, 2018, 47, 6101-6127.	18.7	293
672	Photovoltaic Effect in Graphene/MoS2/Si Van der Waals Heterostructures. Coatings, 2018, 8, 2.	1.2	18
673	Frequency-dependent substrate screening of excitons in atomically thin transition metal dichalcogenide semiconductors. Physical Review B, 2018, 98, .	1.1	20
674	Unraveling the Mechanism of Photoinduced Charge-Transfer Process in Bilayer Heterojunction. ACS Applied Materials & Interfaces, 2018, 10, 25401-25408.	4.0	29
675	Engineering graphene and TMDs based van der Waals heterostructures for photovoltaic and photoelectrochemical solar energy conversion. Chemical Society Reviews, 2018, 47, 4981-5037.	18.7	344
676	Energy and charge transfer effects in two-dimensional van der Waals hybrid nanostructures on periodic gold nanopost array. Applied Physics Letters, 2018, 112, .	1.5	6
677	Ultrafast Energy Dissipation via Coupling with Internal and External Phonons in Two-Dimensional MoS₂. ACS Nano, 2018, 12, 8961-8969.	7.3	61
678	Hybrid coupling enhances photoluminescence of monolayer MoS₂ on plasmonic nanostructures. Optics Letters, 2018, 43, 4128.	1.7	18
679	Nature of Excitons in Bidimensional WSe2 by Hybrid Density Functional Theory Calculations. Nanomaterials, 2018, 8, 481.	1.9	10
680	Light Emission Properties of 2D Transition Metal Dichalcogenides: Fundamentals and Applications. Advanced Optical Materials, 2018, 6, 1800420.	3.6	88
681	Prediction of an extremely long exciton lifetime in a Janus-MoSTe monolayer. Nanoscale, 2018, 10, 19310-19315.	2.8	93
682	Electronic and vibrational properties of PbI2 : From bulk to monolayer. Physical Review B, 2018, 98, .	1.1	49
683	Extrinsic p-type doping of few layered WS2 films with niobium by pulsed laser deposition. Applied Physics Letters, 2018, 113, .	1.5	25
684	Observation of intrinsic dark exciton in Janus-MoSSe heterosturcture induced by intrinsic electric field. Journal of Physics Condensed Matter, 2018, 30, 395001.	0.7	14
685	Effects of the Fermi level energy on the adsorption of O ₂ to monolayer MoS ₂. 2D Materials, 2018, 5, 045025.	2.0	8
686	Role of precursors' ratio for growth of two-dimensional MoS2 structure and investigation on its nonlinear optical properties. Thin Solid Films, 2018, 663, 37-43.	0.8	3
687	Synthesis of transition metal dichalcogenides and their heterostructures. Materials Research Express, 2018, 5, 095904.	0.8	7

#	Article	IF	Citations
688	Tunable topological Nernst effect in two-dimensional transition-metal dichalcogenides. Physical Review B, 2018, 98, .	1.1	13
689	WSe₂/Au vertical Schottky junction photodetector with low dark current and fast photoresponse. Nanotechnology, 2018, 29, 444001.	1.3	27
690	Optoelectronic properties of bottom gate-defined in-plane monolayer WSe₂ pâ€“n junction. Chinese Physics B, 2018, 27, 087303.	0.7	3
691	Electroluminescent Devices Based on 2D Semiconducting Transition Metal Dichalcogenides. Advanced Materials, 2018, 30, e1802687.	11.1	86
692	Ultrafast transient absorption measurements of photocarrier dynamics in monolayer and bulk ReSe₂. Optics Express, 2018, 26, 21501.	1.7	17
693	Photovoltaic Field-Effect Transistors Using a MoS₂ and Organic Rubrene van der Waals Hybrid. ACS Applied Materials & Interfaces, 2018, 10, 29848-29856.	4.0	48
694	Enhanced Carrier Concentration and Electronic Transport by Inserting Graphene into van der Waals Heterostructures of Transition-Metal Dichalcogenides. Physical Review Applied, 2018, 10, .	1.5	19
695	Morphology Engineering in Monolayer MoS₂â€WS₂ Lateral Heterostructures. Advanced Functional Materials, 2018, 28, 1801568.	7.8	67
696	Direct Chemical Vapor Deposition Growth of Monolayer MoS₂ on TiO₂ Nanorods and Evidence for Doping-Induced Strong Photoluminescence Enhancement. Journal of Physical Chemistry C, 2018, 122, 15017-15025.	1.5	38
697	Ultrafast Spontaneous Emission from a Slot-Antenna Coupled WSe₂ Monolayer. ACS Photonics, 2018, 5, 2701-2705.	3.2	17
698	Singleâ€Crystalline Nanobelts Composed of Transition Metal Ditellurides. Advanced Materials, 2018, 30, e1707260.	11.1	18
699	Monolayer Transition Metal Dichalcogenides as Light Sources. Advanced Materials, 2018, 30, e1707627.	11.1	76
700	Wafer-scale synthesis of monolayer WSe2: A multi-functional photocatalyst for efficient overall pure water splitting. Nano Energy, 2018, 51, 54-60.	8.2	45
701	Excitonic processes in atomically-thin MoSe ₂ /MoS ₂ vertical heterostructures. 2D Materials, 2018, 5, 031016.	2.0	12
702	Interfacial charge transfer in WS2 monolayer/CsPbBr3 microplate heterostructure. Frontiers of Physics, 2018, 13, 1.	2.4	17
703	Environmental engineering of transition metal dichalcogenide optoelectronics. Frontiers of Physics, 2018, 13, 1.	2.4	13
704	Field Effect Transistor Based on Layered NiPS 3. Scientific Reports, 2018, 8, 8586.	1.6	62
705	THz-induced thermoelectric and thermal transport in atomic monolayers. , 2018, , 473-509.		0

#	Article	IF	Citations
706	Ultrafast Anisotropic Exciton Dynamics in Nanopatterned MoS₂ Sheets. ACS Photonics, 2018, 5, 3363-3371.	3.2	17
707	Bilayers of Janus WSSe: monitoring the stacking type via the vibrational spectrum. Physical Chemistry Chemical Physics, 2018, 20, 17380-17386.	1.3	56
708	Enhancement of direct and indirect exciton emissions in few-layer WSe₂ at high temperatures. Materials Research Express, 2018, 5, 066209.	0.8	7
709	Luminescence in 2D Materials and van der Waals Heterostructures. Advanced Optical Materials, 2018, 6, 1701296.	3.6	58
710	Lateral heterostructures of hexagonal boron nitride and graphene: BCN alloy formation and microstructuring mechanism. Applied Surface Science, 2018, 455, 1086-1094.	3.1	10
711	Manyâ€Body Complexes in 2D Semiconductors. Advanced Materials, 2019, 31, e1706945.	11.1	255
712	Van der Waals heterostructures for optoelectronics: Progress and prospects. Applied Materials Today, 2019, 16, 435-455.	2.3	117
713	Exciton Polarization and Renormalization Effect for Optical Modulation in Monolayer Semiconductors. ACS Nano, 2019, 13, 9218-9226.	7.3	9
714	Photoinduced doping in monolayer WSe₂ transistors. Applied Physics Express, 2019, 12, 094005.	1.1	3
715	Two-dimensional materials. , 2019, , 165-189.		0
716	First-principles study of metal-semiconductor contact between MX2 (Mâ€¯=â€¯Nb, Pt; Xâ€¯=â€¯S, Se) monolayers. Physics Letters, Section A: General, Atomic and Solid State Physics, 2019, 383, 125867.	0.9	8
717	Biomedical and bioimaging applications of 2D pnictogens and transition metal dichalcogenides. Nanoscale, 2019, 11, 15770-15782.	2.8	22
718	Valleytronics in transition metal dichalcogenides materials. Nano Research, 2019, 12, 2695-2711.	5.8	155
719	Physics of excitons and their transport in two dimensional transition metal dichalcogenide semiconductors. RSC Advances, 2019, 9, 25439-25461.	1.7	24
720	Enhanced Photoâ€Response of Mos 2 Photodetectors by a Laterally Aligned SiO 2 Nanoribbon Array Substrate. ChemNanoMat, 2019, 5, 1272-1279.	1.5	2
721	Enhancing Photoluminescence and Mobilities in WS₂ Monolayers with Oleic Acid Ligands. Nano Letters, 2019, 19, 6299-6307.	4.5	80
722	Two-Dimensional Transition Metal Dichalcogenides: An Overview. , 2019, , 1-27.		4
723	Properties of Transition Metal Dichalcogenides. , 2019, , 69-106.		3

#	Article	IF	Citations
724	Synthesis and Optoelectronic Applications of a Stable p-Type 2D Material: Î±-MnS. ACS Nano, 2019, 13, 12662-12670.	7.3	54
725	Monolayer Excitonic Emission for Imaging Spatial Dispersion of Photonic Crystals. ACS Photonics, 2019, 6, 2312-2319.	3.2	7
726	Dual-Wavelength Passively Mode-Locked Yb-Doped Fiber Laser Based on a SnSe₂-PVA Saturable Absorber. IEEE Photonics Journal, 2019, 11, 1-13.	1.0	4
727	Photoresponse of homostructure WSe2 rectifying diode. AIP Advances, 2019, 9, 075010.	0.6	10
728	Convectionâ€Flowâ€Assisted Preparation of a Strong Electron Dopant, Benzyl Viologen, for Surfaceâ€Charge Transfer Doping of Molybdenum Disulfide. ChemistryOpen, 2019, 8, 908-914.	0.9	6
729	Carbon Nanomaterials and Two-Dimensional Transition Metal Dichalcogenides (2D TMDCs). Advanced Structured Materials, 2019, , 165-245.	0.3	4
730	Scanning Tunneling Microscope-Induced Excitonic Luminescence of a Two-Dimensional Semiconductor. Physical Review Letters, 2019, 123, 027402.	2.9	36
731	Controlled one step thinning and doping of two-dimensional transition metal dichalcogenides. Science China Materials, 2019, 62, 1837-1845.	3.5	10
732	All-2D ReS2 transistors with split gates for logic circuitry. Scientific Reports, 2019, 9, 10354.	1.6	22
733	WSe _(2â" x) Te _x alloys grown by molecular beam epitaxy. 2D Materials, 2019, 6, 045027.	2.0	20
734	Synthesis and Properties of (BiSe)_{0.97}MoSe₂: A Heterostructure Containing Both 2H-MoSe₂ and 1T-MoSe₂. Chemistry of Materials, 2019, 31, 5824-5831.	3.2	14
735	Interface Engineering of Band Evolution and Transport Properties of Bilayer WSe2 under Different Electric Fields. Journal of Physical Chemistry C, 2019, 123, 19812-19819.	1.5	4
736	Scalable Large-Area pâ€"iâ€"n Light-Emitting Diodes Based on WS₂ Monolayers Grown via MOCVD. ACS Photonics, 2019, 6, 1832-1839.	3.2	36
737	Lateral and Vertical MoSe₂â€"MoS₂ Heterostructures via Epitaxial Growth: Triggered by High-Temperature Annealing and Precursor Concentration. Journal of Physical Chemistry Letters, 2019, 10, 5027-5035.	2.1	13
738	Layer-Dependent Interfacial Transport and Optoelectrical Properties of MoS₂ on Ultraflat Metals. ACS Applied Materials & Interfaces, 2019, 11, 31543-31550.	4.0	33
739	Layerâ€Numberâ€Dependent Electronic and Optoelectronic Properties of 2D WSe₂â€Organic Hybrid Heterojunction. Advanced Materials Interfaces, 2019, 6, 1900637.	1.9	18
740	Graphene Wrinkles Enable Spatially Defined Chemistry. Nano Letters, 2019, 19, 5640-5646.	4.5	39
741	Bright electroluminescence in ambient conditions from WSe2 p-n diodes using pulsed injection. Applied Physics Letters, 2019, 115, 011103.	1.5	13

#	Article	IF	Citations
742	Multibit Optoelectronic Memory in Topâ€Floatingâ€Gated van der Waals Heterostructures. Advanced Functional Materials, 2019, 29, 1902890.	7.8	69
743	Investigation on photocatalytic mechanism of graphitic SiC (g-SiC)/MoS₂ van der Waals heterostructured photocatalysts for overall water splitting. Physical Chemistry Chemical Physics, 2019, 21, 15372-15379.	1.3	30
744	Electric-field-induced optical hysteresis in single-layer WSe2. Applied Physics Letters, 2019, 115, 161103.	1.5	3
745	Exciton Luminescence of Wse2 Bilayers. Russian Physics Journal, 2019, 62, 1017-1022.	0.2	2
746	Quantum Multibody Interactions in Halide-Assisted Vapor-Synthesized Monolayer WSe₂ and Its Integration in a High Responsivity Photodetector with Low-Interface Trap Density. Chemistry of Materials, 2019, 31, 9861-9874.	3.2	30
747	Quest for p-Type Two-Dimensional Semiconductors. ACS Nano, 2019, 13, 12294-12300.	7.3	72
748	High-Performance WSe₂ Photodetector Based on a Laser-Induced pâ€“n Junction. ACS Applied Materials & Interfaces, 2019, 11, 43330-43336.	4.0	61
749	Scanning Probe Lithography Patterning of Monolayer Semiconductors and Application in Quantifying Edge Recombination. Advanced Materials, 2019, 31, e1900136.	11.1	27
750	Effect of Dielectric Environment on Excitonic Dynamics in Monolayer WS₂. Advanced Materials Interfaces, 2019, 6, 1901307.	1.9	29
751	WSe₂ Homojunction Devices: Electrostatically Configurable as Diodes, MOSFETs, and Tunnel FETs for Reconfigurable Computing. Small, 2019, 15, e1902770.	5.2	23
752	Temperature-dependent phonon dynamics of supported and suspended monolayer tungsten diselenide. AIP Advances, 2019, 9, .	0.6	27
753	Electronic and Magnetic Properties of Defected Monolayer WSe2 with Vacancies. Nanoscale Research Letters, 2019, 14, 192.	3.1	37
754	Tailoring exciton dynamics of monolayer transition metal dichalcogenides by interfacial electron-phonon coupling. Communications Physics, 2019, 2, .	2.0	27
755	Polarity Tunable Trionic Electroluminescence in Monolayer WSe₂. Nano Letters, 2019, 19, 7470-7475.	4.5	20
756	Photovoltaic activity of WSe2/Si hetero junction. Materials Research Bulletin, 2019, 120, 110602.	2.7	40
757	Multimode Signal Processor Unit Based on the Ambipolar WSe₂â€“Cr Schottky Junction. ACS Applied Materials & Interfaces, 2019, 11, 38895-38901.	4.0	3
758	Waterproof molecular monolayers stabilize 2D materials. Proceedings of the National Academy of Sciences of the United States of America, 2019, 116, 20844-20849.	3.3	32
759	2D boron dichalcogenides from the substitution of Mo with ionic B₂ pair in MoX₂ (X = S, Se and Te): high stability, large excitonic effect and high charge carrier mobility. Journal of Materials Chemistry C, 2019, 7, 1651-1658.	2.7	17

#	Article	IF	Citations
760	Controlled Vapor Growth and Nonlinear Optical Applications of Largeâ€Area 3R Phase WS₂ and WSe₂ Atomic Layers. Advanced Functional Materials, 2019, 29, 1806874.	7.8	92
761	Tuning the electronic structure of GeC/WS2 van der Waals heterostructure by electric field and strain: A first principles study. Computational Materials Science, 2019, 160, 301-308.	1.4	38
762	Symmetric Ultrafast Writing and Erasing Speeds in Quasiâ€Nonvolatile Memory via van der Waals Heterostructures. Advanced Materials, 2019, 31, e1808035.	11.1	50
763	Imaging Carrier Inhomogeneities in Ambipolar Tellurene Field Effect Transistors. Nano Letters, 2019, 19, 1289-1294.	4.5	31
764	Exciton in phosphorene: Strain, impurity, thickness, and heterostructure. Physical Review B, 2019, 99, .	1.1	17
765	Location-selective growth of two-dimensional metallic/semiconducting transition metal dichalcogenide heterostructures. Nanoscale, 2019, 11, 4183-4189.	2.8	16
766	A WSe₂ vertical field emission transistor. Nanoscale, 2019, 11, 1538-1548.	2.8	100
767	Monitoring the crystal orientation of black-arsenic via vibrational spectra. Journal of Materials Chemistry C, 2019, 7, 1228-1236.	2.7	13
768	Transport-map analysis of ionic liquid-gated ambipolar WSe₂ field-effect transistors. Semiconductor Science and Technology, 2019, 34, 075022.	1.0	4
769	Highly Stable Field Emission from a Tungsten Diselenide Monolayer on Zinc Oxide Nanowire by Geometrically Modulating Hot Electrons. Advanced Electronic Materials, 2019, 5, 1900128.	2.6	9
770	Interface charge-transfer induced intralayer excited-state biexcitons in graphene/WS₂ van der Waals heterostructures. Nanoscale, 2019, 11, 13552-13557.	2.8	18
771	Ultrahigh Gauge Factor in Graphene/MoS₂ Heterojunction Field Effect Transistor with Variable Schottky Barrier. ACS Nano, 2019, 13, 8392-8400.	7.3	54
772	On-chip integrated photonic circuits based on two-dimensional materials and hexagonal boron nitride as the optical confinement layer. Journal of Applied Physics, 2019, 125, 230901.	1.1	13
773	Van der Waals materials integrated nanophotonic devices [Invited]. Optical Materials Express, 2019, 9, 384.	1.6	58
774	Dissolved Gas Analysis in Transformer Oil Using Pt-Doped WSe₂ Monolayer Based on First Principles Method. IEEE Access, 2019, 7, 72012-72019.	2.6	58
775	Photostability of Monolayer Transition-Metal Dichalcogenides in Ambient Air and Acidic/Basic Aqueous Solutions. ACS Omega, 2019, 4, 10322-10327.	1.6	11
776	Chemical Vapor Deposition Grown Large-Scale Atomically Thin Platinum Diselenide with Semimetalâ€“Semiconductor Transition. ACS Nano, 2019, 13, 8442-8451.	7.3	87
777	A homogeneous pâ€“n junction diode by selective doping of few layer MoSe₂ using ultraviolet ozone for high-performance photovoltaic devices. Nanoscale, 2019, 11, 13469-13476.	2.8	41

#	Article	IF	Citations
778	Monolayer triphosphates MP₃ (M = Sn, Ge) with excellent basal catalytic activity for hydrogen evolution reaction. Nanoscale, 2019, 11, 12210-12219.	2.8	76
779	Nonvolatile MoTe₂ pâ€“n Diodes for Optoelectronic Logics. ACS Nano, 2019, 13, 7216-7222.	7.3	52
780	Quantum Dots for Hybrid Energy Harvesting: From Integration to Piezoâ€Phototronics. Israel Journal of Chemistry, 2019, 59, 747-761.	1.0	3
781	van der Waals epitaxial growth of ultrathin metallic NiSe nanosheets on WSe2 as high performance contacts for WSe2 transistors. Nano Research, 2019, 12, 1683-1689.	5.8	31
782	Scalable Epitaxial Growth of WSe2 Thin Films on SiO2/Si via a Self-Assembled PtSe2 Buffer Layer. Scientific Reports, 2019, 9, 8017.	1.6	8
783	Exciton aggregation induced photoluminescence enhancement of monolayer WS2. Applied Physics Letters, 2019, 114, .	1.5	11
784	Degenerate electron-doping in two-dimensional tungsten diselenide with a dimeric organometallic reductant. Materials Today, 2019, 30, 26-33.	8.3	14
785	Ultrafast nonlinear absorption and carrier relaxation in ReS2 and ReSe2 films. Journal of Applied Physics, 2019, 125, 173105.	1.1	17
786	Recent Advances in Quantum Effects of 2D Materials. Advanced Quantum Technologies, 2019, 2, 1800111.	1.8	32
787	Hybrid metal nanoantenna 2D-material photovoltaic device. Solar Energy Materials and Solar Cells, 2019, 200, 109918.	3.0	9
788	Point Defects and Localized Excitons in 2D WSe₂. ACS Nano, 2019, 13, 6050-6059.	7.3	127
790	Mechanical responses of WSe₂ monolayers: a molecular dynamics study. Materials Research Express, 2019, 6, 085071.	0.8	17
791	Ultraâ€Long Lifetimes of Single Quantum Emitters in Monolayer WSe₂/hBN Heterostructures. Advanced Quantum Technologies, 2019, 2, 1900022.	1.8	13
792	Ferroelectric-Driven Exciton and Trion Modulation in Monolayer Molybdenum and Tungsten Diselenides. ACS Nano, 2019, 13, 5335-5343.	7.3	61
793	High Optical Response of Niobium-Doped WSe2-Layered Crystals. Materials, 2019, 12, 1161.	1.3	5
794	Controlling Injection Barriers for Ambipolar 2D Semiconductors via Quasiâ€van der Waals Contacts. Advanced Science, 2019, 6, 1801841.	5.6	17
795	Synthesis of Superlattice InSe Nanosheets with Enhanced Electronic and Optoelectronic Performance. ACS Applied Materials & Interfaces, 2019, 11, 18511-18516.	4.0	13
796	Raman fingerprint of stacking order in <mml:math xmlns:mml="http://www.w3.org/1998/Math/MathML"><mml:mrow><mml:msub><mml:mi>HfS</mml:mi><mml:mn>2</mml:mn></mml:msub></mml:mrow></mml:math> heterobilayer. Physical Review B, 2019, 99, .	1.1	26

#	Article	IF	Citations
797	Room temperature nanocavity laser with interlayer excitons in 2D heterostructures. Science Advances, 2019, 5, eaav4506.	4.7	108
798	Tuning the Magnetic and Electronic Properties of Janus MoSSe Nanoribbon by Edge Modification: A Firstâ€Principles Study. Physica Status Solidi (B): Basic Research, 2019, 256, 1900106.	0.7	8
799	Ultrafast carrier dynamics in two-dimensional transition metal dichalcogenides. Journal of Materials Chemistry C, 2019, 7, 4304-4319.	2.7	51
800	High-Performance WS₂ Monolayer Light-Emitting Tunneling Devices Using 2D Materials Grown by Chemical Vapor Deposition. ACS Nano, 2019, 13, 4530-4537.	7.3	56
801	Electrical control of spatial resolution in mixed-dimensional heterostructured photodetectors. Proceedings of the National Academy of Sciences of the United States of America, 2019, 116, 6586-6593.	3.3	20
802	Metalâ€Guided Selective Growth of 2D Materials: Demonstration of a Bottomâ€Up CMOS Inverter. Advanced Materials, 2019, 31, e1900861.	11.1	36
803	High capacity conversion anodes in Li-ion batteries: A review. International Journal of Hydrogen Energy, 2019, 44, 10852-10905.	3.8	88
804	Lithographically patterned metallic conduction in single-layer MoS2 via plasma processing. Npj 2D Materials and Applications, 2019, 3, .	3.9	21
805	Lateral WSe₂ pâ€“n Junction Device Electrically Controlled by a Singleâ€Gate Electrode. Advanced Optical Materials, 2019, 7, 1900051.	3.6	19
806	Tailoring electronic properties and Schottky barrier in sandwich heterostructure based on graphene and tungsten diselenide. Diamond and Related Materials, 2019, 94, 129-136.	1.8	18
807	Thermally driven reversible photoluminescence modulation in WS2/VO2 heterostructure. Applied Surface Science, 2019, 480, 680-688.	3.1	7
808	Versatile Crystal Structures and (Opto)electronic Applications of the 2D Metal Monoâ€, Diâ€, and Triâ€Chalcogenide Nanosheets. Advanced Functional Materials, 2019, 29, 1900040.	7.8	58
809	Laser synthesis and functionalization of nanostructures. International Journal of Extreme Manufacturing, 2019, 1, 012002.	6.3	15
810	Design strategies for twoâ€dimensional material photodetectors to enhance device performance. InformaÄnÃ-MateriÃ¡ly, 2019, 1, 33-53.	8.5	158
811	Surface-diffusion-limited growth of atomically thin WS₂ crystals from coreâ€“shell nuclei. Nanoscale, 2019, 11, 8706-8714.	2.8	18
812	Electroluminescence from multi-particle exciton complexes in transition metal dichalcogenide semiconductors. Nature Communications, 2019, 10, 1709.	5.8	100
813	Characterization of atomic defects on the photoluminescence in twoâ€dimensional materials using transmission electron microscope. InformaÄnÃ-MateriÃ¡ly, 2019, 1, 85-97.	8.5	46
814	Solvent engineering for strong photoluminescence enhancement of monolayer molybdenum disulfide in redox-active molecular treatment. Applied Physics Express, 2019, 12, 051014.	1.1	5

#	Article	IF	Citations
815	MoTe₂ van der Waals homojunction pâ€“n diode with low resistance metal contacts. Nanoscale, 2019, 11, 9518-9525.	2.8	54
816	WS₂ monolayer-based light-emitting devices in a vertical pâ€“n architecture. Nanoscale, 2019, 11, 8372-8379.	2.8	20
817	Improvements in the Performance of a Visibleâ€“NIR Photodetector Using Horizontally Aligned TiS₃ Nanoribbons. ACS Omega, 2019, 4, 6180-6191.	1.6	33
818	Neutral and defect-induced exciton annihilation in defective monolayer WS₂. Nanoscale, 2019, 11, 7913-7920.	2.8	36
819	Nondestructive hole doping enabled photocurrent enhancement of layered tungsten diselenide. 2D Materials, 2019, 6, 024002.	2.0	7
820	Transient photoconductivity and free carrier dynamics in a monolayer WS₂ probed by time resolved Terahertz spectroscopy. Nanotechnology, 2019, 30, 265706.	1.3	20
821	Lateral heterostructures and one-dimensional interfaces in 2D transition metal dichalcogenides. Journal of Physics Condensed Matter, 2019, 31, 213001.	0.7	32
822	Experimental progress on layered topological semimetals. 2D Materials, 2019, 6, 032001.	2.0	26
823	Recent Developments in Controlled Vaporâ€Phase Growth of 2D Group 6 Transition Metal Dichalcogenides. Advanced Materials, 2019, 31, e1804939.	11.1	100
824	Dynamical screening in monolayer transition-metal dichalcogenides and its manifestations in the exciton spectrum. Journal of Physics Condensed Matter, 2019, 31, 203001.	0.7	38
825	Black Phosphorus-IGZO van der Waals Diode with Low-Resistivity Metal Contacts. ACS Applied Materials & Interfaces, 2019, 11, 10959-10966.	4.0	31
826	A Self-Limited Atomic Layer Deposition of WS₂ Based on the Chemisorption and Reduction of Bis(t-butylimino)bis(dimethylamino) Complexes. Chemistry of Materials, 2019, 31, 1881-1890.	3.2	24
827	Seamless Fabrication and Threshold Engineering in Monolayer MoS₂ Dualâ€Gated Transistors via Hydrogen Silsesquioxane. Advanced Electronic Materials, 2019, 5, 1800888.	2.6	13
828	Tuning carrier concentration in a superacid treated MoS2 monolayer. Scientific Reports, 2019, 9, 1989.	1.6	18
829	Translate and Summarize Complaints of Patient to Electronic Health Record by BiLSTM-CNN Attention model. , 2019, , .		1
830	Photo-amplification in Bipolar $mathbf{WSe}_{2}$ Transistors with Electrostatic Gating. , 2019, , .		0
831	Equilibrium shape of single-layer hexagonal boron nitride islands on iridium. Scientific Reports, 2019, 9, 19553.	1.6	6
832	Tunable WSe2 phototransistor enabled by electrostatically doped lateral p-n homojunction. , 2019, , .		0

#	Article	IF	Citations
833	Reconfigurable Local Photoluminescence of Atomically-Thin Semiconductors via Ferroelectric-Assisted Effects. Nanomaterials, 2019, 9, 1620.	1.9	3
834	Characterization and Stability of Janus TiXY (X/Y = S, Se, and Te) Monolayers. Journal of Physical Chemistry C, 2019, 123, 29922-29931.	1.5	30
835	Two-dimensional MgX₂Se₄ (X = Al, Ga) monolayers with tunable electronic properties for optoelectronic and photocatalytic applications. Nanoscale, 2019, 11, 19806-19813.	2.8	21
836	A unipolar nonvolatile resistive switching behavior in a layered transition metal oxide. Nanoscale, 2019, 11, 20497-20506.	2.8	24
837	Length- and Thickness-Dependent Optical Response of Liquid-Exfoliated Transition Metal Dichalcogenides. Chemistry of Materials, 2019, 31, 10049-10062.	3.2	57
838	High performance room temperature p-type injection in few-layered tungsten diselenide films from cobalt and palladium contacts. Materials Research Express, 0, , .	0.8	2
839	Methane-Mediated Vapor Transport Growth of Monolayer WSe2 Crystals. Nanomaterials, 2019, 9, 1642.	1.9	1
840	Explaining observed stability of excitons in highly excited CdSe nanoplatelets. Physical Review B, 2019, 100, .	1.1	14
841	Optical fingerprint of bright and dark localized excitonic states in atomically thin 2D materials. Physical Chemistry Chemical Physics, 2019, 21, 26077-26083.	1.3	7
842	p-MoS₂/n-InSe van der Waals heterojunctions and their applications in all-2D optoelectronic devices. RSC Advances, 2019, 9, 35039-35044.	1.7	15
843	Progress, Challenges, and Opportunities for 2D Material Based Photodetectors. Advanced Functional Materials, 2019, 29, 1803807.	7.8	884
844	Electrically-Transduced Chemical Sensors Based on Two-Dimensional Nanomaterials. Chemical Reviews, 2019, 119, 478-598.	23.0	521
845	Symmetry-Controlled Reversible Photovoltaic Current Flow in Ultrathin All 2D Vertically Stacked Graphene/MoS₂/WS₂/Graphene Devices. ACS Applied Materials & Interfaces, 2019, 11, 2234-2242.	4.0	32
846	Recent progress in synthesis, properties, and applications of hexagonal boron nitride-based heterostructures. Nanotechnology, 2019, 30, 074003.	1.3	31
847	Stress-induced bandgap renormalization in atomic crystals. Solid State Communications, 2019, 288, 18-21.	0.9	7
848	Tribo-piezoelectricity in Janus transition metal dichalcogenide bilayers: A first-principles study. Nano Energy, 2019, 56, 33-39.	8.2	58
849	Doping of Monolayer Transition-Metal Dichalcogenides via Physisorption of Aromatic Solvent Molecules. Journal of Physical Chemistry Letters, 2019, 10, 540-547.	2.1	52
850	Tunable and enhanced light emission in hybrid WS2-optical-fiber-nanowire structures. Light: Science and Applications, 2019, 8, 8.	7.7	51

#	Article	IF	Citations
851	Probing exciton species in atomically thin WS₂â€“graphene heterostructures. JPhys Materials, 2019, 2, 025001.	1.8	5
852	Current Rectification in a Structure: ReSe2/Au Contacts on Both Sides of ReSe2. Nanoscale Research Letters, 2019, 14, 1.	3.1	401
853	Two Dimensional Î²-InSe with Layer-Dependent Properties: Band Alignment, Work Function and Optical Properties. Nanomaterials, 2019, 9, 82.	1.9	43
854	Nonlinear Nanophotonics With 2D Transition Metal Dichalcogenides. , 2019, , 305-318.		5
855	Stable monolayer of the RuO₂ structure by the Peierls distortion. Philosophical Magazine, 2019, 99, 376-385.	0.7	18
856	New Oneâ€Dimensional Material Nb₂Se₉: Theoretical Prediction of Indirect to Direct Band Gap Transition due to Dimensional Reduction. Physica Status Solidi - Rapid Research Letters, 2019, 13, 1800517.	1.2	20
857	Investigation of multiband plasmonic metamaterial perfect absorbers based on graphene ribbons by the phase-coupled method. Carbon, 2019, 141, 481-487.	5.4	110
858	Modulation of the electronic properties of two-dimensional MoTe2/WSe2 heterostructure by electrical field. Physica E: Low-Dimensional Systems and Nanostructures, 2019, 108, 90-95.	1.3	14
859	TiS₂ Monolayer as an Emerging Ultrathin Bifunctional Catalyst: Influence of Defects and Functionalization. ChemPhysChem, 2019, 20, 608-617.	1.0	24
860	Recent Advances in Flexible Inorganic Light Emitting Diodes: From Materials Design to Integrated Optoelectronic Platforms. Advanced Optical Materials, 2019, 7, 1800936.	3.6	75
861	Dirac Fermion and Plasmon Dynamics in Graphene and 3D Topological Insulators. Advanced Optical Materials, 2020, 8, 1801334.	3.6	13
862	ZrS3/MS2 and ZrS3/MXY (M Mo, W; X, Y S, Se, Te; Xâ€â‰ Y) type-II van der Waals hetero-bilayers: Prospective candidates in 2D excitonic solar cells. Applied Surface Science, 2020, 499, 143894.	3.1	51
863	Optical Properties and Light-Emission Device Applications of 2-D Layered Semiconductors. Proceedings of the IEEE, 2020, 108, 676-703.	16.4	19
864	Recent Developments and Novel Applications of Thin Film, Lightâ€Emitting Transistors. Advanced Functional Materials, 2020, 30, 1905269.	7.8	53
865	Controlling exciton transport in monolayer MoSe₂ by dielectric screening. Nanoscale Horizons, 2020, 5, 139-143.	4.1	19
866	Emerging 2D Layered Materials for Perovskite Solar Cells. Advanced Energy Materials, 2020, 10, 1902253.	10.2	79
867	Two-dimensional materials toward future photovoltaic devices. , 2020, , 117-158.		2
868	Role of metal contacts and effect of annealing in high performance 2D WSe2 field-effect transistors. Surface and Coatings Technology, 2020, 381, 125084.	2.2	19

#	Article	IF	Citations
869	High rectification ratio metal-insulator-semiconductor tunnel diode based on single-layer MoS₂. Nanotechnology, 2020, 31, 075202.	1.3	6
870	Enhanced bulk photovoltaic effect in ZnO:Bi x (p-type)/MoS2 (n-type) heterostructure by tuning Bi content. Semiconductor Science and Technology, 2020, 35, 015006.	1.0	0
871	Inorganic 2D Luminescent Materials: Structure, Luminescence Modulation, and Applications. Advanced Optical Materials, 2020, 8, 1900978.	3.6	37
872	Tunable electric properties of bilayer MX2 (Mâ€¯=â€¯Ge, Sn; Xâ€¯=â€¯S, Se) with different strain and external electric field. Physica B: Condensed Matter, 2020, 581, 411673.	1.3	5
874	Introduction to Carbon-Based Nanostructures. , 2020, , 1-10.		0
875	The New Family of Two-Dimensional Materials and van der Waals Heterostructures. , 2020, , 70-91.		0
876	Quantum Transport: General Concepts. , 2020, , 92-119.		0
877	Klein Tunneling and Ballistic Transport in Graphene and Related Materials. , 2020, , 120-144.		0
878	Quantum Transport in Disordered Graphene-Based Materials. , 2020, , 145-209.		0
879	Control of spin and valley Hall effects in monolayer transition metal dichalcogenides by magnetic proximity effect. Journal of Applied Physics, 2020, 127, 023903.	1.1	8
880	Optical performance and growth mechanism of a 2D WS₂â€“MoWS₂ hybrid heterostructure fabricated by a one-step CVD strategy. CrystEngComm, 2020, 22, 660-665.	1.3	9
883	Electronic Properties of Carbon-Based Nanostructures. , 2020, , 11-69.		0
884	Quantum Hall Effects in Graphene. , 2020, , 210-236.		0
885	Spin-Related Phenomena. , 2020, , 237-277.		0
886	Ab Initio and Multiscale Quantum Transport in Graphene-Based Materials. , 2020, , 293-353.		0
890	Ultrafast growth of large single crystals of monolayer WS2 and WSe2. National Science Review, 2020, 7, 737-744.	4.6	64
891	Light-triggered two-dimensional lateral homogeneous p-n diodes for opto-electrical interconnection circuits. Science Bulletin, 2020, 65, 293-299.	4.3	29
892	Drain-engineered carbon-nanotube-film field-effect transistors with high performance and ultra-low current leakage. Nano Research, 2020, 13, 1875-1881.	5.8	13

#	Article	IF	Citations
893	Direct Imaging of Individual Molecular Binding to Clean Nanopore Edges in 2D Monolayer MoS₂. ACS Nano, 2020, 14, 153-165.	7.3	19
894	WSe₂ Nanosheets Synthesized by a Solvothermal Process as Advanced Nanofluids for Thermal Solar Energy. ACS Sustainable Chemistry and Engineering, 2020, 8, 1627-1636.	3.2	20
895	Tunneling-based rectification and photoresponsivity in black phosphorus/hexagonal boron nitride/rhenium diselenide van der Waals heterojunction diode. Nanoscale, 2020, 12, 3455-3468.	2.8	40
896	A high-beam-quality passively Q-switched 2ÂÎ¼m solid-state laser with a WSe2 saturable absorber. Optics and Laser Technology, 2020, 125, 105960.	2.2	12
897	Quantitative Mapping of the Charge Density in a Monolayer of MoS₂ at Atomic Resolution by Off-Axis Electron Holography. ACS Nano, 2020, 14, 524-530.	7.3	10
898	2D semiconducting materials for electronic and optoelectronic applications: potential and challenge. 2D Materials, 2020, 7, 022003.	2.0	168
899	Centimeterâ€Scale and Visible Wavelength Monolayer Lightâ€Emitting Devices. Advanced Functional Materials, 2020, 30, 1907941.	7.8	20
900	Artificial Optoelectronic Synapses Based on Ferroelectric Field-Effect Enabled 2D Transition Metal Dichalcogenide Memristive Transistors. ACS Nano, 2020, 14, 746-754.	7.3	190
901	Ultrafast Carrier Dynamics in Two-Dimensional Electron Gas-like K-Doped MoS₂. Journal of Physical Chemistry C, 2020, 124, 19187-19195.	1.5	0
902	High performance complementary WS₂ devices with hybrid Gr/Ni contacts. Nanoscale, 2020, 12, 21280-21290.	2.8	27
903	Carbon Nanomaterials for Halide Perovskitesâ€Based Hybrid Photodetectors. Advanced Materials Technologies, 2020, 5, 2000643.	3.0	9
904	Temperature- and power-dependent phonon properties of suspended few layers of tungsten diselenide. Vibrational Spectroscopy, 2020, 111, 103169.	1.2	10
905	Lateral Monolayer MoSe₂â€“WSe₂ pâ€“n Heterojunctions with Giant Builtâ€in Potentials. Small, 2020, 16, e2002263.	5.2	50
906	The highly-efficient light-emitting diodes based on transition metal dichalcogenides: from architecture to performance. Nanoscale Advances, 2020, 2, 4323-4340.	2.2	41
907	Electro-optical properties of monolayer and bilayer boron-doped <mml:math xmlns:mml="http://www.w3.org/1998/Math/MathML" altimg="si1.svg"><mml:mrow><mml:msub><mml:mtext>C</mml:mtext><mml:mn>3</mml:mn></mml:msub></mml:mrow></mml:mat Tunable electronic structure via strain engineering and electric field. Carbon, 2020, 168, 220-229.	5.4	66
908	Transition metal dichalcogenides based two-dimensional heterostructures for optoelectronic applications. , 2020, , 125-149.		15
909	Photonic and optoelectronic properties of layered semiconductors. Applied Nanoscience (Switzerland), 2020, 10, 3933-3938.	1.6	2
910	Machine learning in materials modelingâ€”fundamentals and the opportunities in 2D materials. , 2020, , 445-468.		7

#	Article	IF	Citations
911	Growth of 2-D MoS2 thin film by facile electrochemical deposition. AIP Conference Proceedings, 2020, , .	0.3	0
912	Modulation Doping via a Two-Dimensional Atomic Crystalline Acceptor. Nano Letters, 2020, 20, 8446-8452.	4.5	44
913	Modification of the Electronic Transport in Atomically Thin WSe₂ by Oxidation. Advanced Materials Interfaces, 2020, 7, 2000422.	1.9	11
914	Substrate effect on the photoluminescence of chemical vapor deposition transferred monolayer WSe2. Journal of Applied Physics, 2020, 128, 043101.	1.1	16
915	Two-dimensional functional materials: from properties to potential applications. International Journal of Smart and Nano Materials, 2020, 11, 247-264.	2.0	14
916	Electric-double-layer pâ€“iâ€“n junctions in WSe2. Scientific Reports, 2020, 10, 12890.	1.6	4
917	Ab initio calculations of structural and electronic properties of WSe2 compound. Materials Today: Proceedings, 2020, 31, S130-S133.	0.9	2
918	Photocarrier Dynamics in TlGaS₂ Nanoflakes and van der Waals Heterostructures with Hexagonal Boron Nitride and WS₂ Nanoflakes: Implications for Optoelectronic Applications. ACS Applied Nano Materials, 2020, 3, 8702-8707.	2.4	3
919	Atomic-Scale Interface Engineering for Constructing p-CuPc/n-CdS Coreâ€“Shell Heterojunctions toward Light-Harvesting Application. ACS Applied Energy Materials, 2020, 3, 8765-8773.	2.5	2
920	Effect of sulfosalt and polymers on performance parameter of SPR biosensor. Optical and Quantum Electronics, 2020, 52, 1.	1.5	16
921	Naturally occurring van der Waals materials. Npj 2D Materials and Applications, 2020, 4, .	3.9	75
922	Progress and Prospects in Transition-Metal Dichalcogenide Research Beyond 2D. Chemical Reviews, 2020, 120, 12563-12591.	23.0	163
923	Integrated single photon emitters. AVS Quantum Science, 2020, 2, .	1.8	40
924	Control of the Schottky Barrier and Contact Resistance at Metalâ€“WSe₂ Interfaces by Polymeric Doping. Advanced Electronic Materials, 2020, 6, 2000616.	2.6	24
926	Emergent phenomena and proximity effects in two-dimensional magnets and heterostructures. Nature Materials, 2020, 19, 1276-1289.	13.3	213
927	Excitonic Lasers in Atomically Thin 2D Semiconductors. , 2020, 2, 1328-1342.		12
928	Biexcitons in highly excited CdSe nanoplatelets. Physical Review B, 2020, 102, .	1.1	9
929	Neutral Exciton Diffusion in Monolayer MoS₂. ACS Nano, 2020, 14, 13433-13440.	7.3	62

#	Article	IF	Citations
930	Multioperationâ€Mode Lightâ€Emitting Fieldâ€Effect Transistors Based on van der Waals Heterostructure. Advanced Materials, 2020, 32, e2003567.	11.1	12
931	A Self-Powered Photovoltaic Photodetector Based on a Lateral WSe₂-WSe₂ Homojunction. ACS Applied Materials & Interfaces, 2020, 12, 44934-44942.	4.0	71
932	Trion induced photoluminescence of a doped MoS2 monolayer. Journal of Chemical Physics, 2020, 153, 044132.	1.2	25
933	WSe₂ Homojunction pâ€“n Diode Formed by Photoinduced Activation of Mid-Gap Defect States in Boron Nitride. ACS Applied Materials & Interfaces, 2020, 12, 42007-42015.	4.0	34
934	A review of molybdenum disulfide (MoS₂) based photodetectors: from ultra-broadband, self-powered to flexible devices. RSC Advances, 2020, 10, 30529-30602.	1.7	211
935	Ab-initio investigation of preferential triangular self-formation of oxide heterostructures of monolayer $$hbox {WSe}_{2}$$. Scientific Reports, 2020, 10, 21737.	1.6	1
936	Investigating the lattice dynamics and electronic structure of monolayer PdTe2. AIP Conference Proceedings, 2020, , .	0.3	1
937	Se intercalation between <mml:math xmlns:mml="http://www.w3.org/1998/Math/MathML"><mml:mrow><mml:mi>Pt</mml:mi><mml:msub><mml:mi>Se</mml:mi><mml:m and the Pt surface during synthesis of <mml:math xmlns:mml="http://www.w3.org/1998/Math/MathML"><mml:mrow><mml:mi>Pt</mml:mi><mml:msub><mml:mi>Se</mml:mi><mml:m by direct selenization of Pt(111). Physical Review B, 2020, 102, .	1.1	3
938	Gate-controlled spinâ€“valleyâ€“layer locking in bilayer transition-metal dichalcogenides. Nanoscale, 2020, 12, 22281-22288.	2.8	9
939	Mechanisms and Applications of Steady-State Photoluminescence Spectroscopy in Two-Dimensional Transition-Metal Dichalcogenides. ACS Nano, 2020, 14, 14579-14604.	7.3	56
940	Operational Limits and Failure Mechanisms in All-2D van der Waals Vertical Heterostructure Devices with Long-Lived Persistent Electroluminescence. ACS Nano, 2020, 14, 15533-15543.	7.3	7
941	Stable single-layers of calcium halides (CaX₂, X = F, Cl, Br, I). Journal of Chemical Physics, 2020, 152, 164116.	1.2	13
942	Robust room temperature emissions of trion in darkish WSe2 monolayers: effects of dark neutral and charged excitonic states. Journal of Physics Condensed Matter, 2020, 32, 365702.	0.7	7
943	2D Tungsten Chalcogenides: Synthesis, Properties and Applications. Advanced Materials Interfaces, 2020, 7, 2000002.	1.9	39
944	Large area chemical vapour deposition grown transition metal dichalcogenide monolayers automatically characterized through photoluminescence imaging. Npj 2D Materials and Applications, 2020, 4, .	3.9	20
945	2D materials beyond graphene toward Si integrated infrared optoelectronic devices. Nanoscale, 2020, 12, 11784-11807.	2.8	59
946	Recent Progress on Lightâ€Emitting Electrochemical Cells with Nonpolymeric Materials. Advanced Functional Materials, 2020, 30, 1908641.	7.8	33
947	Thermal Evaporation of Large-Area SnS₂ Thin Films with a UV-to-NIR Photoelectric Response for Flexible Photodetector Applications. ACS Applied Materials & Interfaces, 2020, 12, 24940-24950.	4.0	46

#	Article	IF	Citations
948	Charge transport in nnn and npn phosphorene junctions: The use of phosphorene pn junctions as rectifiers. Physica E: Low-Dimensional Systems and Nanostructures, 2020, 124, 114239.	1.3	11
949	Emerging Opportunities for Electrostatic Control in Atomically Thin Devices. ACS Nano, 2020, 14, 6498-6518.	7.3	51
950	Charge carrier scattering and ultrafast Auger dynamics in two-dimensional superatomic semiconductors. Applied Physics Letters, 2020, 116, 201109.	1.5	1
951	Origins of Fermi Level Pinning between Tungsten Dichalcogenides (WS2, WTe2) and Bulk Metal Contacts: Interface Chemistry and Band Alignment. Journal of Physical Chemistry C, 2020, 124, 14550-14563.	1.5	19
952	Synthesis and Applications of Wide Bandgap 2D Layered Semiconductors Reaching the Green and Blue Wavelengths. ACS Applied Electronic Materials, 2020, 2, 1777-1814.	2.0	50
953	2D pn junctions driven out-of-equilibrium. Nanoscale Advances, 2020, 2, 3252-3262.	2.2	6
954	Observation of the Interlayer Exciton Gases in WSe₂ -p:WSe₂ Heterostructures. ACS Photonics, 2020, 7, 1622-1627.	3.2	7
955	Three-particle states and brightening of intervalley excitons in a doped <mml:math xmlns:mml="http://www.w3.org/1998/Math/MathML"><mml:msub><mml:mi>MoS</mml:mi><mml:mn>2</mml:mn></mml:msub></mml monolayer. Physical Review B, 2020, 101, .	1.1	15
956	Carrier polarity modulation of molybdenum ditelluride (MoTe₂) for phototransistor and switching photodiode applications. Nanoscale, 2020, 12, 15687-15696.	2.8	26
957	Photo-responsive MoS₂/organic-rubrene heterojunction field-effect-transistor: application to photo-triggered ternary inverter. Semiconductor Science and Technology, 2020, 35, 065020.	1.0	15
958	Modulation of carrier lifetime in MoS2 monolayer by uniaxial strain. Chinese Physics B, 2020, 29, 077201.	0.7	4
959	Tuning Electrical and Optical Properties of MoSe₂ Transistors via Elemental Doping. Advanced Materials Technologies, 2020, 5, 2000307.	3.0	15
960	Electrically controlled dielectric band gap engineering in a two-dimensional semiconductor. Physical Review B, 2020, 101, .	1.1	17
961	Excitonic complexes and optical gain in two-dimensional molybdenum ditelluride well below the Mott transition. Light: Science and Applications, 2020, 9, 39.	7.7	35
962	Decorating a WSe2 monolayer with Au nanoparticles: A study combined first-principles calculation with material genome approach. Surface and Coatings Technology, 2020, 388, 125563.	2.2	3
963	Evidence for the Dominance of Carrier-Induced Band Gap Renormalization over Biexciton Formation in Cryogenic Ultrafast Experiments on MoS₂ Monolayers. Journal of Physical Chemistry Letters, 2020, 11, 2658-2666.	2.1	17
964	Facile p-Doping of Few-Layer MoTe₂ by Controllable Surface Oxidation toward High-Performance Complementary Devices. ACS Applied Electronic Materials, 2020, 2, 920-926.	2.0	19
965	Breaking symmetry in device design for self-driven 2D material based photodetectors. Nanoscale, 2020, 12, 8109-8118.	2.8	29

#	Article	IF	Citations
966	A gate-tunable symmetric bipolar junction transistor fabricatedviafemtosecond laser processing. Nanoscale Advances, 2020, 2, 1733-1740.	2.2	10
967	Layer-Dependent and In-Plane Anisotropic Properties of Low-Temperature Synthesized Few-Layer PdSe₂ Single Crystals. ACS Nano, 2020, 14, 4963-4972.	7.3	64
968	Electrically pumped WSe2-based light-emitting van der Waals heterostructures embedded in monolithic dielectric microcavities. 2D Materials, 2020, 7, 031006.	2.0	16
969	High-Performance p-BP/n-PdSe₂ Near-Infrared Photodiodes with a Fast and Gate-Tunable Photoresponse. ACS Applied Materials & Interfaces, 2020, 12, 19625-19634.	4.0	67
970	Metalâ€“organic chemical vapor deposition of 2D van der Waals materialsâ€”The challenges and the extensive future opportunities. APL Materials, 2020, 8, .	2.2	45
971	Ultrafast machine vision with 2D material neural network image sensors. Nature, 2020, 579, 62-66.	13.7	546
972	Enhanced Spin Seebeck Effect in Monolayer Tungsten Diselenide Due to Strong Spin Current Injection at Interface. Advanced Functional Materials, 2020, 30, 2003192.	7.8	22
973	Reconfigurable logic and neuromorphic circuits based on electrically tunable two-dimensional homojunctions. Nature Electronics, 2020, 3, 383-390.	13.1	191
974	Polarized Lightâ€Emitting Diodes Based on Anisotropic Excitons in Fewâ€Layer ReS₂. Advanced Materials, 2020, 32, e2001890.	11.1	49
975	Ferroelectric field-effect transistors for logic and in-situ memory applications. Nanotechnology, 2020, 31, 424007.	1.3	9
976	Thermally Induced Defects on WSe₂. Journal of Physical Chemistry C, 2020, 124, 15337-15346.	1.5	25
977	Photoactivation of Strong Photoluminescence in Superacid-Treated Monolayer Molybdenum Disulfide. ACS Applied Materials & Interfaces, 2020, 12, 36496-36504.	4.0	24
978	Broadband optical properties of monolayer and bulk MoS2. Npj 2D Materials and Applications, 2020, 4, .	3.9	112
979	Computational discovery of two-dimensional HfO₂ zoo based on evolutionary structure search. Physical Chemistry Chemical Physics, 2020, 22, 4481-4489.	1.3	5
980	MoTe₂ pâ€“n Homojunctions Defined by Ferroelectric Polarization. Advanced Materials, 2020, 32, e1907937.	11.1	115
981	Outâ€ofâ€Plane Homojunction Enabled High Performance SnS₂ Lateral Phototransistor. Advanced Optical Materials, 2020, 8, 1901971.	3.6	27
982	Multifunctional and high-performance GeSe/PdSe₂heterostructure device with a fast photoresponse. Journal of Materials Chemistry C, 2020, 8, 4743-4753.	2.7	47
983	Observation of the hot-phonon effect in monolayer MoS₂. Nanotechnology, 2020, 31, 235712.	1.3	16

#	Article	IF	Citations
984	Temperature-dependent Raman spectroscopy studies of 1â€“5-layer WSe2. Nano Research, 2020, 13, 591-595.	5.8	34
985	Quasi-two-dimensional magnon identification in antiferromagnetic<mml:math xmlns:mml="http://www.w3.org/1998/Math/MathML"><mml:mrow><mml:mi>FeP</mml:mi><mml:msub><mml:mi mathvariant="normal">S</mml:mi><mml:mn>3</mml:mn></mml:msub></mml:mrow></mml:math>via magneto-Raman spectroscopy. Physical Review B, 2020, 101, .	1.1	53
986	Fano resonances from plasmon-exciton coupling in hetero-bilayer WSe2-WS2 on Au nanorod arrays. Photonics and Nanostructures - Fundamentals and Applications, 2020, 41, 100783.	1.0	1
987	First principles study for band engineering of MoS2 monolayer with Mn doping. Solid State Communications, 2020, 309, 113844.	0.9	12
988	Dynamical screening effects of substrate phonons on two-dimensional excitons. Physical Review B, 2020, 101, .	1.1	12
989	Low-loss composite photonic platform based on 2D semiconductor monolayers. Nature Photonics, 2020, 14, 256-262.	15.6	140
990	Quantum properties and applications of 2D Janus crystals and their superlattices. Applied Physics Reviews, 2020, 7, .	5.5	156
991	WSe₂ 2D pâ€type semiconductorâ€based electronic devices for information technology: Design, preparation, and applications. InformaÄnÂ-MateriÂ¡ly, 2020, 2, 656-697.	8.5	115
992	A high-efficiency electrocatalyst for hydrogen evolution based on tree-like amorphous MoS2 nanostructures prepared by glancing angle deposition. Journal of Solid State Chemistry, 2020, 286, 121255.	1.4	9
993	Octahedrally coordinated single layered CaF₂: robust insulating behaviour. Physical Chemistry Chemical Physics, 2020, 22, 2949-2954.	1.3	11
994	Hematite at its thinnest limit. 2D Materials, 2020, 7, 025029.	2.0	13
995	Two-dimensional electronic devices modulated by the activation of donor-like states in boron nitride. Nanoscale, 2020, 12, 18171-18179.	2.8	28
996	Transient Absorption Microscopy of Layered Crystal AsSbS₃. Journal of Physical Chemistry A, 2020, 124, 1047-1052.	1.1	8
997	Valley phonons and exciton complexes in a monolayer semiconductor. Nature Communications, 2020, 11, 618.	5.8	128
998	Strong Lightâ€“Matter Interactions Enabled by Polaritons in Atomically Thin Materials. Advanced Optical Materials, 2020, 8, 1901473.	3.6	56
999	Quantum Transport beyond DC. , 2020, , 278-292.		0
1001	Excitons in two-dimensional atomic layer materials from time-dependent density functional theory: mono-layer and bi-layer hexagonal boron nitride and transition-metal dichalcogenides. Physical Chemistry Chemical Physics, 2020, 22, 2908-2916.	1.3	12
1002	Few-Layer <mml:math xmlns:mml="http://www.w3.org/1998/Math/MathML" display="inline" overflow="scroll"><mml:mi>Î²</mml:mi></mml:math> - <mml:math xmlns:mml="http://www.w3.org/1998/Math/MathML" display="inline" overflow="scroll"><mml:mrow><mml:mi>Sn</mml:mi><mml:mi>Se</mml:mi></mml:mrow></mml:math> with Strong Visible Light Absorbance and Ultrahigh Carrier Mobility. Physical Review Applied, 2020, 13, .	1.5	8

#	Article	IF	Citations
1003	Resonant Tunneling Spectroscopy to Probe the Giant Stark Effect in Atomically Thin Materials. Advanced Materials, 2020, 32, e1906942.	11.1	18
1004	Gate-Modulated Ultrasensitive Visible and Near-Infrared Photodetection of Oxygen Plasma-Treated WSe₂ Lateral pn-Homojunctions. ACS Applied Materials & Interfaces, 2020, 12, 23261-23271.	4.0	41
1005	P-type laser-doped WSe₂/MoTe₂ van der Waals heterostructure photodetector. Nanotechnology, 2020, 31, 295201.	1.3	25
1006	Near-Unity Light Absorption in a Monolayer WS₂ Van der Waals Heterostructure Cavity. Nano Letters, 2020, 20, 3545-3552.	4.5	48
1007	Photogating WS₂ Photodetectors Using Embedded WSe₂ Charge Puddles. ACS Nano, 2020, 14, 4559-4566.	7.3	87
1008	Ambipolar device simulation based on the drift-diffusion model in ion-gated transition metal dichalcogenide transistors. Npj Computational Materials, 2020, 6, .	3.5	5
1009	Interlayer excitons in van der Waals heterostructures: Binding energy, Stark shift, and field-induced dissociation. Scientific Reports, 2020, 10, 5537.	1.6	46
1010	Magneto-electronics, transport properties, and tuning effects of arsenene armchair nanotubes doped with transition metal atoms. Nanotechnology, 2020, 31, 315206.	1.3	15
1011	Mid-infrared Polarized Emission from Black Phosphorus Light-Emitting Diodes. Nano Letters, 2020, 20, 3651-3655.	4.5	69
1012	Nonvolatile Programmable WSe₂ Photodetector. Advanced Optical Materials, 2020, 8, 2000417.	3.6	16
1013	Large-area 2D TMD layers for mechanically reconfigurable electronic devices. Journal Physics D: Applied Physics, 2020, 53, 313002.	1.3	22
1014	Layer-resolved absorption of light in arbitrarily anisotropic heterostructures. Physical Review B, 2020, 101, .	1.1	29
1015	Diamond membranes for photonic devices. Semiconductors and Semimetals, 2021, 104, 173-217.	0.4	1
1016	Strongly Quantum-Confined Blue-Emitting Excitons in Chemically Configurable Multiquantum Wells. ACS Nano, 2021, 15, 4085-4092.	7.3	21
1017	Two-dimensional materials for light emitting applications: Achievement, challenge and future perspectives. Nano Research, 2021, 14, 1912-1936.	5.8	34
1018	Staggered band offset induced high performance opto-electronic devices: Atomically thin vertically stacked GaSe-SnS2 van der Waals p-n heterostructures. Applied Surface Science, 2021, 535, 147480.	3.1	16
1019	Building Functional Memories and Logic Circuits with 2D Boron Nitride. Advanced Functional Materials, 2021, 31, 2004733.	7.8	22
1020	2D Material Based Synaptic Devices for Neuromorphic Computing. Advanced Functional Materials, 2021, 31, 2005443.	7.8	165

#	Article	IF	Citations
1021	Emerging Lightâ€Emitting Materials for Photonic Integration. Advanced Materials, 2021, 33, e2003733.	11.1	25
1022	2D Hybrid Halide Perovskites: Synthesis, Properties, and Applications. Solar Rrl, 2021, 5, .	3.1	20
1023	Single nanoflake-based PtSe2 pâ€“n junction (in-plane) formed by optical excitation of point defects in BN for ultrafast switching photodiodes. Journal of Materials Chemistry C, 2021, 9, 199-207.	2.7	23
1024	Ambipolar 2D Semiconductors and Emerging Device Applications. Small Methods, 2021, 5, e2000837.	4.6	39
1025	Gateâ€Controlled Polarityâ€Reversible Photodiodes with Ambipolar 2D Semiconductors. Advanced Functional Materials, 2021, 31, 2007559.	7.8	38
1026	The first-principles and BTE investigation of phonon transport in 1T-TiSe₂. Physical Chemistry Chemical Physics, 2021, 23, 1627-1638.	1.3	9
1027	Sequential lithium deposition on hexagonal boron nitride monolayer on Ir(111): Identifying intercalation and adsorption. Surface Science, 2021, 706, 121786.	0.8	3
1028	Twoâ€dimensional Boron Nitride for Electronics and Energy Applications. Energy and Environmental Materials, 2022, 5, 10-44.	7.3	11
1029	Twoâ€Dimensional Materials for Integrated Photonics: Recent Advances and Future Challenges. Small Science, 2021, 1, 2000053.	5.8	56
1030	Stable Janus TaSe2 single-layers via surface functionalization. Applied Surface Science, 2021, 538, 148064.	3.1	7
1031	Atomically Thin Hexagonal Boron Nitride and Its Heterostructures. Advanced Materials, 2021, 33, e2000769.	11.1	71
1032	Substitutional doping in 2D transition metal dichalcogenides. Nano Research, 2021, 14, 1668-1681.	5.8	92
1033	A two-step chemical vapor deposition process for the growth of continuous vertical heterostructure WSe₂/h-BN and its optical properties. RSC Advances, 2021, 11, 16962-16969.	1.7	7
1034	Photodetectors based on homojunctions of transition metal dichalcogenides. Wuli Xuebao/Acta Physica Sinica, 2021, 70, 177301-177301.	0.2	1
1035	Microsphere-coupled light emission control of van der Waals heterostructures. Nanoscale, 2021, 13, 4262-4268.	2.8	2
1036	Structural and surface morphological studies of WSe2 2-D material. AIP Conference Proceedings, 2021, , .	0.3	1
1037	Reversible photoluminescence modulation of monolayer MoS₂ on a ferroelectric substrate by light irradiation and thermal annealing. Physical Chemistry Chemical Physics, 2021, 23, 17265-17270.	1.3	0
1038	The effect of the stacking arrangement on the device behavior of bilayer MoS2 FETs. Journal of Computational Electronics, 2021, 20, 161-168.	1.3	6

#	Article	IF	Citations
1039	Controllable preparation and photoelectric applications of two-dimensional in-plane and van der Waals heterostructures. Wuli Xuebao/Acta Physica Sinica, 2021, 70, 027901-027901.	0.2	5
1040	Solution-Processable Carbon and Graphene Quantum Dots Photodetectors. Lecture Notes in Nanoscale Science and Technology, 2021, , 157-214.	0.4	1
1041	Recent progress and challenges based on two-dimensional material photodetectors. Nano Express, 2021, 2, 012001.	1.2	31
1042	Chromgruppe: Elemente der sechsten Nebengruppe. , 2021, , 573-622.		0
1043	Fast and high photoresponsivity gallium telluride/hafnium selenide van der Waals heterostructure photodiode. Journal of Materials Chemistry C, 2021, 9, 7110-7118.	2.7	10
1044	Metal halide perovskite nanocrystals: application in high-performance photodetectors. Materials Advances, 2021, 2, 856-879.	2.6	18
1045	Direct growth of tungsten disulfide on gallium nitride and the photovoltaic characteristics of the heterojunctions. Semiconductor Science and Technology, 2021, 36, 025016.	1.0	3
1046	Plasmonic metasurfaces for probing two-dimensional materials. AIP Conference Proceedings, 2021, , .	0.3	0
1047	Non-invasively improving the Schottky barrier of MoS₂/metal contacts by inserting a SiC layer. Physical Chemistry Chemical Physics, 2021, 23, 14796-14802.	1.3	6
1048	Ideal PN photodiode using doping controlled WSe₂â€“MoSe₂ lateral heterostructure. Journal of Materials Chemistry C, 2021, 9, 3504-3512.	2.7	16
1049	2D Homojunctions for Electronics and Optoelectronics. Advanced Materials, 2021, 33, e2005303.	11.1	66
1050	Giant Photoluminescence Enhancement and Resonant Charge Transfer in Atomically Thin Two-Dimensional Cr₂Ge₂Te₆/WS₂ Heterostructures. ACS Applied Materials & Interfaces, 2021, 13, 7423-7433.	4.0	19
1051	Highly Selective Synthesis of Monolayer or Bilayer WSe₂ Single Crystals by Pre-annealing the Solid Precursor. Chemistry of Materials, 2021, 33, 1307-1313.	3.2	20
1052	Unusual Strain Dependence of Quasiparticle Electronic Structure, Exciton, and Optical Properties in Blue Phosphorene. Physical Review Applied, 2021, 15, .	1.5	9
1053	Recent Advances in Twoâ€Dimensional Heterostructures: From Band Alignment Engineering to Advanced Optoelectronic Applications. Advanced Electronic Materials, 2021, 7, 2001174.	2.6	34
1054	Recent Advances in Multiâ€Layer Lightâ€Emitting Heterostructure Transistors. Small, 2021, 17, e2007661.	5.2	14
1055	Role of Ferromagnetic Monolayer WSe₂ Flakes in the Pt/Y₃Fe₅O₁₂ Bilayer Structure in the Longitudinal Spin Seebeck Effect. ACS Applied Materials & Interfaces, 2021, 13, 15783-15790.	4.0	14
1056	Gate-Tunable Plasmon-Enhanced Photodetection in a Monolayer MoS₂ Phototransistor with Ultrahigh Photoresponsivity. Nano Letters, 2021, 21, 3083-3091.	4.5	68

#	Article	IF	Citations
1057	Lightâ€“Matter Interaction Enhancement in Anisotropic 2D Black Phosphorus via Polarization-Tailoring Nano-Optics. ACS Photonics, 2021, 8, 1120-1128.	3.2	20
1058	Highly Sensitive, Ultrafast, and Broadband Photoâ€Detecting Fieldâ€Effect Transistor with Transitionâ€Metal Dichalcogenide van der Waals Heterostructures of MoTe₂ and PdSe₂. Advanced Science, 2021, 8, e2003713.	5.6	65
1059	Atomic-Layer Controlled Interfacial Band Engineering at Two-Dimensional Layered PtSe₂/Si Heterojunctions for Efficient Photoelectrochemical Hydrogen Production. ACS Nano, 2021, 15, 4627-4635.	7.3	27
1060	Controllable n-type doping in WSe2 monolayer via construction of anion vacancies. Chinese Chemical Letters, 2021, 32, 3118-3122.	4.8	9
1061	Regulation of vertical and biaxial strain on electronic and optical properties of G-GaN-G sandwich heterostructure. Journal of Materials Science, 2021, 56, 11402-11413.	1.7	3
1062	Low-Loss Integrated Nanophotonic Circuits with Layered Semiconductor Materials. Nano Letters, 2021, 21, 2709-2718.	4.5	24
1063	Hierarchical WSe2 nanoflower as a cathode material for rechargeable Mg-ion batteries. Journal of Colloid and Interface Science, 2021, 588, 378-383.	5.0	69
1064	Preferential hole defect formation in monolayer WSe2 by electron-beam irradiation. Physical Review Materials, 2021, 5, .	0.9	4
1065	Strong Photoluminescence Enhancement from Bilayer Molybdenum Disulfide via the Combination of UV Irradiation and Superacid Molecular Treatment. Applied Sciences (Switzerland), 2021, 11, 3530.	1.3	2
1066	Two-dimensional nanomaterials with engineered bandgap: Synthesis, properties, applications. Nano Today, 2021, 37, 101059.	6.2	82
1067	Electronic, magnetism and optical properties of transition metals adsorbed puckered arsenene. Superlattices and Microstructures, 2021, 152, 106852.	1.4	62
1068	Understanding Substrate-Guided Assembly in van der Waals Epitaxy by in Situ Laser Crystallization within a Transmission Electron Microscope. ACS Nano, 2021, 15, 8638-8652.	7.3	7
1069	Excitonic Emission in Atomically Thin Electroluminescent Devices. Laser and Photonics Reviews, 2021, 15, 2000587.	4.4	7
1070	Ultralarge Photoluminescence Enhancement of Monolayer Molybdenum Disulfide by Spontaneous Superacid Nanolayer Formation. ACS Applied Materials & Interfaces, 2021, 13, 25280-25289.	4.0	8
1071	MoSe₂â€“Cu_{2â€“x}S/GaAs Heterostructure-Based Self-Biased Two Color-Band Photodetectors with High Detectivity. Journal of Physical Chemistry C, 2021, 125, 10768-10776.	1.5	9
1072	Nonvolatile Electric Control of Exciton Complexes in Monolayer MoSe₂ with Two-Dimensional Ferroelectric CuInP₂S₆. ACS Applied Materials & Interfaces, 2021, 13, 24250-24257.	4.0	11
1073	Optical bandgap control in Al2O3/TiO2 heterostructures by plasma enhanced atomic layer deposition: Toward quantizing structures and tailored binary oxides. Spectrochimica Acta - Part A: Molecular and Biomolecular Spectroscopy, 2021, 252, 119508.	2.0	9
1074	2D Semiconductor Nanomaterials and Heterostructures: Controlled Synthesis and Functional Applications. Nanoscale Research Letters, 2021, 16, 94.	3.1	20

#	Article	IF	Citations
1075	Atomically Thin Sheets of Leadâ€Free 1D Hybrid Perovskites Feature Tunable Whiteâ€Light Emission from Selfâ€Trapped Excitons. Advanced Materials, 2021, 33, e2100518.	11.1	15
1076	Synthesis of lateral heterostructure of 2D materials for optoelectronic devices: challenges and opportunities. Emergent Materials, 2021, 4, 923-949.	3.2	14
1077	Perspectives on photodetectors based on selenides and their van der Waals heterojunctions. Applied Physics Letters, 2021, 118, 190501.	1.5	9
1078	Synergistic enhancement of photoluminesent intensity in monolayer molybdenum disulfide embedded with plasmonic nanostructures for catalytic sensing. 2D Materials, 0, , .	2.0	4
1079	Enhanced Exciton Binding Energy, Zeeman Splitting and Spin Polarization in Hybrid Layered Nanosheets Comprised of (Cd, Mn)Se and Nitrogen-Doped Graphene Oxide: Implication for Semiconductor Devices. Nanotechnology, 2021, 32, .	1.3	0
1080	Development of photovoltaic solar cells based on heterostructure of layered materials: challenges and opportunities. Emergent Materials, 2021, 4, 881-900.	3.2	6
1081	Molecular Doping of 2D Indium Selenide for Ultrahigh Performance and Lowâ€Power Consumption Broadband Photodetectors. Advanced Functional Materials, 2021, 31, 2103353.	7.8	17
1082	Optical properties of two-dimensional AlOCl, BaFCl, and BiOCl monolayers using the density functional theory. Optik, 2021, 236, 166678.	1.4	2
1083	Inducing and Probing Localized Excitons in Atomically Thin Semiconductors via Tipâ€Enhanced Cavityâ€Spectroscopy. Advanced Functional Materials, 2021, 31, 2102893.	7.8	22
1084	Layer-Dependent Photoabsorption and Photovoltaic Effects in Two-Dimensional <mml:math xmlns:mml="http://www.w3.org/1998/Math/MathML" display="inline" overflow="scroll"><mml:msub><mml:mi>Bi</mml:mi><mml:mn>2</mml:mn></mml:msub><mml:msub><mml:mrow><mml:mrow><mml:mathvariant="normal">O</mml:mi></mml:mrow></mml:mrow><mml:mn>2</mml:mn></mml:msub><mml:mi>X</mml:mi></mml:ma		

#	Article	IF	Citations
1093	Bandâ€tailored van der Waals heterostructure for multilevel memory and artificial synapse. InformaÄnÃ-MateriÃ¡ly, 2021, 3, 917-928.	8.5	59
1094	Dimensionality-Inhibited Chemical Doping in Two-Dimensional Semiconductors: The Phosphorene and MoS₂ from Charge-Correction Method. Nano Letters, 2021, 21, 6711-6717.	4.5	14
1095	Experimental Adhesion Energy in van der Waals Crystals and Heterostructures from Atomically Thin Bubbles. Physical Review Letters, 2021, 127, 046101.	2.9	36
1096	Spatial Control of Dynamic pâ€“iâ€“n Junctions in Transition Metal Dichalcogenide Light-Emitting Devices. ACS Nano, 2021, 15, 12911-12921.	7.3	8
1097	Roomâ€Temperature Chiral Lightâ€Emitting Diode Based on Strained Monolayer Semiconductors. Advanced Materials, 2021, 33, e2100601.	11.1	16
1098	Spontaneous Polarity Flipping in a 2D Heterobilayer Induced by Fluctuating Interfacial Carrier Flows. Nano Letters, 2021, 21, 6773-6780.	4.5	7
1099	Neutralizing Defect States in MoS₂ Monolayers. ACS Applied Materials & Interfaces, 2021, 13, 44686-44692.	4.0	8
1100	Defects inducing anomalous exciton kinetics in monolayer WS2. Nano Research, 2022, 15, 1616-1622.	5.8	9
1101	Unraveling the synergetic mechanism of physisorption and chemisorption in laser-irradiated monolayer WS2. Nano Research, 2021, 14, 4274-4280.	5.8	6
1102	Nature of optical excitations and bandgap of Re_xMo_{1â^'x}S₂ alloy at nanoscale probed from high resolution low loss electron energy loss spectroscopy. Journal of Physics Condensed Matter, 2021, 33, 455901.	0.7	0
1103	Polarized photoluminescence spectroscopy in WS₂, WSe₂ atomic layers and heterostructures by cylindrical vector beams*. Chinese Physics B, 2021, 30, 087802.	0.7	1
1104	Two-dimensional heterostructures and their device applications: progress, challenges and opportunitiesâ€”review. Journal Physics D: Applied Physics, 2021, 54, 433001.	1.3	30
1105	Polarization-insensitive broadband absorption enhancement with few-layer MoS2 film. Physics Letters, Section A: General, Atomic and Solid State Physics, 2021, 408, 127511.	0.9	4
1106	Enhanced Dielectric Screening and Photoluminescence from Nanopillar-Strained MoS₂ Nanosheets: Implications for Strain Funneling in Optoelectronic Applications. ACS Applied Nano Materials, 2021, 4, 8101-8107.	2.4	12
1107	Observation of double indirect interlayer exciton in MoSe2/WSe2 heterostructure. Nano Research, 2022, 15, 2661-2666.	5.8	17
1108	Two-Dimensional Materials for Advanced Solar Cells. , 0, , .		0
1109	Recent progress of silicon integrated light emitters and photodetectors for optical communication based on two-dimensional materials. Optical Materials Express, 2021, 11, 3298.	1.6	7
1110	Modulation of trion and exciton formation in monolayer WS₂ by dielectric and substrate engineering. 2D Materials, 2021, 8, 045032.	2.0	3

#	Article	IF	Citations
1111	Exciton Transitions in Monolayer WS₂ Activated by Swift Heavy Ion Irradiation. Journal of Physical Chemistry C, 2021, 125, 20389-20396.	1.5	6
1112	Wet Chemistry Vitrification and Metalâ€toâ€Semiconductor Transition of 2D Gray Arsenene Nanoflakes. Advanced Functional Materials, 2021, 31, 2106529.	7.8	11
1113	First-Principles Investigation of Structural, Raman and Electronic Characteristics of Single Layer Ge3N4. Applied Surface Science, 2021, 572, 151361.	3.1	1
1114	Gate-controlled MoTe2 homojunction for sub-thermionic subthreshold swing tunnel field-effect transistor. Nano Today, 2021, 40, 101263.	6.2	19
1115	Anisotropy of effective masses induced by strain in Janus MoSSe and WSSe monolayers. Physica E: Low-Dimensional Systems and Nanostructures, 2021, 134, 114826.	1.3	7
1116	Gas (CO and NO) adsorption and sensing based on transition metals functionalized Janus MoSSe. Applied Surface Science, 2021, 565, 150509.	3.1	13
1117	Vibrational and optical identification of GeO₂ and GeO single layers: a first-principles study. Physical Chemistry Chemical Physics, 2021, 23, 21307-21315.	1.3	3
1118	Gate-tunable the interface properties of GaAsâ€“WSe2 (1Dâ€“2D) vdWs heterojunction for high-responsivity, self-powered photodetector. Applied Physics Letters, 2021, 118, .	1.5	31
1119	Excitons in bulk black phosphorus evidenced by photoluminescence at low temperature. 2D Materials, 2021, 8, 021001.	2.0	12
1120	The catalyst-free growth of layer-structured CuInSe₂/Î²-In₂Se₃ microwires for ultrasensitive self-powered photodetectors based on a lateral pâ€“n junction. Journal of Materials Chemistry C, 2021, 9, 9484-9491.	2.7	8
1121	Raman spectrum of Janus transition metal dichalcogenide monolayers WSSe and MoSSe. Physical Review B, 2021, 103, .	1.1	63
1122	Design and tailoring of two-dimensional Schottky, PN and tunnelling junctions for electronics and optoelectronics. Nanoscale, 2021, 13, 6713-6751.	2.8	30
1123	Van der Waals Bipolar Junction Transistor Using Vertically Stacked Twoâ€Dimensional Atomic Crystals. Advanced Functional Materials, 2019, 29, 1807893.	7.8	46
1124	Electronic and Optoelectronic Applications Based on 2D Novel Anisotropic Transition Metal Dichalcogenides. Advanced Science, 2017, 4, 1700231.	5.6	219
1125	Measurement of the Optical Dielectric Function of Monolayer Transition Metal Dichalcogenides: MoS2, MoSe2, WS2, and WSe2. Springer Theses, 2016, , 33-43.	0.0	16
1126	Effects of dielectric stoichiometry on the photoluminescence properties of encapsulated WSe2 monolayers. Nano Research, 2018, 11, 1399-1414.	5.8	12
1128	Substrate-Dependent Exciton Diffusion and Annihilation in Chemically Treated MoS₂ and WS₂. Journal of Physical Chemistry C, 2020, 124, 12175-12184.	1.5	51
1129	Atomically thin quantum light-emitting diodes. , 0, .		1

#	Article	IF	Citations
1130	Complex band structures of transition metal dichalcogenide monolayers with spinâ€“orbit coupling effects. Journal of Physics Condensed Matter, 2016, 28, 355301.	0.7	7
1131	Excitons in two-dimensional van der Waals heterostructures. Journal Physics D: Applied Physics, 2021, 54, 053001.	1.3	8
1132	Role of defects and phonons in bandgap dynamics of monolayer WS2 at high carrier densities. JPhys Materials, 2020, 4, 015005.	1.8	7
1133	Engineering of optical and electronic band gaps in transition metal dichalcogenide monolayers through external dielectric screening. Physical Review Materials, 2017, 1, .	0.9	83
1134	Revealing electronic nature of broad bound exciton bands in two-dimensional semiconducting <mml:math xmlns:mml="http://www.w3.org/1998/Math/MathML"><mml:mrow><mml:mi mathvariant="normal">W</mml:mi><mml:msub><mml:mi mathvariant="normal">S</mml:mi><mml:mn>2</mml:mn></mml:msub></mml:mrow></mml:math> and <mml:math xmlns:mml="http://www.w3.org/1998/Math/MathML"><mml:mrow><mml:mi>Mo</mml:mi><mml:msub><mml:mi	0.9	19
1135	Magnetic properties of transition metal dichalcogenides-Fe/Ir(111) interfaces from first principles. Physical Review Materials, 2018, 2, .	0.9	4
1136	Ab initio study of magnetic nanopatterning of a hybrid transition metal dichalcogenides/Ir(111) system via magnetic clusters. Physical Review Materials, 2019, 3, .	0.9	4
1137	Bright trion emission from semiconductor nanoplatelets. Physical Review Materials, 2020, 4, .	0.9	24
1138	Anisotropic exciton excitations and optical properties of Hittorf's phosphorene. Physical Review Research, 2020, 2, .	1.3	10
1139	Controlled growth of 2D heterostructures and prevention of TMD oxidation. , 2018, , .		2
1140	Chiral light-matter interactions using spin-valley states in transition metal dichalcogenides. Optics Express, 2019, 27, 21367.	1.7	19
1141	Strong plasmon-exciton coupling in MIM waveguide-resonator systems with WS₂ monolayer. Optics Express, 2020, 28, 205.	1.7	26
1142	Auger-type process in ultrathin ReS₂. Optical Materials Express, 2020, 10, 1092.	1.6	17
1143	Radially polarized light beams from spin-forbidden dark excitons and trions in monolayer WSe₂. Optical Materials Express, 2020, 10, 1273.	1.6	10
1144	All-optical dynamic tuning of local excitonic emission of monolayer MoS2 by integration with Ge2Sb2Te5. Nanophotonics, 2020, 9, 2351-2359.	2.9	4
1145	Tunable electronic structure of two-dimensional transition metal chalcogenides for optoelectronic applications. Nanophotonics, 2020, 9, 1675-1694.	2.9	44
1146	Electronic properties of graphene/ZnO 2D-2D composite. Semiconductor Physics, Quantum Electronics and Optoelectronics, 2018, 21, 65-72.	0.3	5
1147	Controlling plasmon-exciton interactions through photothermal reshaping. Opto-Electronic Advances, 2020, 3, 19001701-19001708.	6.4	12

#	Article	IF	Citations
1149	Synthesis and Characterization of Highly Crystalline Vertically Aligned WSe2 Nanosheets. Applied Sciences (Switzerland), 2020, 10, 874.	1.3	31
1150	Excitons in Two-Dimensional Materials. , 0, , .		6
1151	Novel p-n junctions based on ambipolar two-dimensional crystals. Wuli Xuebao/Acta Physica Sinica, 2017, 66, 217302.	0.2	4
1152	Electrically driven strain-induced deterministic single-photon emitters in a van der Waals heterostructure. Science Advances, 2021, 7, eabj3176.	4.7	28
1153	Highâ€Speed Electroluminescence Modulation in Monolayer WS₂. Advanced Materials Technologies, 2022, 7, 2100915.	3.0	6
1154	Interlayer Excitons in Transition Metal Dichalcogenide Semiconductors for 2D Optoelectronics. Advanced Materials, 2022, 34, e2107138.	11.1	28
1155	pâ€GeSe/nâ€ReS₂ Heterojunction Rectifier Exhibiting A Fast Photoresponse with Ultraâ€High Frequencyâ€Switching Applications. Advanced Materials Interfaces, 2021, 8, 2100705.	1.9	29
1156	Ultrafast and Highly Stable Photodetectors Based on p-GeSe/n-ReSe₂ Heterostructures. ACS Applied Materials & Interfaces, 2021, 13, 47882-47894.	4.0	26
1157	Electrochemical growth of two-dimensional MoS2 nanosheets for development of femtomolar Hg(II) ion label-free biosensor. Chemical Physics Letters, 2021, 784, 139115.	1.2	3
1158	The valley degree of freedom of an electron. Wuli Xuebao/Acta Physica Sinica, 2015, 64, 187301.	0.2	3
1159	Electrical Properties and Photo-response of FETs based on Few-layer WS2 Nanoflakes. , 2016, , .		0
1160	Antenna-Coupled Optoelectronics With Two-Dimensional Materials. , 2016, , .		1
1161	Chapter 11: Perspective. , 2017, , 177-186.		0
1162	Bright Electroluminescence from Back-Gated WSe2 P-N Junctions Using Pulsed Injection. , 2018, , .		0
1163	Controllable coherent plasmon-exciton interaction in MoS2 monolayer with gold nanorods through photothermal reshaping. , 2019, , .		0
1164	Chromgruppe: Elemente der sechsten Nebengruppe. , 2019, , 1-51.		0
1165	1D and 2D materials, and flexible substrates. , 2019, , .		0
1166	Electric field induced variations of excited state lifetimes and photoluminescence spectra in 2D heterostructures. , 2019, , .		1

#	Article	IF	Citations
1167	Resonant photocurrent from a single quantum emitter in tungsten diselenide. 2D Materials, 2020, 7, 045021.	2.0	4
1168	2D Layered Material Alloys: Synthesis and Application in Electronic and Optoelectronic Devices. Advanced Science, 2022, 9, e2103036.	5.6	38
1169	Enhanced optoelectronics performances of multilayer Sb0.1Mo0.9Se2/SnSe2 heterostructure. Journal of Materials Science: Materials in Electronics, 2021, 32, 28739-28749.	1.1	1
1170	Electrically Pumped Light-emitting Device Based on MoTe2 Directly Integrated with Doped Silicon. , 2020, , .		0
1171	Realization of strong coupling between 2D excitons and cavity photons at room temperature. Optics Letters, 2020, 45, 6571.	1.7	5
1172	Inter-Layer interaction induced electronic properties in partially oxidized transition metal dichalcogenides. AIP Conference Proceedings, 2020, , .	0.3	0
1173	Biexcitons do not form in MoS2 monolayers from optical pumping at 6 K. , 2020, , .		0
1174	First Principles Based Compact Model for 2D-Channel MOSFETs. , 2020, , .		1
1175	Charge Transfer at the Heteroâ€Interface of WSe₂/InSe Induces Efficient Doping to Achieve Multiâ€Functional Lateral Homoâ€Junctions. Advanced Electronic Materials, 2021, 7, 2100584.	2.6	5
1176	High-Temperature-Induced Intervalley Carrier Transfer in Two-Dimensional Semiconductors: WSe2 versus WS2. Journal of Physical Chemistry C, 2021, 125, 23922-23928.	1.5	0
1177	The gate tunable 2D pn junction driven out-of-equilibrium. Journal of Applied Physics, 2021, 130, .	1.1	1
1178	Electrical Modulation of Exciton Complexes in Light-Emitting Tunnel Transistors of a van der Waals Heterostructure. ACS Photonics, 2021, 8, 3455-3461.	3.2	3
1179	The electrical conductivity of solution-processed nanosheet networks. Nature Reviews Materials, 2022, 7, 217-234.	23.3	75
1180	Direct and indirect excitons in two-dimensional covalent organic frameworks. Chinese Journal of Chemical Physics, 2020, 33, 569-577.	0.6	2
1181	Spontaneous formation of atomically thin p-n homojunction diodes in exfoliated graphenic medium intended for rectifiers. Physica Scripta, 2021, 96, 015807.	1.2	0
1182	Quantum transport: general concepts. , 0, , 91-117.		1
1183	Trap-free exciton dynamics in monolayer WS₂via oleic acid passivation. Nanoscale, 2021, 13, 20126-20133.	2.8	4
1184	Valley-contrasting interband transitions and excitons in symmetrically biased dice model. Physical Review B, 2021, 104, .	1.1	5

#	Article	IF	Citations
1185	Effects of Halogen Substitution on the Optoelectronic Properties of Two-Dimensional All-Inorganic Double Perovskite <mml:math xmlns:mml="http://www.w3.org/1998/Math/MathML" display="inline" overflow="scroll"><mml:msub><mml:mi>Cs</mml:mi><mml:mn>4</mml:mn></mml:msub><mml:mrow><mml:mi>Ag</mml:mi><mml:mi></mml:mi>		

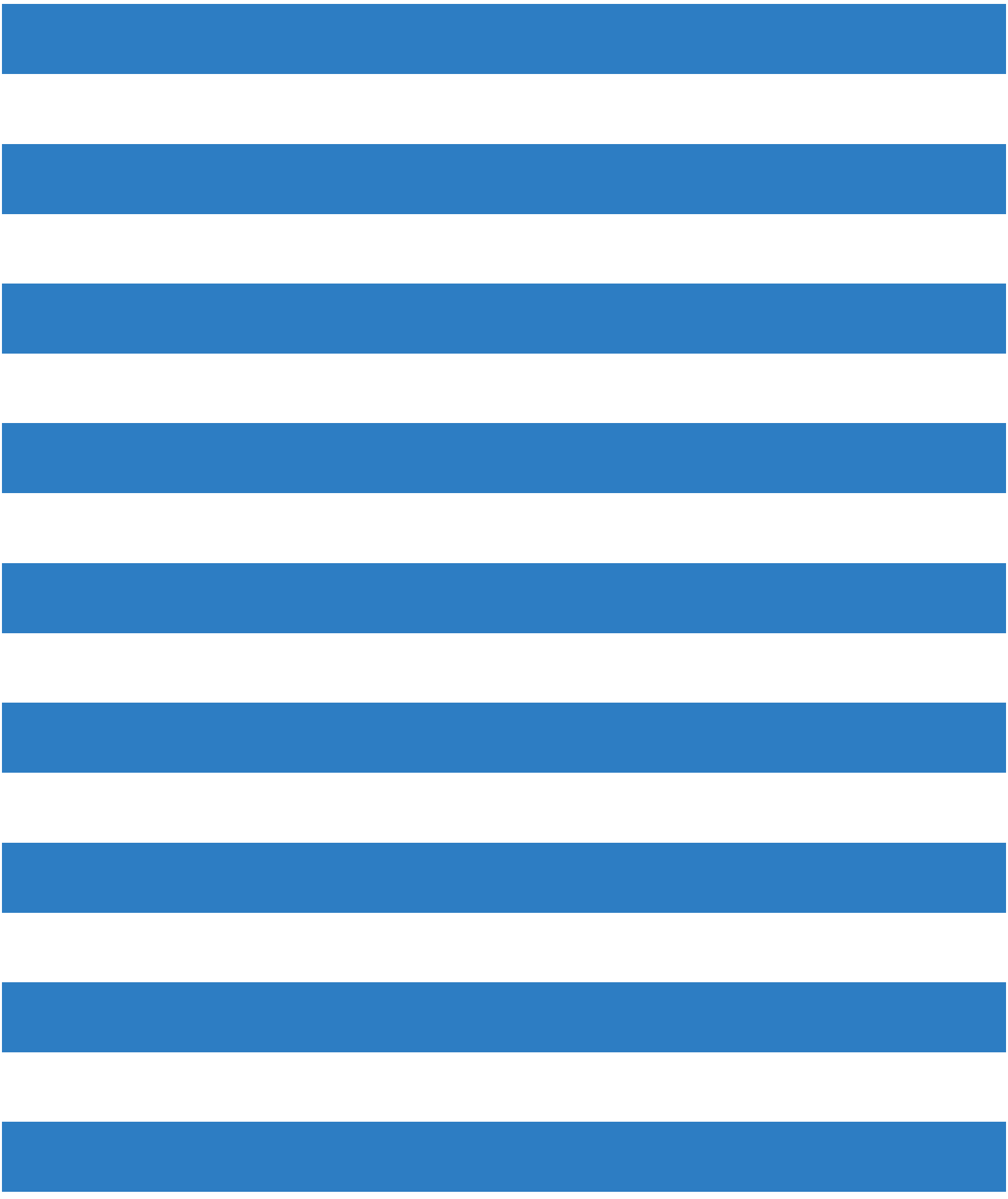

#	Article	IF	Citations
1204	One order enhancement of charge carrier relaxation rate by tuning structural and optical properties in annealed cobalt doped MoS₂ nanosheets. New Journal of Chemistry, 2022, 46, 1877-1895.	1.4	1
1205	Plasmon-enhanced photoluminescence from MoS₂ monolayer with topological insulator nanoparticle. Nanophotonics, 2022, 11, 995-1001.	2.9	8
1206	Recent progress on transition metal diselenides from formation and modification to applications. Nanoscale, 2022, 14, 1075-1095.	2.8	21
1207	Valleytronics in two-dimensional materials with line defect. Nanotechnology, 2022, 33, 212001.	1.3	22
1208	Injection-free multiwavelength electroluminescence devices based on monolayer semiconductors driven by an alternating field. Science Advances, 2022, 8, eabl5134.	4.7	13
1210	Transition Metal Dichalcogenides: Properties, Synthetic Routes and Applications. RSC Nanoscience and Nanotechnology, 2022, , 417-441.	0.2	0
1211	Drift-dominant exciton funneling and trion conversion in 2D semiconductors on the nanogap. Science Advances, 2022, 8, eabm5236.	4.7	21
1212	Exciton Emissions in Bilayer WSe₂ Tuned by the Ferroelectric Polymer. Journal of Physical Chemistry Letters, 2022, 13, 1636-1643.	2.1	3
1213	Design and analysis of III-V two-dimensional van der Waals heterostructures for ultra-thin solar cells. Applied Surface Science, 2022, 586, 152799.	3.1	16
1214	Few-Layer WS₂â€“WSe₂ Lateral Heterostructures: Influence of the Gas Precursor Selenium/Tungsten Ratio on the Number of Layers. ACS Nano, 2022, 16, 1198-1207.	7.3	16
1215	Quantum emitters and detectors based on 2D van der Waals materials. Nanoscale, 2022, 14, 5289-5313.	2.8	12
1216	Magnetic single-layer nanoribbons of manganese oxide: edge- and width-dependent electronic properties. Journal of Materials Chemistry C, 2022, 10, 7567-7574.	2.7	1
1217	Design and Analysis of Iii-V Two-Dimensional Van Der Waals Heterostructures for Ultra-Thin Solar Cells. SSRN Electronic Journal, 0, , .	0.4	0
1218	Construction and physical properties of low-dimensional structures for nanoscale electronic devices. Physical Chemistry Chemical Physics, 2022, 24, 9082-9117.	1.3	3
1219	Detection of dielectric screening effect by excitons in two-dimensional semiconductors and its application. Wuli Xuebao/Acta Physica Sinica, 2022, 71, 127102.	0.2	2
1220	Preparation of NbAs Single Crystal by the Seed Growth Process. Crystals, 2022, 12, 249.	1.0	1
1221	A Waveguide-Integrated Two-Dimensional Light-Emitting Diode Based on p-Type WSe₂/n-Type CdS Nanoribbon Heterojunction. ACS Nano, 2022, 16, 4371-4378.	7.3	17
1222	Nearâ€Infrared Electroluminescent Lightâ€Emitting Transistors Based on CVDâ€Synthesized Ambipolar ReSe₂ Nanosheets. Advanced Optical Materials, 2022, 10, .	3.6	3

#	Article	IF	Citations
1223	Enhanced valley splitting of WSe2 in twisted van der Waals WSe2/CrI3 heterostructures. Npj Computational Materials, 2022, 8, .	3.5	13
1224	CRYSTALLINE AND NANOSTRUCTURED MATERIALS BASED ON TRANSITION METAL DICHALCOGENIDES: SYNTHESIS AND ELECTRONIC PROPERTIES. Journal of Structural Chemistry, 2022, 63, 176-226.	0.3	6
1225	Enhanced lightâ€“matter interaction in two-dimensional transition metal dichalcogenides. Reports on Progress in Physics, 2022, 85, 046401.	8.1	74
1226	Versatile band structure and electronâ€"phonon coupling in layered PtSe2 with strong interlayer interaction. Nano Research, 2022, 15, 6613-6619.	5.8	8
1227	Strong reduction of thermal conductivity of WSe₂ with introduction of atomic defects. Nanotechnology, 2022, 33, 275706.	1.3	4
1228	Engineering the Optoelectronic Properties of 2D Hexagonal Boron Nitride Monolayer Films by Sulfur Substitutional Doping. ACS Applied Materials & Interfaces, 2022, 14, 16453-16461.	4.0	10
1229	Delayed Thermal Relaxation in Lateral Heterostructures of Transition-Metal Dichalcogenides. Journal of Physical Chemistry C, 2022, 126, 6815-6824.	1.5	0
1230	Anisotropic exciton states and excitonic absorption spectra in a freestanding monolayer black phosphorus. Physica E: Low-Dimensional Systems and Nanostructures, 2022, 141, 115238.	1.3	6
1231	Doping level and environment dependence of structural stability and magnetic properties in Mn-doped WS2 bilayer in first principles. Current Applied Physics, 2022, 39, 1-7.	1.1	1
1232	Enhanced magnetic anisotropy in two-dimensional <mml:math xmlns:mml="http://www.w3.org/1998/Math/MathML" display="inline" id="d1e370" altimg="si3.svg"><mml:mrow><mml:mn>2</mml:mn><mml:mi>H</mml:mi><mml:mo linebreak="goodbreak" linebreakstyle="after">â^'</mml:mo><mml:mi>T</mml:mi><mml:mi>a</mml:mi><mml:msub><mml:mrow><mml:mi>S</mml:mi></mml by self-intercalation: A DFT study. Journal of Magnetism and Magnetic Materials, 2022, 553, 168988.	1.0	5
1233	Tactile tribotronic reconfigurable p-n junctions for artificial synapses. Science Bulletin, 2022, 67, 803-812.	4.3	26
1234	Growth of MoS₂â€“Nb-doped MoS₂ lateral homojunctions: A monolayer <i>p</i>â€“<i>n</i> diode by substitutional doping. APL Materials, 2021, 9, 121115.	2.2	5
1235	Ultrasensitive and Broadâ€Spectrum Photodetectors Based on InSe/ReS₂ Heterostructure. Advanced Optical Materials, 2022, 10, .	3.6	28
1236	Recent advances in the controlled chemical vapor deposition growth of bilayer 2D single crystals. Journal of Materials Chemistry C, 2022, 10, 13324-13350.	2.7	10
1237	Enhancement of photoluminescence of monolayer transition metal dichalcogenide by subwavelength TiO₂ grating. Wuli Xuebao/Acta Physica Sinica, 2022, 71, 087801.	0.2	0
1238	Properties and applications of quantum dots derived from two-dimensional materials. Advances in Physics: X, 2022, 7, .	1.5	11
1239	Review of recent progress, challenges, and prospects of 2D materials-based short wavelength infrared photodetectors. Journal Physics D: Applied Physics, 2022, 55, 313001.	1.3	12
1240	Klein tunneling and ballistic transport in graphene and related materials. , 0, , 118-142.		0

#	Article	IF	Citations
1241	Quantum transport in disordered graphene-based materials. , 0, , 143-218.		0
1242	Ab initio and multiscale quantum transport in graphene-based materials. , 0, , 232-299.		0
1243	Electronic structure calculations: the density functional theory (DFT). , 0, , 314-331.		0
1244	Electronic structure calculations: the many-body perturbation theory (MBPT). , 0, , 332-337.		0
1245	Green's functions and ab initio quantum transport in the Landauerâ€“BÃ¼ttiker formalism. , 0, , 338-357.		0
1246	On the importance of electronâ€“electron and electronâ€“phonon scatterings and energy renormalizations during carrier relaxation in monolayer transition-metal dichalcogenides. Journal of Physics Condensed Matter, 2022, 34, 285601.	0.7	2
1247	Resolving the Mechanism of Acoustic Plasmon Instability in Graphene Doped by Alkali Metals. International Journal of Molecular Sciences, 2022, 23, 4770.	1.8	5
1248	Electrically tunable guided mode resonance grating for switchable photoluminescence. Applied Physics Letters, 2022, 120, 191108.	1.5	0
1249	Light emission properties of mechanical exfoliation induced extended defects in hexagonal boron nitride flakes. 2D Materials, 2022, 9, 035018.	2.0	5
1250	Theory of Excitons in Atomically Thin Semiconductors: Tight-Binding Approach. Nanomaterials, 2022, 12, 1582.	1.9	7
1251	Formation of van der Waals Stacked pâ€“n Homojunction Optoelectronic Device of Multilayered ReSe₂ by Cr Doping. Advanced Optical Materials, 2022, 10, .	3.6	8
1252	A Review on Materials and Methods for the Fabrication of Microcavity Laser. International Journal of Applied Engineering and Management Letters, 0, , 27-42.	0.0	0
1253	Gold nanoparticles decorated 2D-WSe2 as a SERS substrate. Spectrochimica Acta - Part A: Molecular and Biomolecular Spectroscopy, 2022, 278, 121349.	2.0	3
1254	Scalable production of p-MoTe₂/n-MoS₂ heterostructure array and its application for self-powered photodetectors and CMOS inverters. 2D Materials, 2022, 9, 035015.	2.0	4
1255	Exciton binding energy and screening length in two-dimensional semiconductors. Physical Review B, 2022, 105, .	1.1	8
1256	A Review on MX2 (MÂ=ÂMo, W and XÂ=ÂS, Se) layered material for opto-electronic devices. Advances in Natural Sciences: Nanoscience and Nanotechnology, 2022, 13, 023001.	0.7	5
1257	Optothermal and temperature reliant phonon dynamics probed by Raman spectroscopy. Physica B: Condensed Matter, 2022, , 414074.	1.3	1
1258	Pristine PN junction toward atomic layer devices. Light: Science and Applications, 2022, 11, .	7.7	21

#	Article	IF	Citations
1260	Simple Fabrication of Photodetectors Based on MoS2 Nanoflakes and Ag Nanoparticles. Sensors, 2022, 22, 4695.	2.1	0
1261	Hexagonal Boron Nitride for Nextâ€Generation Photonics and Electronics. Advanced Materials, 2023, 35, .	11.1	43
1263	Efficiency Roll-Off Free Electroluminescence from Monolayer WSe₂. Nano Letters, 2022, 22, 5316-5321.	4.5	11
1264	Room Temperature Fluorescence Blinking in MoS₂ Atomic Layers by Single Photon Energy Transfer. Laser and Photonics Reviews, 2022, 16, .	4.4	5
1265	Electronic, Magnetic, and Optical Properties of Metal Adsorbed g-ZnO Systems. Frontiers in Chemistry, 0, 10, .	1.8	6
1266	Optical nonlinearities in the excited carrier density of atomically thin transition metal dichalcogenides. Physical Review B, 2022, 106, .	1.1	2
1267	The non-volatile electrostatic doping effect in MoTe2 field-effect transistors controlled by hexagonal boron nitride and a metal gate. Scientific Reports, 2022, 12, .	1.6	3
1268	Fewâ€layered MoS₂ Based Vertical van der Waals pâ€n Homojunction by Highlyâ€efficient N₂ Plasma Implantation. Advanced Electronic Materials, 2022, 8, .	2.6	8
1269	Atomic-Scale Insights into the Lateral and Vertical Epitaxial Growth in Two-Dimensional Pd₂Se₃â€“MoS₂ Heterostructures. ACS Nano, 2022, 16, 10260-10272.	7.3	3
1270	Reversible Chargeâ€Polarity Control for Multioperationâ€Mode Transistors Based on van der Waals Heterostructures. Advanced Science, 2022, 9, .	5.6	6
1271	Growth, structure, electrical and optical properties of transition metal chalcogenide crystals synthesized by improved chemical vapor transport technique for semiconductor technologies. Progress in Crystal Growth and Characterization of Materials, 2022, 68, 100578.	1.8	4
1272	Positively Charged Biexcitons in Monolayer WSe₂ in Type-I GaSe/WSe₂ van der Waals Heterostructures: Implications for the Biexciton Laser. ACS Applied Nano Materials, 2022, 5, 10628-10635.	2.4	0
1273	Nondestructive and local mapping photoresponse of WSe2 by electrostatic force microscopy. Ultramicroscopy, 2022, 240, 113590.	0.8	2
1274	Laser Irradiation Effect on the p-GaSe/n-HfS₂ PN-Heterojunction for High-Performance Phototransistors. ACS Applied Materials & Interfaces, 2022, 14, 35927-35939.	4.0	6
1275	High-Temperature Annealing Effects on Atomically Thin Tungsten Diselenide Field-Effect Transistor. Applied Sciences (Switzerland), 2022, 12, 8119.	1.3	5
1276	Two-dimensional complementary gate-programmable PN junctions for reconfigurable rectifier circuit. Nano Research, 2023, 16, 1252-1258.	5.8	8
1277	First-principles insights into the spin-valley physics of strained transition metal dichalcogenides monolayers. New Journal of Physics, 2022, 24, 083004.	1.2	16
1278	Recent Advances in Tunable Metasurfaces: Materials, Design, and Applications. ACS Nano, 2022, 16, 13339-13369.	7.3	54

#	Article	IF	Citations
1279	Probing Chemical Vapor Deposition Growth Mechanism of Polycrystalline MoSe₂ by Near-Field Photoluminescence. Journal of Physical Chemistry C, 2022, 126, 13821-13829.	1.5	5
1280	Tunable Emission from Localized Excitons Deterministically Positioned in Monolayer pâ€“n Junctions. ACS Photonics, 2022, 9, 3067-3074.	3.2	5
1281	Room-temperature electrical control of polarization and emission angle in a cavity-integrated 2D pulsed LED. Nature Communications, 2022, 13, .	5.8	8
1282	Advances in Two-Dimensional Materials for Optoelectronics Applications. Crystals, 2022, 12, 1087.	1.0	18
1283	Direct observation of ultrafast carrier coupling dynamics in monolayer graphene/metal system. International Journal of Heat and Mass Transfer, 2022, 197, 123322.	2.5	2
1284	Programmable Photoâ€Induced Doping in 2D Materials. Advanced Materials Interfaces, 2022, 9, .	1.9	12
1285	Effect of an ultra-thin 2D transport layer on eco-friendly Perovskite/CIGS tandem solar cell: A numerical study. , 2022, 170, 207398.		6
1286	Quantification of the dielectric constant of MoS2 and WSe2 Nanosheets by electrostatic force microscopy. Materials Characterization, 2022, 193, 112313.	1.9	3
1287	Electrical modulation of excitonic transition in monolayer tungsten disulfide on periodically poled ferroelectric substrates. Current Applied Physics, 2022, 43, 90-96.	1.1	1
1288	Effect of surface preparation on PtSe2 crystal surface morphology. Surface Science, 2023, 727, 122181.	0.8	0
1289	Local strain and tunneling current modulate excitonic luminescence in MoS₂ monolayers. RSC Advances, 2022, 12, 24922-24929.	1.7	3
1290	Quantification of the Dielectric Constant of Mos_2 and Wse_2 Nanosheets by Electrostatic Force Microscopy. SSRN Electronic Journal, 0, , .	0.4	0
1291	Perovskite-transition metal dichalcogenides heterostructures: recent advances and future perspectives. , 2022, 1, 220006-220006.		17
1292	Single charge control of localized excitons in heterostructures with ferroelectric thin films and two-dimensional transition metal dichalcogenides. Nanoscale, 2022, 14, 14537-14543.	2.8	1
1293	Growth of Multilayer Wse2/Bi2o2se Heterostructures for Photodetection Without Lithography. SSRN Electronic Journal, 0, , .	0.4	0
1294	Highly Enhanced Many-body Interactions in Anisotropic 2D Semiconductors. RSC Nanoscience and Nanotechnology, 2022, , 76-125.	0.2	1
1295	Waveguide Integrated MoTe2 Photodetector with High speed and energy efficient. , 2022, , .		4
1296	Size-Dependent Mutual Charge Transfer between B- and P-Codoped Si Quantum Dots and Monolayer MoS₂. Journal of Physical Chemistry C, 2022, 126, 16401-16408.	1.5	1

#	Article	IF	Citations
1297	A field-effect WSe₂/Si heterojunction diode. Chinese Physics B, 2023, 32, 018505.	0.7	2
1298	Photoluminescence Path Bifurcations by Spin Flip in Two-Dimensional CrPS₄. ACS Nano, 2022, 16, 16385-16393.	7.3	7
1299	Basal Plane Functionalization of Niobium Disulfide Nanosheets with Cyclopentadienyl Manganese(I) Dicarbonyl. Inorganic Chemistry, 2022, 61, 14824-14832.	1.9	3
1300	The Recent Progress of Two-Dimensional Transition Metal Dichalcogenides and Their Phase Transition. Crystals, 2022, 12, 1381.	1.0	6
1301	Coherent dynamics of multi-spin V$${}_{{{{{{{{{m{B}}}}}}}}}^{-}$$ center in hexagonal boron nitride. Nature Communications, 2022, 13, .	5.8	25
1302	A multimode photodetector with polarization-dependent near-infrared responsivity using the tunable split-dual gates control. IScience, 2022, 25, 105164.	1.9	3
1303	Investigation of two-dimensional HfS₂/PtSSe heterostructure with strong visible light adsorption and strain tunable bandgap. Journal Physics D: Applied Physics, 2022, 55, 475301.	1.3	2
1304	Monolayer-like lattice dynamics in bulk WSe2. Materials Today Physics, 2022, 28, 100856.	2.9	4
1305	Exciton tuning in monolayer WSe₂viasubstrate induced electron doping. Nanoscale Advances, 2022, 4, 5102-5108.	2.2	7
1306	Role of tilt grain boundaries on the structural integrity of WSe₂ monolayers. Physical Chemistry Chemical Physics, 2022, 24, 27241-27249.	1.3	5
1307	Electrostatic and Environmental Control of the Trion Fine Structure in Transition Metal Dichalcogenide Monolayers. Nanomaterials, 2022, 12, 3728.	1.9	2
1308	Pâ€Type 2D Semiconductors for Future Electronics. Advanced Materials, 2023, 35, .	11.1	15
1309	Prediction of electronic and optical properties of monoclinic 1Tâ€™-phase OsSe2 monolayer using DFT principles. Materials Today Communications, 2022, 33, 104764.	0.9	5
1310	Programmable Photovoltaics of Metalâ€Oxideâ€Semiconductor Junction. Advanced Electronic Materials, 0, , 2200672.	2.6	0
1311	Prediction of new 2D Hf2Br2N2 monolayer as a promising candidate for photovoltaic applications. Materials Chemistry and Physics, 2023, 294, 126979.	2.0	51
1312	Electronic, mechanical and optical properties of the new 1T dipolonide PdPo2 and PtPo2 monolayers: A comparative study with 1T Pd and Pt-based dichalcogenides. Physica E: Low-Dimensional Systems and Nanostructures, 2023, 146, 115548.	1.3	0
1313	Structural, electronic and optical properties of monolayer InGeX₃ (Xâ€‰=â€‰S, Se, Te) by first-principles calculations. Journal of Physics Condensed Matter, 2023, 35, 064002.	0.7	0
1314	Synthesis of Ultrathin Topological Insulator Î²â€Ag₂Te and Ag₂Te/WSe₂â€Based Highâ€Performance Photodetector. Small, 2023, 19, .	5.2	7

#	Article	IF	Citations
1315	Recent Advances in Two-dimensional p-type Metal Chalcogenidesï¼š synthesis, doping strategies and applications. Journal Physics D: Applied Physics, 0, , .	1.3	0
1316	Chromgruppe: Elemente der sechsten Nebengruppe. , 2022, , 1-52.		0
1317	AC-driven multicolor electroluminescence from a hybrid WSe₂ monolayer/AlGaInP quantum well light-emitting device. Nanoscale, 2023, 15, 1347-1356.	2.8	3
1318	Emerging trends in van der Waals 2D TMD heterojunction bipolar transistors. Journal of Materials Chemistry C, 2023, 11, 1648-1667.	2.7	3
1319	Self-powered, ultra-fast and high photoresponsivity of MoTe2/HfSe2 heterostructure broadband photovoltaic device. Materials Science in Semiconductor Processing, 2023, 155, 107204.	1.9	4
1320	Polaronic Trions Induced by Strong Interfacial Coupling in Monolayer WSe ₂. Advanced Electronic Materials, 0, , 2200852.	2.6	2
1321	Plasmonic Slot Waveguide - Integrated MoTe2 Photodetector with 30-GHz Bandwidth at Telecom Wavelength. , 2022, , .		1
1322	Dielectric Function of 2D Tungsten Disulfide in Homoâ€•and Heterobilayer Stacking. Advanced Materials Interfaces, 2023, 10, .	1.9	3
1323	A roadmap to decipher ultrafast photophysics in two-dimensional nanomaterials. Journal of Chemical Physics, 2023, 158, .	1.2	6
1324	Band Alignments, Electronic Structure, and Core-Level Spectra of Bulk Molybdenum Dichalcogenides (MoS₂, MoSe₂, and MoTe₂). Journal of Physical Chemistry C, 2022, 126, 21022-21033.	1.5	4
1325	Tip-Induced and Electrical Control of the Photoluminescence Yield of Monolayer WS₂. Nano Letters, 2022, 22, 9244-9251.	4.5	3
1326	Two-dimensional optoelectronic devices for silicon photonic integration. Journal of Materiomics, 2023, 9, 551-567.	2.8	3
1327	2D Materials in the Display Industry: Status and Prospects. Advanced Materials, 2023, 35, .	11.1	3
1328	Graphene and Two-Dimensional Materials-Based Flexible Electronics for Wearable Biomedical Sensors. Electronics (Switzerland), 2023, 12, 45.	1.8	3
1329	Impact of Dispersion Force Schemes on Liquid Systems: Comparing Efficiency and Drawbacks for Well-Targeted Test Cases. Molecules, 2022, 27, 9034.	1.7	1
1332	Highâ€Performance Solutionâ€Processed 2D Pâ€Type WSe₂ Transistors and Circuits through Molecular Doping. Advanced Materials, 2023, 35, .	11.1	13
1333	Two/Quasi-two-dimensional perovskite-based heterostructures: construction, properties and applications. International Journal of Extreme Manufacturing, 2023, 5, 012004.	6.3	8
1334	A review of the synthesis, properties, and applications of 2D transition metal dichalcogenides and their heterostructures. Materials Chemistry and Physics, 2023, 297, 127332.	2.0	29

#	Article	IF	Citations
1335	Anisotropic phonon dispersion and optoelectronic properties of few-layer HfS₂. Journal of Materials Chemistry C, 2023, 11, 2608-2618.	2.7	2
1336	Lightâ€Triggered and Polarityâ€Switchable Homojunctions for Optoelectronic Logic Devices. Advanced Optical Materials, 2023, 11, .	3.6	5
1337	Ion-gel-based light-emitting devices using transition metal dichalcogenides and hexagonal boron nitride heterostructures. Japanese Journal of Applied Physics, 0, , .	0.8	0
1338	Laser Etching of Quasi-1D TiS3 Nanoribbons by Raman Spectrophotometer. Bulletin of the Russian Academy of Sciences: Physics, 2022, 86, S135-S140.	0.1	1
1339	Homogeneous in-plane WSe₂ Pâ€“N junctions for advanced optoelectronic devices. Nanoscale, 2023, 15, 4940-4950.	2.8	5
1340	2D materials for optoelectronics. , 2023, , 207-258.		0
1341	A Review on the Materials and Applications of Nanophotonics. , 2023, , 116-140.		1
1342	Gate Tunable Lateral 2D Pn Junctions: An Analytical Study of Its Electrostatics. IEEE Nanotechnology Magazine, 2023, 22, 52-57.	1.1	0
1343	Layer-Structured Anisotropic Metal Chalcogenides: Recent Advances in Synthesis, Modulation, and Applications. Chemical Reviews, 2023, 123, 3329-3442.	23.0	23
1344	Two Dimensional Heterostructures for Optoelectronics: Current Status and Future Perspective. Molecules, 2023, 28, 2275.	1.7	2
1345	First-principles calculations to investigate electronic band structure, optical and mechanical properties of new CaFCl monolayer. Results in Physics, 2023, 45, 106251.	2.0	4
1346	Thermal Stability and Sublimation of Two-Dimensional Co₉Se₈ Nanosheets for Ultrathin and Flexible Nanoelectronic Devices. ACS Applied Nano Materials, 2023, 6, 2421-2428.	2.4	0
1347	Impact of synthesis temperature and precursor ratio on the crystal quality of MOCVD WSe₂ monolayers. Nanotechnology, 2023, 34, 205602.	1.3	2
1348	A direction-sensitive photodetector based on the two-dimensional WSe2/MoSe2 lateral heterostructure with enhanced photoresponse. Results in Physics, 2023, 46, 106271.	2.0	2
1349	Bright and Efficient Lightâ€Emitting Devices Based on 2D Transition Metal Dichalcogenides. Advanced Materials, 2023, 35, .	11.1	10
1350	Growth of Multilayer WSe₂/Bi₂O₂Se Heterostructures for Photodetection without Lithography. Crystal Growth and Design, 2023, 23, 2092-2098.	1.4	4
1351	Photoluminescence manipulation in two-dimensional transition metal dichalcogenides. Journal of Materiomics, 2023, 9, 768-786.	2.8	2
1352	Tungsten dichalcogenide WS_{2x}Se_{2â^'2x} films via single source precursor low-pressure CVD and their (thermo-)electric properties. Journal of Materials Chemistry A, 2023, 11, 9635-9645.	5.2	3

#	Article	IF	Citations
1353	Lead halide perovskite sensitized WSe2 photodiodes with ultrahigh open circuit voltages. ELight, 2023, 3, .	11.9	13
1354	Intrinsic Control of Interlayer Exciton Generation in Van der Waals Materials via Janus Layers. Nano Letters, 0, , .	4.5	1
1355	Silver nanowire electrodes for transparent light emitting devices based on WS₂ monolayers. Nanotechnology, 2023, 34, 285201.	1.3	1
1356	On-Chip Ultralow-Threshold Tunable CdSSe Nanobelt Lasers Excited by the Emission of Linked ZnO Nanowire. Journal of Physical Chemistry Letters, 0, , 3861-3868.	2.1	0
1357	Perspectives and recent advances of two-dimensional III-nitrides: Material synthesis and emerging device applications. Applied Physics Letters, 2023, 122, .	1.5	5
1364	Dielectrics for Two-Dimensional Transition-Metal Dichalcogenide Applications. ACS Nano, 2023, 17, 9870-9905.	7.3	8
1367	2D materials for intelligent devices. Science China: Physics, Mechanics and Astronomy, 2023, 66, .	2.0	4
1370	Reduced Absorption Due to Defect-Localized Interlayer Excitons in Transition-Metal Dichalcogenideâ€“Graphene Heterostructures. Nano Letters, 2023, 23, 5995-6001.	4.5	2
1383	Enhanced Emission of Molybdenum Disulfide by Organicâ€“Inorganic Hybrid Heterojunctions. , 0, , .		0
1385	Chromgruppe: Elemente der sechsten Nebengruppe. , 2023, , 589-640.		0
1393	p-Type Two-Dimensional Semiconductors: From Materials Preparation to Electronic Applications. Nano-Micro Letters, 2023, 15, .	14.4	2
1403	Contemporary innovations in two-dimensional transition metal dichalcogenide-based Pâ€“N junctions for optoelectronics. Nanoscale, 2023, 16, 14-43.	2.8	1